②

AFWAL-TR-88-3080

SUPERPLASTIC FORMED ALUMINUM-LITHIUM AIRCRAFT STRUCTURE
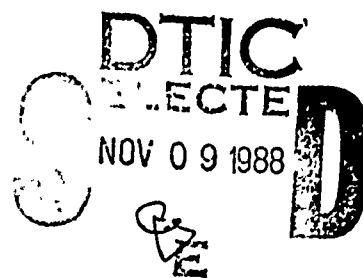
G.R. Martin, et al

Rockwell International
P.O. Box 92098
Los Angeles, CA   90009

October 1988

Interim Report for Period April 1987 - April 1988

AD-A200 245

Approved for Public Release; Distribution Unlimited

DTIC
ELECTE
NOV 0 9 1988
D

FLIGHT DYNAMICS LABORATORY
AIR FORCE WRIGHT AERONAUTICAL LABORATORIES
AIR FORCE SYSTEMS COMMAND
WRIGHT-PATTERSON AIR FORCE BASE, OHIO   45433-6553

88 11 07 033

NOTICE

WHEN GOVERNMENT DRAWINGS, SPECIFICATIONS, OR OTHER DATA ARE USED FOR ANY PURPOSE OTHER THAN IN CONNECTION WITH A DEFINITELY GOVERNMENT-RELATED PROCUREMENT, THE UNITED STATES GOVERNMENT INCURS NO RESPONSIBILITY OR ANY OBLIGATION WHATSOEVER. THE FACT THAT THE GOVERNMENT MAY HAVE FORMULATED OR IN ANY WAY SUPPLIED THE SAID DRAWINGS, SPECIFICATIONS, OR OTHER DATA, IS NOT TO BE REGARDED BY IMPLICATION, OR OTHERWISE IN ANY MANNER CONSTRUED, AS LICENSING THE HOLDER, OR ANY OTHER PERSON OR CORPORATION; OR AS CONVEYING ANY RIGHTS OR PERMISSION TO MANUFACTURE, USE, OR SELL ANY PATENTED INVENTION THAT MAY IN ANY WAY BE RELATED THERETO.

THIS REPORT HAS BEEN REVIEWED BY THE OFFICE OF PUBLIC AFFAIRS (ASD/CPA) AND IS RELEASABLE TO THE NATIONAL TECHNICAL INFORMATION SERVICE (NTIS). AT NTIS, IT WILL BE AVAILABLE TO THE GENERAL PUBLIC, INCLUDING FOREIGN NATIONS.

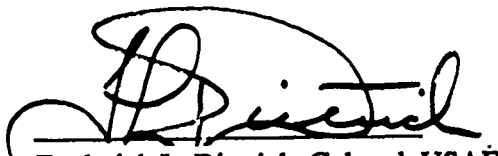THIS TECHNICAL REPORT HAS BEEN REVIEWED AND IS APPROVED FOR PUBLICATION.

Larry G. Kelly
Structural Concepts Branch
Structures Division

James P. Belloto
Structural Concepts Evaluation Group
Structural Concepts Branch

FOR THE COMMANDER

Frederick L. Dietrich, Colonel, USAF
Chief, Structures Division

IF YOUR ADDRESS HAS CHANGED, IF YOU WISH TO BE REMOVED FROM OUR MAILING LIST, OR IF THE ADDRESSEE IS NO LONGER EMPLOYED BY YOUR ORGANIZATION PLEASE NOTIFY AFWAL/FIBC , WRIGHT-PATTERSON AFB, OH 45433-6553 TO HELP US MAINTAIN A CURRENT MAILING LIST.

COPIES OF THIS REPORT SHOULD NOT BE RETURNED UNLESS RETURN IS REQUIRED BY SECURITY CONSIDERATIONS, CONTRACTUAL OBLIGATIONS, OR NOTICE ON A SPECIFIC DOCUMENT.

SECURITY CLASSIFICATION OF THIS PAGE   *AD-A200 243*

REPORT DOCUMENTATION PAGE

Form Approved
OMB No. 0704-0188

1a. REPORT SECURITY CLASSIFICATION	1b. RESTRICTIVE MARKINGS
2a. SECURITY CLASSIFICATION AUTHORITY UNCLASSIFIED **2b. DECLASSIFICATION/DOWNGRADING SCHEDULE**	**3. DISTRIBUTION/AVAILABILITY OF REPORT** Approved for public release, distribution Unlimited.

4. PERFORMING ORGANIZATION REPORT NUMBER(S) NA-88-1347L	5. MONITORING ORGANIZATION REPORT NUMBER(S) AFWAL-TR-88-3080

6a. NAME OF PERFORMING ORGANIZATION ROCKWELL INTERNATIONAL	6b. OFFICE SYMBOL *(If applicable)*	7a. NAME OF MONITORING ORGANIZATION Flight Dynamics Laboratory (AFWAL/FIBCB) Air Force Wright Aeronautical Laboratories
6c. ADDRESS *(City, State, and ZIP Code)* P.O. BOX 92098 LOS ANGELES, CA 90009		7b. ADDRESS *(City, State, and ZIP Code)* WRIGHT-PATTERSON AFB, OH 45433-6553

8a. NAME OF FUNDING/SPONSORING ORGANIZATION FLIGHT DYNAMICS LABORATORY	8b. OFFICE SYMBOL *(If applicable)* AFWAL/FIBC B	9. PROCUREMENT INSTRUMENT IDENTIFICATION NUMBER F33615-87-C-3223

8c. ADDRESS *(City, State, and ZIP Code)* WRIGHT-PATTERSON AFB AFWAL/FIBC, OH 45433-6553	10. SOURCE OF FUNDING NUMBERS			
	PROGRAM ELEMENT NO. 62201F	PROJECT NO. 2401	TASK NO 03	WORK UNIT ACCESSION NO. 79

11. TITLE *(Include Security Classification)*
SUPERPLASTIC FORMED ALUMINUM-LITHIUM AIRCRAFT STRUCTURE

12. PERSONAL AUTHOR(S)
G.R. Martin, et al

13a. TYPE OF REPORT INTERIM	13b. TIME COVERED FROM APR 1987 TO APR 1988	14. DATE OF REPORT *(Year, Month, Day)* 1988 October	15. PAGE COUNT 134

16. SUPPLEMENTARY NOTATION

17. COSATI CODES			18. SUBJECT TERMS *(Continue on reverse if necessary and identify by block number)*
FIELD	GROUP	SUB-GROUP	SUPERPLASTIC FORMING, ALUMINUM LITHIUM, ADVANCED JOINING, ADVANCED ALUMINUM, AIRFRAMES. (JES)
01	0103	010303	
11	1106	110601	

19. ABSTRACT *(Continue on reverse if necessary and identify by block number)*
This program selects, designs, fabricates, and evaluates SPF Al-Li airframe parts using advanced joining technology; it also screens and evaluates SPF Al-Li alloys for application to candidate parts. Factors used in part selection include supportability, technical risk, and required development. A design trade study modifies and improves the advanced SPF Al-Li candidate parts by implementing efficient design concepts and advanced joining methods. Design and joining methods are evaluated using material from the same lots used for material evaluation. Demonstration parts and the required tooling are fabricated using criteria generated from producibility evaluations. Finally, the demonstration parts are subjected to verification testing as prescribed in the test plan.

20. DISTRIBUTION/AVAILABILITY OF ABSTRACT ☒ UNCLASSIFIED/UNLIMITED ☐ SAME AS RPT. ☐ DTIC USERS	21. ABSTRACT SECURITY CLASSIFICATION UNCLASSIFIED
22a. NAME OF RESPONSIBLE INDIVIDUAL Mr James P. Belloto	22b. TELEPHONE *(Include Area Code)* (513) 255-2582/21	22c. OFFICE SYMBOL AFWAL/FIBCB

DD Form 1473, JUN 86   *Previous editions are obsolete.*

SECURITY CLASSIFICATION OF THIS PAGE

FOREWORD

This interim report documents work performed under contract F33615-C-3223 for the Flight Dynamics Laboratory, Air Force Wright Aeronautical Laboratories, Aeronautical Systems Division, Wright Patterson Air Force Base, Ohio 45433-6553. Mr. Richard L. Rolfes was Air Force program manager from program inception through March 1988. Current program manager is Mr. James Belloto; program inquiries should be directed to him at (513)255-2582.

Mr. Gardner R. Martin is Rockwell program manager and Mrs. Claire Anton is deputy program manager. Mr. Dean Klivans is responsible for the design trade study conducted during Task 1; Mrs. M. A. Ramsey is responsible for technical documentation.

Subcontracting to Rockwell is Lockheed Aeronautical Systems Company who is providing the SPF designs and conducting weight-cost design studies; Messrs. P. S. McAuliffe, J. C. George, M. K. Guess, and H. R. Pearson are Lockheed personnel assigned to the program. Alcoa Laboratories, Dr. C. C. Bampton, principal investigator, is also subcontracting to Rockwell and is conducting a study of post-SPF engineering allowables. Drs. R. A.Grimm and R. M. Rivett are principal investigators for the Edison Welding Institute metal-to-composite investigation. Finally, Washington State University is developing and optimizing a heat treatment for 8091 aluminum-lithium; Dr. C. H. Hamilton is principal investigator supported by Mr. R. D. Tucker.

The Rockwell Science Center is providing support in the areas of material evaluation and selection and detailed evaluation for superplastic forming and joining parameters for aluminum-lithium alloys. Drs. A. K. Ghosh and C. Gandhi are principal investigators.

Period of performance for this interim report is 30 April 1987 (program go-ahead) through 30 April 1988.

Accession For	
NTIS GRA&I	☒
DTIC TAB	☐
Unannounced	☐
Justification	

By	
Distribution/	
Availability Codes	
Dist	Avail and/or Special
A-1	

DTIC COPY INSPECTED

TABLE OF CONTENTS

TABLE OF CONTENTS (Continued)

TABLE OF CONTENTS (Concluded)

LIST OF ILLUSTRATIONS

LIST OF ILLUSTRATIONS (Continued)

LIST OF ILLUSTRATIONS (Continued)

LIST OF ILLUSTRATIONS (Continued)

LIST OF ILLUSTRATIONS (Continued)

LIST OF ILLUSTRATIONS (Concluded)

LIST OF TABLES

1.0 INTRODUCTION

The advent of organic composite materials has motivated a drive in the aluminum industry to offer competitive materials for aerospace structural applications. Aluminum-lithium (Al-Li) alloys, among those materials developed to provide a competitive alternative to composites, offer the aerospace industry an opportunity to dramatically increase the performance and overall efficiency of aluminum airframe structures. The addition of lithium to the alloy decreases the density of the material while increasing the specific modulus and strength of the metal. Other areas which make Al-Li attractive compared with conventional aluminum alloys are the increase in fatigue crack growth resistance and the ability to maintain good strength retention at moderate elevated temperatures (350°F).

Laboratory work indicates that several Al-Li alloys can be processed for superplastic behavior. Superplastic forming (SPF) has emerged as an important manufacturing process for reducing both part cost (decreasing the labor intensity level) and weight (decreasing part and fastener count) in the structure. Superplastic forming allows significant reductions in manufacturing, assembly and tooling costs normally incurred with conventional built-up structures. Innovative joining technologies used in conjunction with SPF structure can significantly reduce the cost of an aircraft and can improve the structural durability and performance by eliminating mechanical fasteners. Other avenues where advanced joining technologies may open up new generations of high performance aluminum structure for integration into Air Force systems are metal-composite bonding or joining.

1.1 OBJECTIVE

The objective of this program is to select, design, fabricate and structurally assess the performance of superplastically-formed aluminum-lithium component(s) representative of near-term advanced airframe structure. Incorporated into this processing technology thrust is the addition of advanced joining techniques including metal-to-metal and metal-to-composite joining. The scope of the program demonstrates the SPF technology relative to aluminum-lithium alloys and critically assesses and, using SPF Al-Li technology, validates the structural integrity of fabricated airframe components.

To achieve the program's overall objective, tasks relative to technical approach and corresponding effort were identified and scoped. Specific areas to be addressed include:

1. Select and subsequently evaluate/characterize Al-Li material for program application

2. Survey an advanced near-term aircraft system to identify suitable structure (components) for SPF conversions

3. Evaluate candidate parts to identify those with the greatest payoffs

4. Select suitable SPF-conversion/demonstration parts and conduct detailed design/trade studies

5. Fabricate test structure including the producibility testing required for part fabrication

6. Develop a suitable environment/loading test envelope and structurally test the selected structure under suitable test conditions

7. Assess the data base developed for material/structure performance

1.2 PROGRAM OVERVIEW

The program is divided into five tasks; these tasks are further divided into subtasks and are as follows:

1.2.1 TASK 1 - PART SELECTION AND DESIGN

Select candidate SPF Al-Li airframe parts for design which includes a design trade study, fabrication, test and evaluation.

1.2.1.1 Candidate Demonstration Parts

From an existing prototype aircraft, select parts which are either primary structure or significantly loaded secondary structure to utilize and maximize the unique payoff advantages of SPF Al-Li and (possibly) advanced joining techniques.

1.2.1.2 Design Trade Study

Conduct a design trade study for the candidate demonstration parts and select a demonstration part(s) which represents the greatest combination of payoff and technology advancement.

1.2.1.3 Detailed Part Design

Considering supportability, generate a complete structural design to meet all requirements of the baseline component on the demonstration part(s). Prepare a comprehensive manufacturing plan for the demonstration part(s).

1.2.2   TASK 2 - MATERIAL EVALUATION AND SELECTION

Initially screen available Al-Li alloys for application to candidate SPF part(s). One of the screened alloys will be selected for more detailed characterization and for fabrication of the demonstration part(s).

1.2.2.1 Candidate Al-Li Alloys

Evaluate only near-term "production" alloys procured from cne of the major aluminum producers.

1.2.2.2 Candidate Alloy Evaluation

Evaluate superplastic, mechanical, and service properties for selection of one alloy for detailed evaluation.

1.2.2.3 Detailed Alloy Evaluation

Evaluate (in detail) the superplastic forming parameters, mechanical properties and service properties of the selected alloy.

1.2.2.4 Superplastic Forming Evaluation

Characterize the optimum superplastic forming parameters, microstructure, strain rate(s), temperature, back pressure, forming limits, and cavitation behavior of the selected alloy.

1.2.2.5 Design Data Generation

Generate preliminary data base of post-SPF and heat-treated mechanical and service properties to determine the affect of superplastic forming on these properties.

1.2.2.6 Heat Treatment Evaluation

Optimize post-SPF mechanical properties through solution heat treatment and artificial aging parameters.

1.2.3 TASK 3 - DESIGN CONCEPT EVALUATION

Verify SPF designs and joining concepts for the demonstration part with material from the same lot that will be used to fabricate the demonstration components.

1.2.3.1 SPF Design Concept Evaluation

Verify the producibility of the SPF demonst..⌐.ion part(s) and the fabrication of subcomponents representative of the severest areas of forming on the SPF demonstration part(s).

1.2.3.2 Joining Concept Evaluation

Develop and optimize the joining concepts defined during the design trade study which is required for the demonstration part(s).

1.2.3.3 Production and Design Data

Verify producibility and bond strength by fabrication of test coupons which simulate the processing conditions of demonstration parts followed by tests (of coupons) to failure.

1.2.4 TASK 4 - DEMONSTRATION PART FABRICATION

Design and machine required tooling to fabricate the demonstration part(s).

1.2.4.1 Tooling Design and Fabrication

Interactively design the demonstration part tooling using the part designs. Following consideration of the producibility test results, the tool design will be modified.

1.2.4.2 Demonstration Part Fabrication

Fabricate the demonstration part(s) according to the manufacturing plan developed under Task 1 - Part Selection and Design.

1.2.5 TASK 5 - DEMONSTRATION PART(S) TESTING AND EVALUATION

1.2.5.1 Test Plan Development

Plan a complete structural test program to validate the static strength, durability, and damage tolerance requirements of the demonstration part(s). Define loading and instrumentation requirements and develop testing requirements; these test requirements will be coordinated with the Air Force.

1.2.5.2 Test Article Fabrication

Fabricate and fit the demonstration part(s) with any load introduction, boundary condition, and other necessary hardware for testing. Install any internal or hidden gauges required for data gathering.

1.2.5.3 Testing

Package and ship demonstration part(s) to WPAFB for testing by Air Force according to the test plan previously developed. Evaluate, interpret, and summarize resultant Air Force test data for inclusion in final report.

1.2.5.4 Final Evaluation

Evaluate cost, weight, performance and structural integrity of the demonstration part(s).

1.3 PROGRAM TEAM ACTIVITIES

A team of subcontractors with a wide range of expertise is being utilized in performance of the contract. The subcontractors and their responsibilities are:

1. Lockheed Aeronautical Systems Company. Lockheed is providing the SPF aircraft designs, participating in the trade studies, and will assist Rockwell in the development of a test plan for the demonstration part(s).

2. Washington State University. Washington State is developing the heat treatment parameters to optimize post SPF strength and toughness.

3. Alcoa Laboratories. The Alcoa Laboratory is performing Task 1.3, Design Data Generation of the Post-formed SPF Material.

4. Edison Welding Institute. Edison is developing a metal-to-composite joining system with 8091 Al-Li and Cypac.

In addition to subcontractor support, Rockwell Science Center is providing material evaluation and selection as well as the detailed alloy evaluation for the superplastic-forming parameters. In addition, they will develop the metal-to-metal advanced joining concepts and techniques.

1.4 SCHEDULE

The program consists of five tasks:

The development effort comprises three tasks: Task 1, Part Selection and Design; Task 2, Material Evaluation and Selection; and Task 3, Design Concept Evaluation.

The fabrication and test effort comprises two tasks: Task 4, Demonstration Part Fabrication and Task 5, Demonstration Part Testing and Evaluation.

The program master schedule is shown in Figure 1-1, it spans 24-months for overall completion of technical work (12 months for the development effort and 12 months for fabrication and test). Both efforts are efficiently planned with concurrent operation of all development tasks and some overlap of the two tasks in the fabrication and test phase.

MAJOR MILESTONES

	1987	1988	1989
	MAY JUN JUL AUG SEP OCT NOV DEC	JAN FEB MAR APR MAY JUN JUL AUG SEP OCT NOV DEC	JAN FEB MAR APR MAY JUN JUL AUG SEP

TASK 1 PART SELECTION & DESIGN
CANDIDATE DEMO PARTS

DESIGN TRADE STUDY

DETAILED PARTS STUDY

TASK 2 MATERIAL EVALUATION & SELECTION
CANDIDATE AL-LI ALLOYS
CANDIDATE ALLOY SCREENING
DETAIL ALLOY EVALUATION
SPF EVALUATION
DESIGN DATA GENERATION
HEAT TREAT EVALUATION

TASK 3 DESIGN CONCEPT EVALUATION
SPF DESIGN CONCEPT EVALUATION
JOINING CONCEPT EVALUATION
METAL-METAL
METAL-COMPOSITE
PRODUCTION & DESIGN DATA

TASK 4 DEMO PART(S) FABRICATION
TOOLING DESIGN & FABRICATION
DEMO PART(S) FABRICATION

TASK 5 DEMO PART(S) TEST & EVALUATION
TEST PLAN DEVELOPMENT
TEST ARTICLE FAB/DEL
TESTING

FINAL EVALUATION

STATUS 30 APRIL 1988

DEL DWGS TO AIR FORCE
FINAL DWGS TO NAAO

START TOOLING
START FAB
FAB COMP

START DEV
START FAB
DEL TEST PLAN TO AF
DEL TEST ARTICLE TO AF

LEGEND
NAAO MILESTONE
ROCKWELL/SCIENCE CENTER MILESTONE
LOCKHEED/CALAC MILESTONE
ALCOA MILESTONE
EDISON WELDING INST MILESTONE
WASH STATE UNIV MILESTONE
AIR FORCE MILESTONE (AFWAL)
INDICATES AN INTERFACE MILESTONE
CHANGE IN LINE FROM PREVIOUS ISSUE
SCHEDULE SLIP

Figure 1.   SPF Aluminum-Lithium Airframe Structure Master Program Schedule

2.0 PROGRAM ACTIVITIES

Technical effort during this reporting period (program go-ahead through 30 April 1988) covered Tasks 1 through 3.

Task 1 activities focused on the acquisition of nine SPF designs from Lockheed. The designs were subjected to an initial qualitative trade study which decreased the number of possible payoff designs.

Task 2 activities included the selection of an Al-Li alloy. The alloy selected was subjected to an intense, detailed evaluation of its superplastic forming parameters and mechanical properties. These activities will continue until the material evaluation is complete. The formed material for the design data generation is available and testing should commence upon completion of heat treatment of the material to optimum mechanical parameters. The heat treatment study provided strengths which are acceptable for aerospace primary structure application.

During Task 3 a metal-composite joining study and an effort to form producibility parts which characterized SPF formability for the material relative to varying amounts of strain were initiated.

2.1 TASK 1 - PART SELECTION AND DESIGN

2.1.1 CANDIDATE DEMONSTRATION PARTS

Generic Advanced Tactical Fighter (ATF) parts which would lend themselves to SPF Al-Li design were selected based on the following criteria: (1) potential for cost saving by reducing piece and fastener count and by reducing or eliminating labor intensive operations (2) potential for an overall weight reduction in the part (3) significant structural loads (4) complex part shapes (5) appropriate part size (6) durability and damage tolerance and (7) reliability and maintainability. The SPF geometries selected were not highly complex (e.g., deep draws or multiple contours) but exhibited sufficient complexity to demonstrate the technology for Al-Li. The candidate parts permit use of current SPF sheet sizes and forming press capabilities.

2.1.2 DESIGN TRADE STUDY

2.1.2.1 Candidate Aluminum-Lithium Parts

Candidate SPF aircraft parts were provided by Lockheed Aeronautical Systems Company from their ATF configurations. These configurations, (Figures 2-1 through 2-15) were selected to represent primary or significantly loaded secondary structure with some degree of difficulty for superplastic forming. The candidate parts were evaluated under both a qualitative design and a detailed design trade study. Following the qualitative design study, three candidate demonstration parts were selected from the list of parts. The
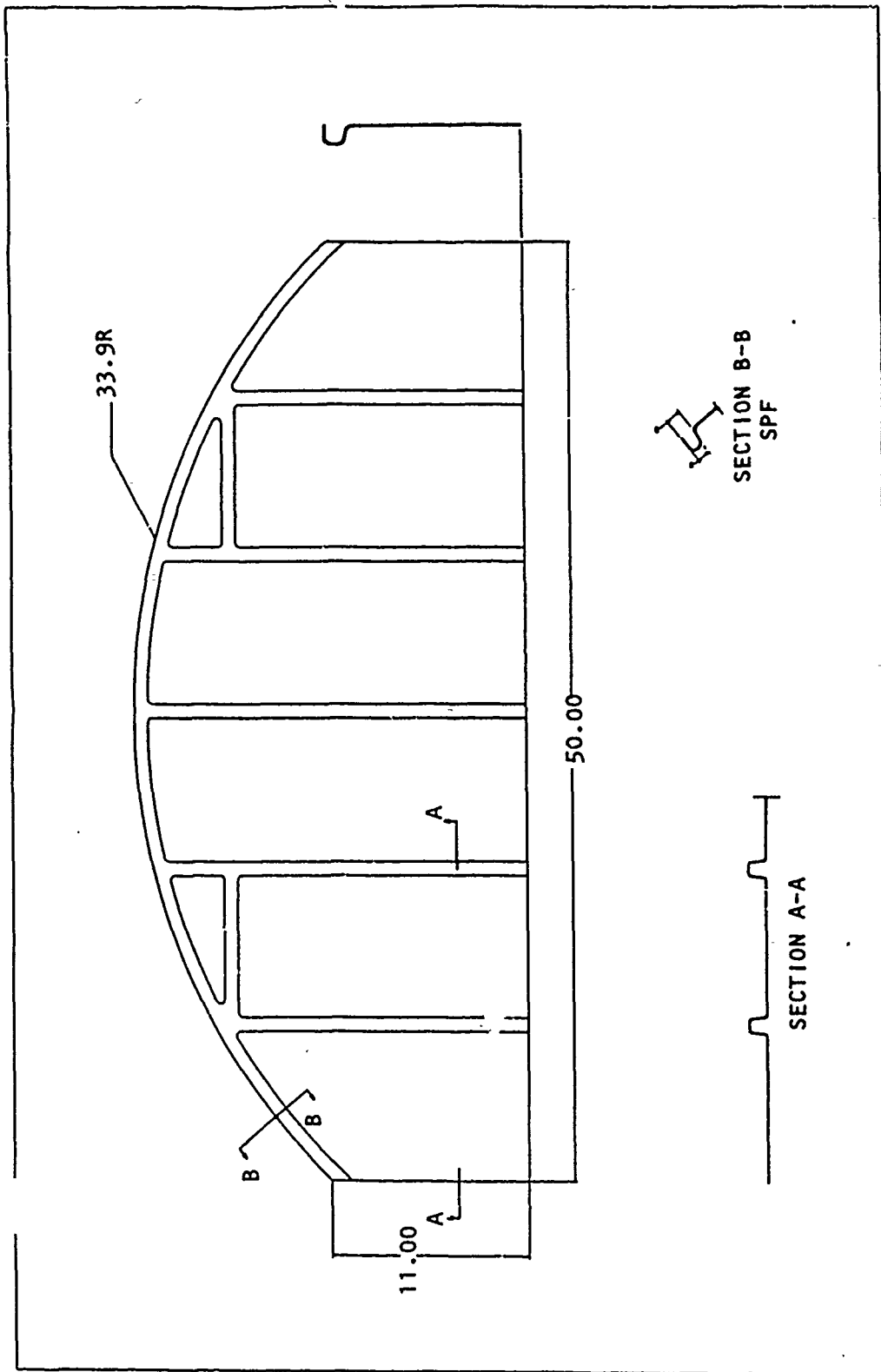
Figure 2-1. Superplastic Forming Concept 1 – ATF Bulkhead Cockpit Foot Support; Provided by Lockheed Aeronautical Systems Company (Formerly Lockheed-California Company)

1.06 TYPICAL

43.24

12.5

16.19

40.00R
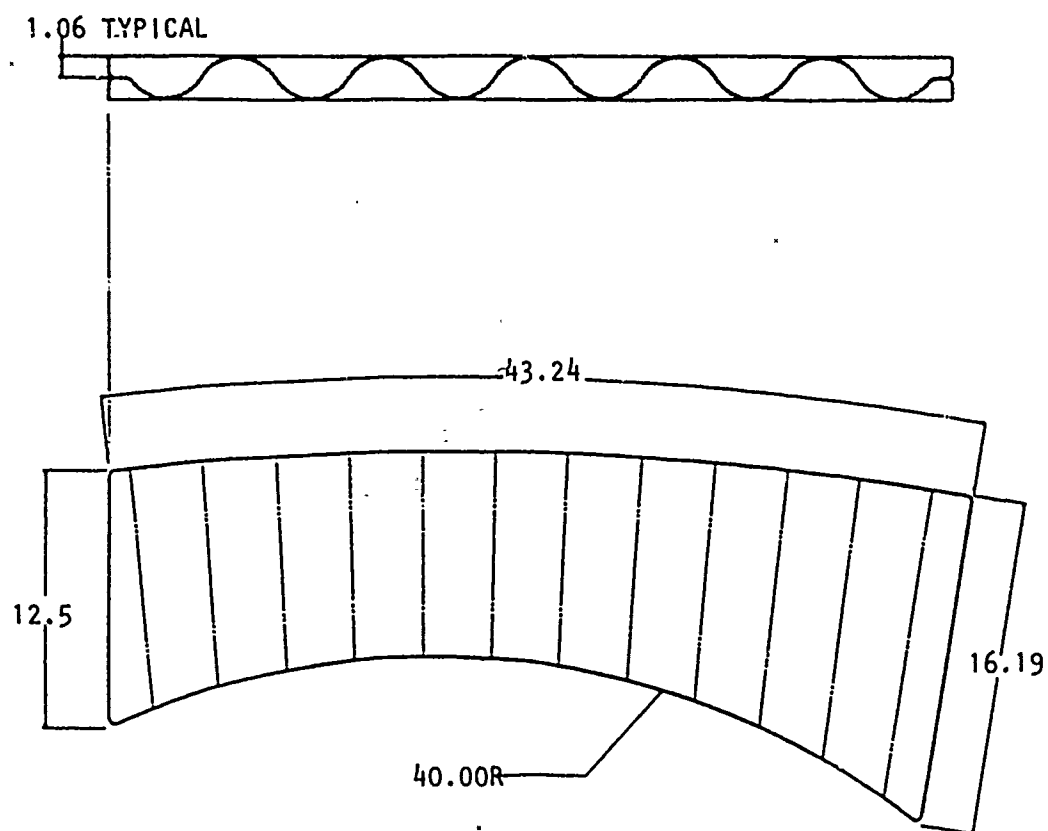
Figure 2-2. Superplastic Forming Concept 2 - ATF Intermediate Fuselage
Upper Frame; Provided by Lockheed Aeronautical Systems
Company (Formerly Lockheed-California Company)
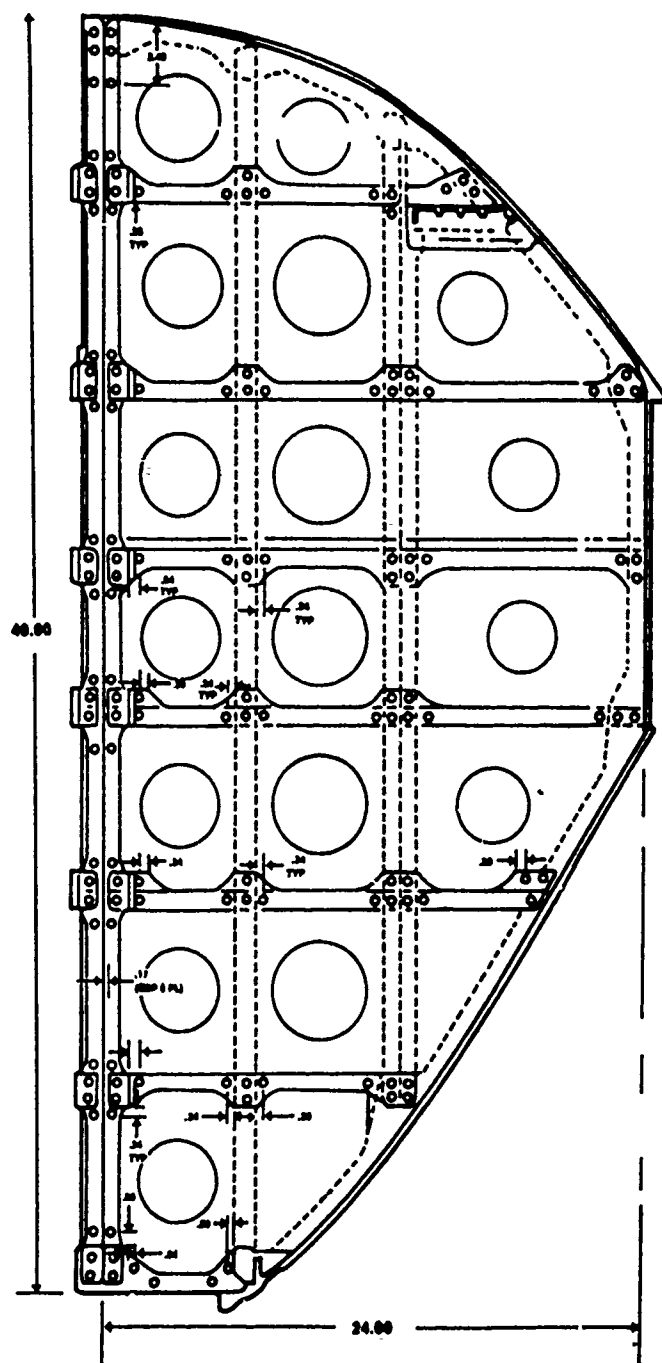
Figure 2-3. Conventional Concept 3 - ATF Bulkhead Forward Fuselage;
Provided by Lockheed Aeronautical Systems Company
(Formerly Lockheed-California Company)
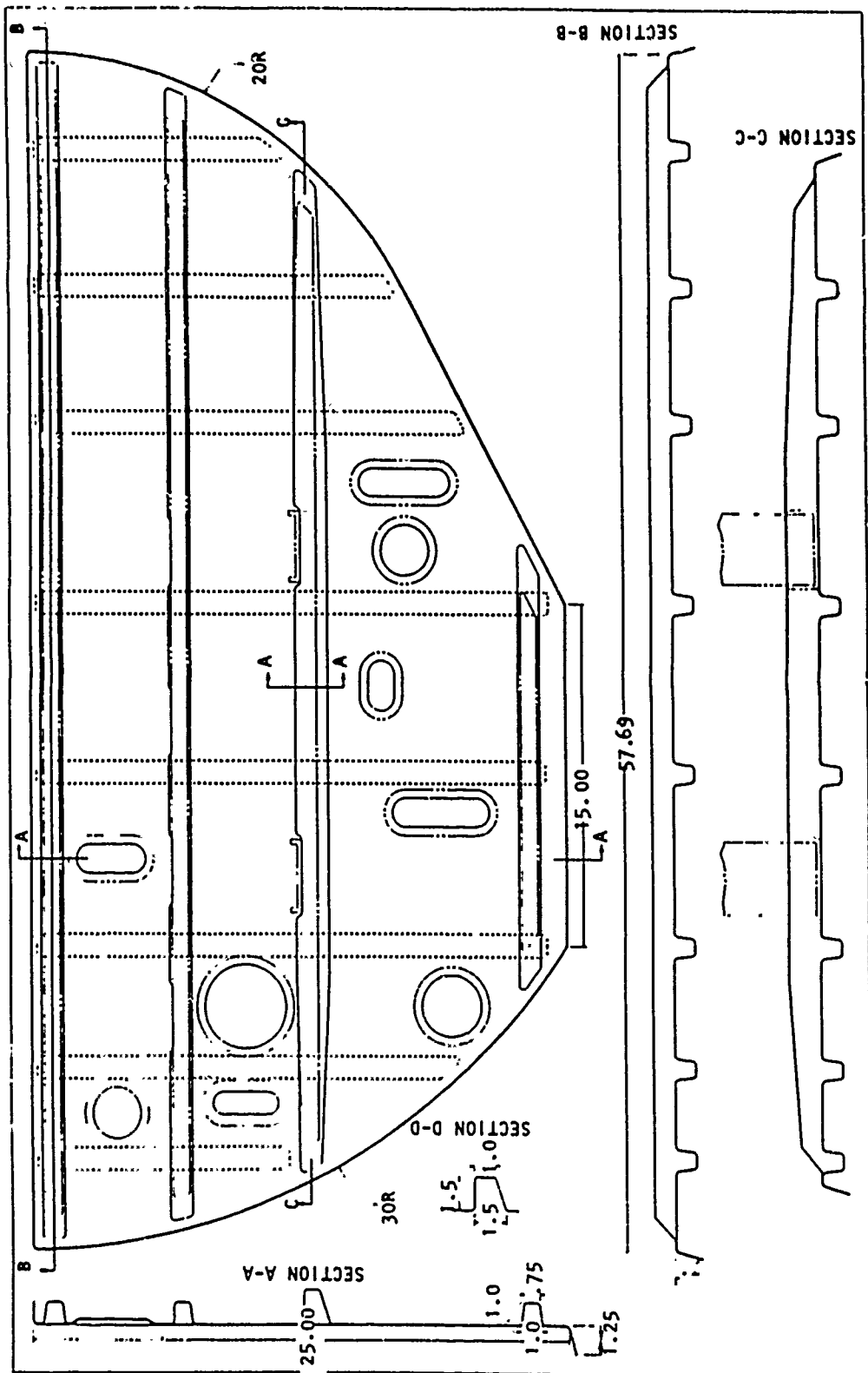
Figure 2-4. Superplastic Forming Concept 3 – ATF Bulkhead Forward Fuselage; Provided by Lockheed Aeronautical Systems Company (Formerly Lockheed-California Company)
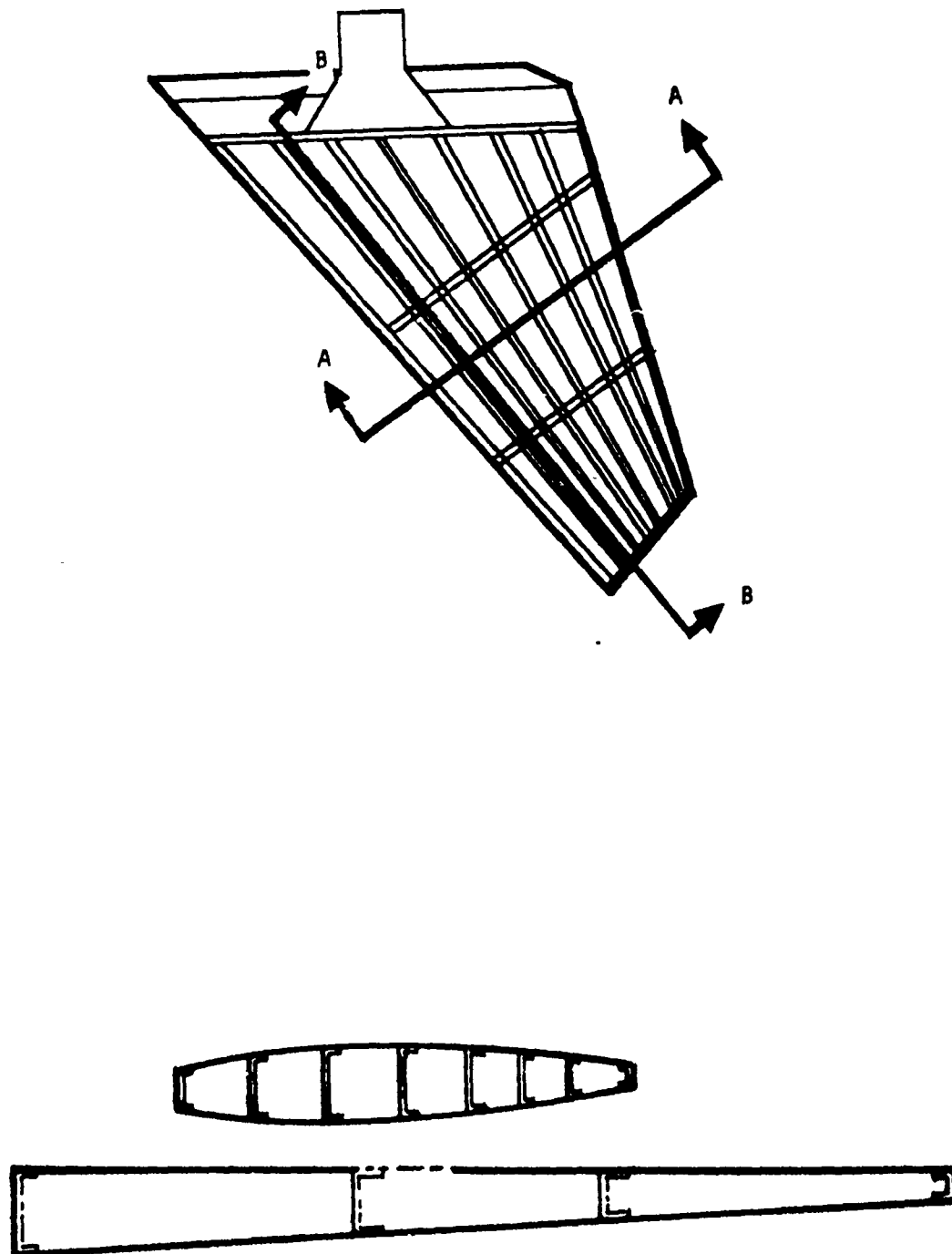
Figure 2-5. Conventional Concept 4 - ATF Vertical Stabilizer; Provided by Lockheed Aeronautical Systems Company (Formerly Lockheed California Company)
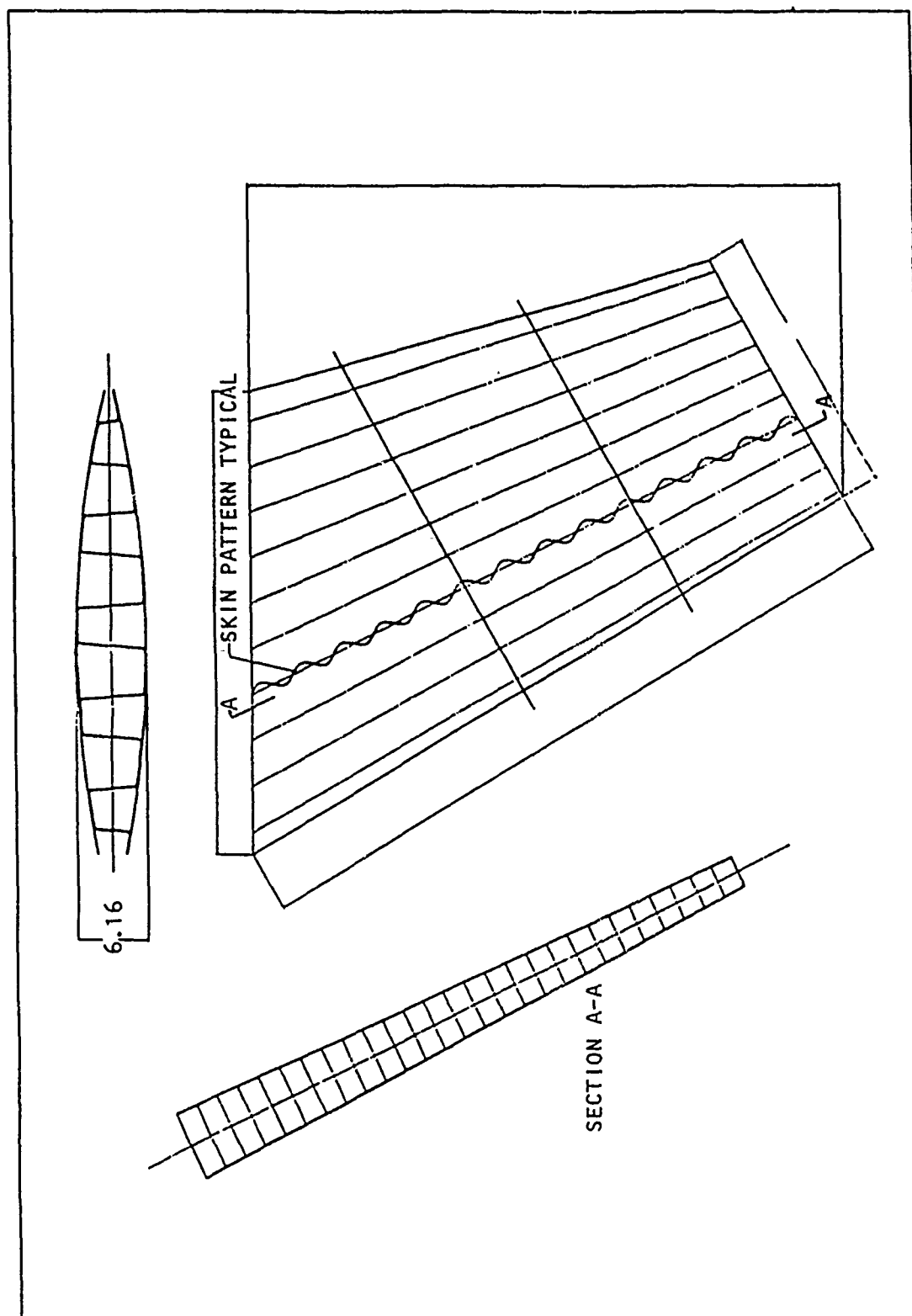
Figure 2-6. Superplastic Forming Concept 4 - ATF Vertical Stabilizer; Provided by Lockheed Aeronautical Systems Company (Formerly Lockheed-California Company)

OUTER FLANGE

FLANGE CURVES
TO SEAL UP
ON THE FUSELAGE
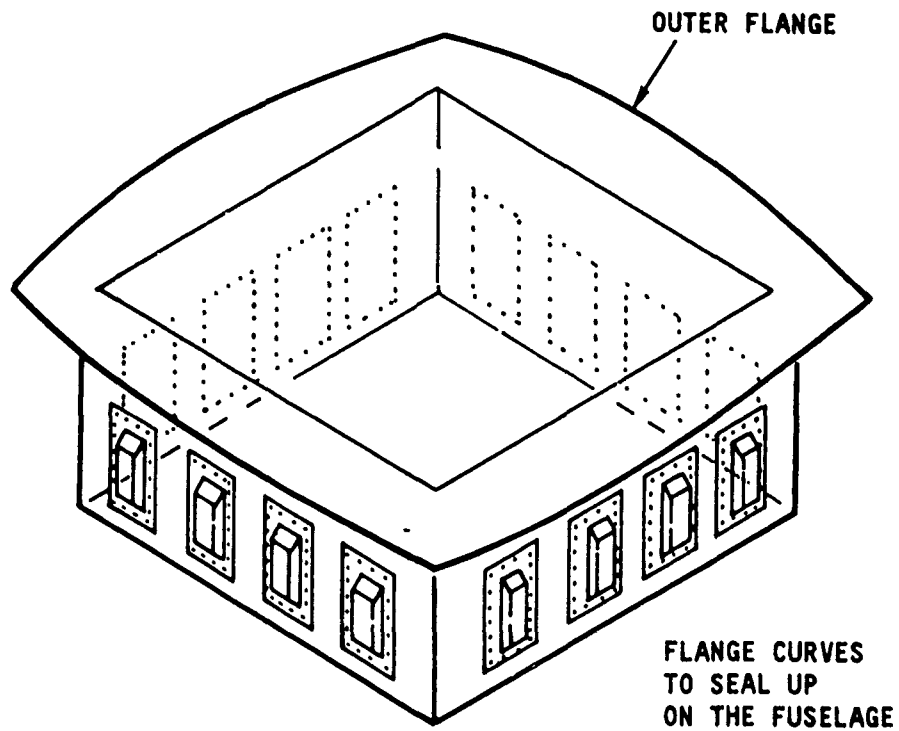
Figure 2-7. Conventional Concept 5 - ATF Antenna Box; Provided by
Lockheed Aeronautical Systems Company (Formerly Lockheed
California Company)
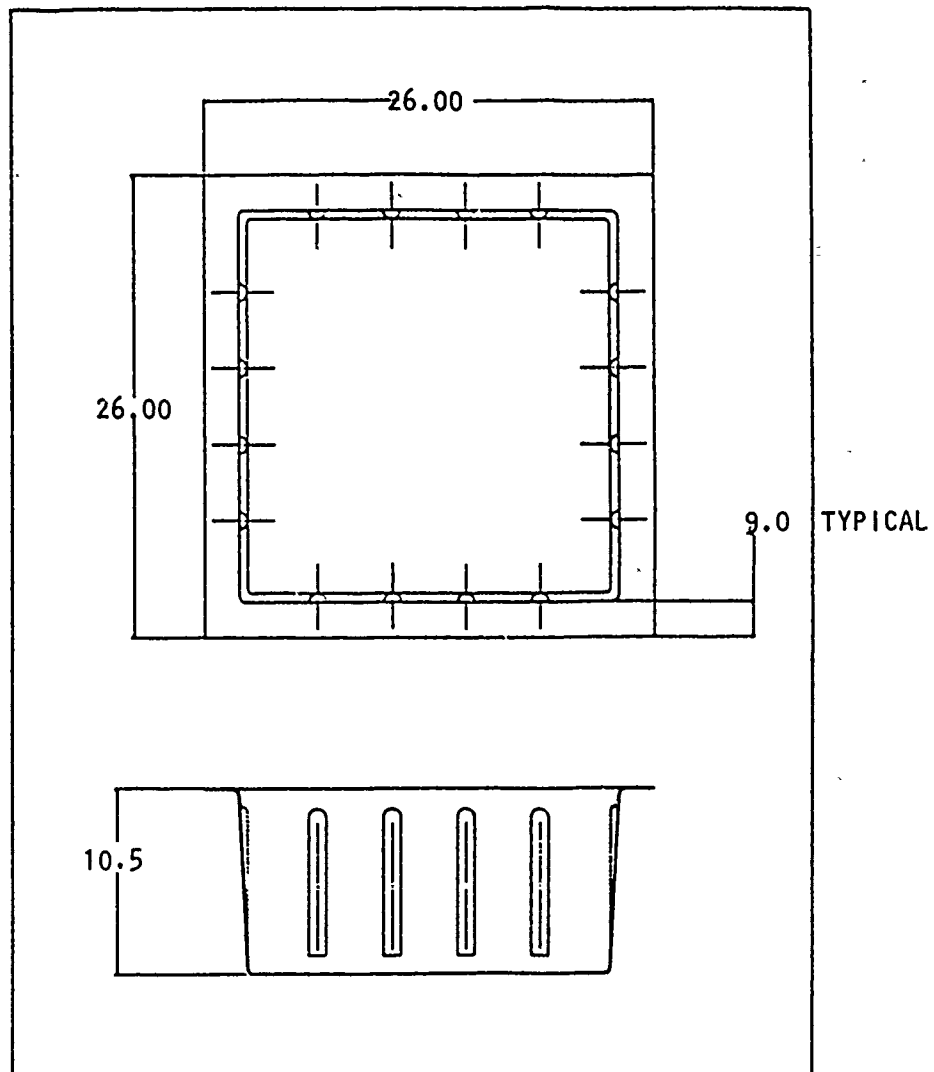
Figure 2-8. Superplastic Forming Concept 5 - ATF Antenna Box; Provided by Lockheed Aeronautical Systems Company (Formerly Lockheed California)
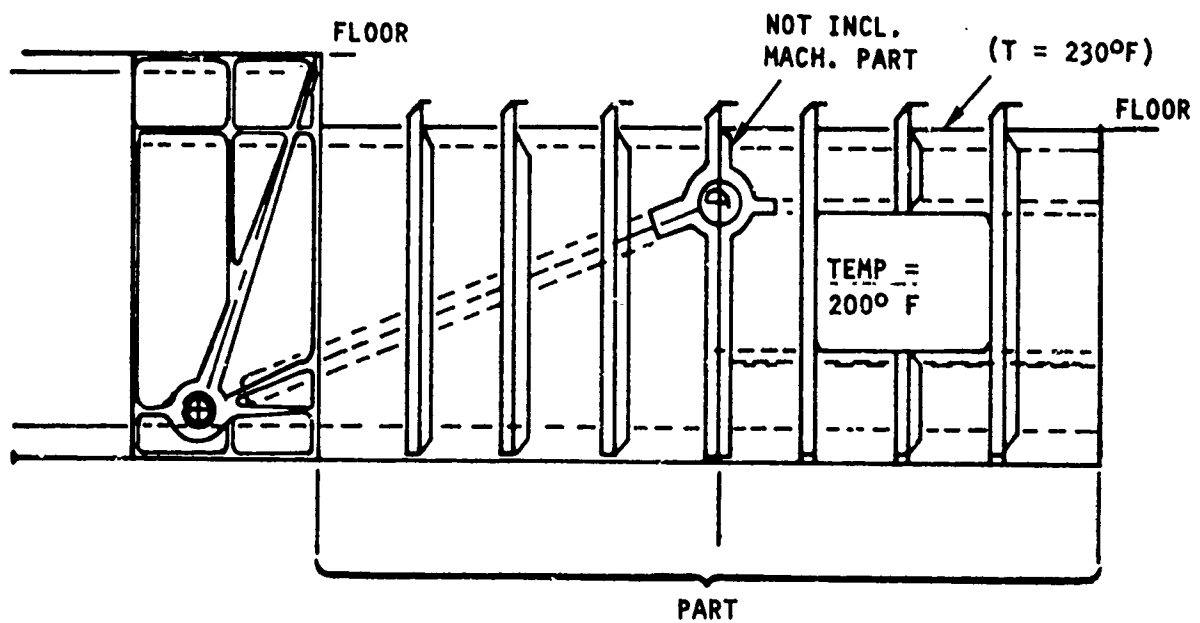
Figure 2-9. Conventional Concept 6 - ATF Nose Wheel Keel Beam; Provided
by Lockheed Aeronautical Systems Company (Formerly Lockheed
California Company)
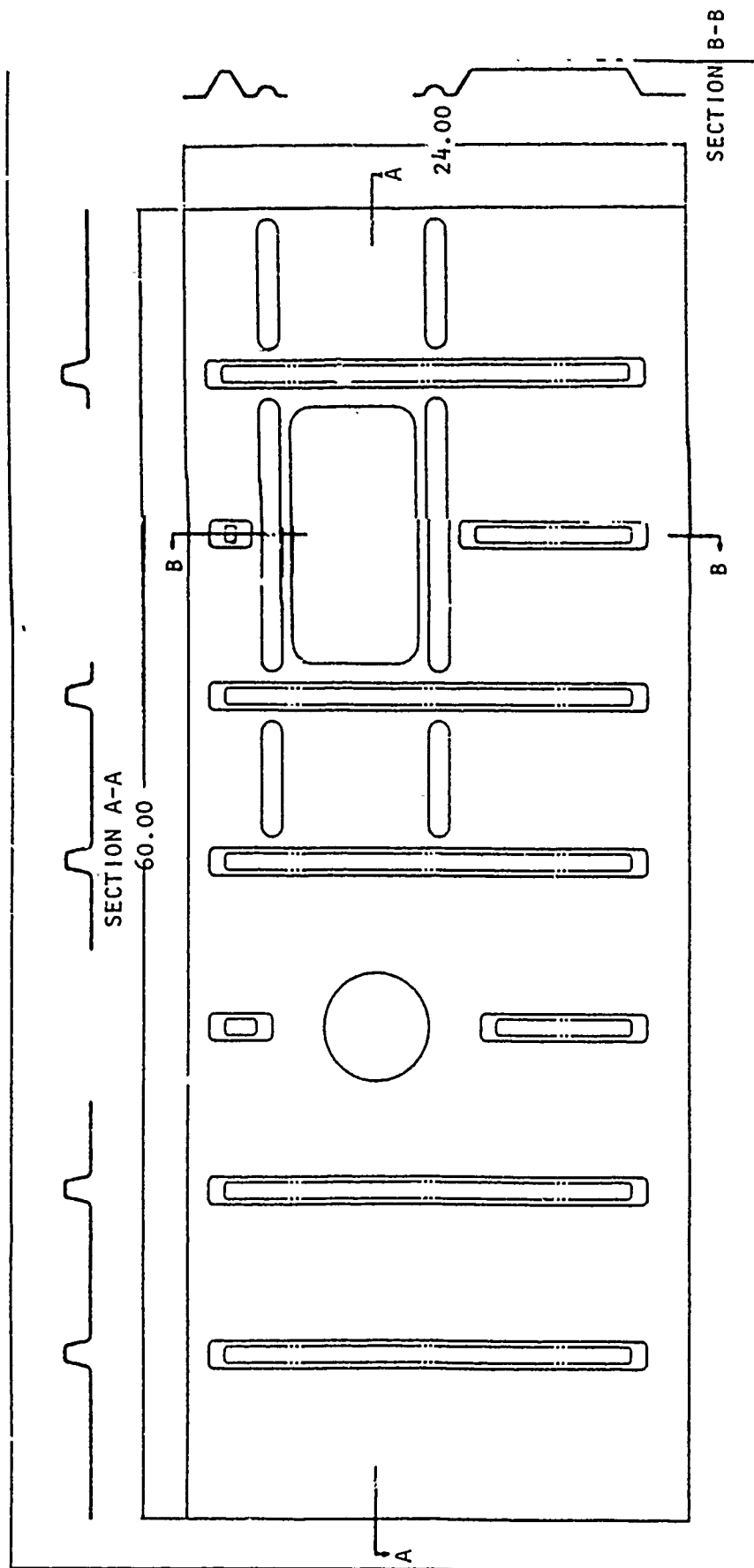
Figure 2-10. Superplastic Forming Concept 6 – ATF Nose Wheel Keel Beam; Provided by Lockheed Aeronautical Systems Company (Formerly Lockheed-California Company)
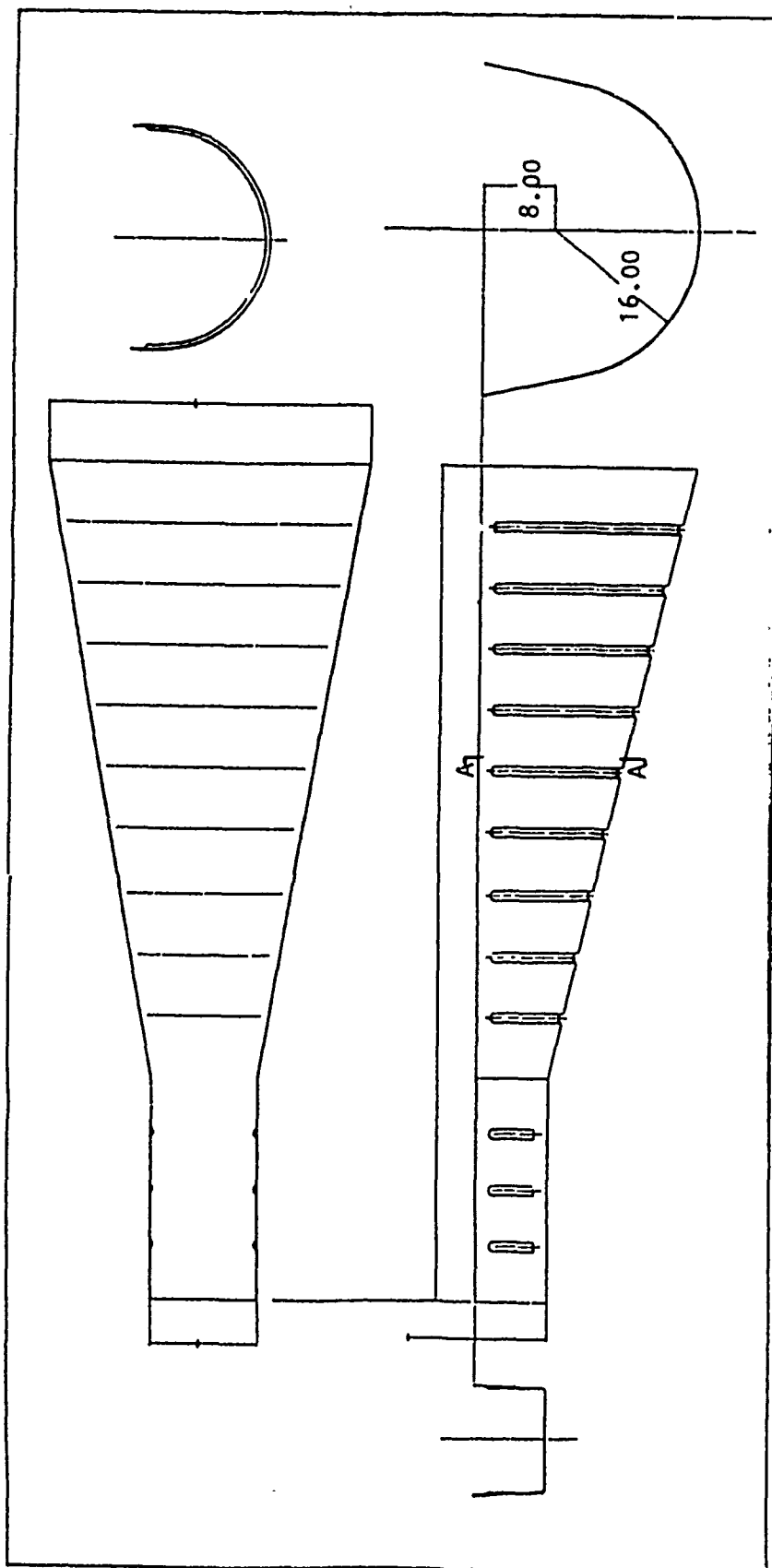
Figure 2-11. Superplastic Forming Concept 7 - ATF Gun Trough; Provided by Lockheed Aeronautical Systems Company (Formerly Lockheed-California Company)
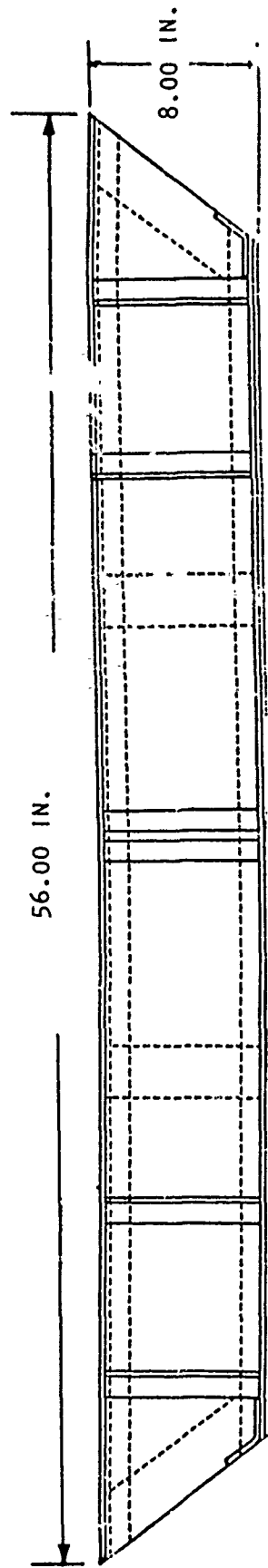
Figure 2-12. Conventional Concept 8 - ATF Floor Support; Provided by Lockheed Aeronautical Systems Company (Formerly Lockheed-California Company)
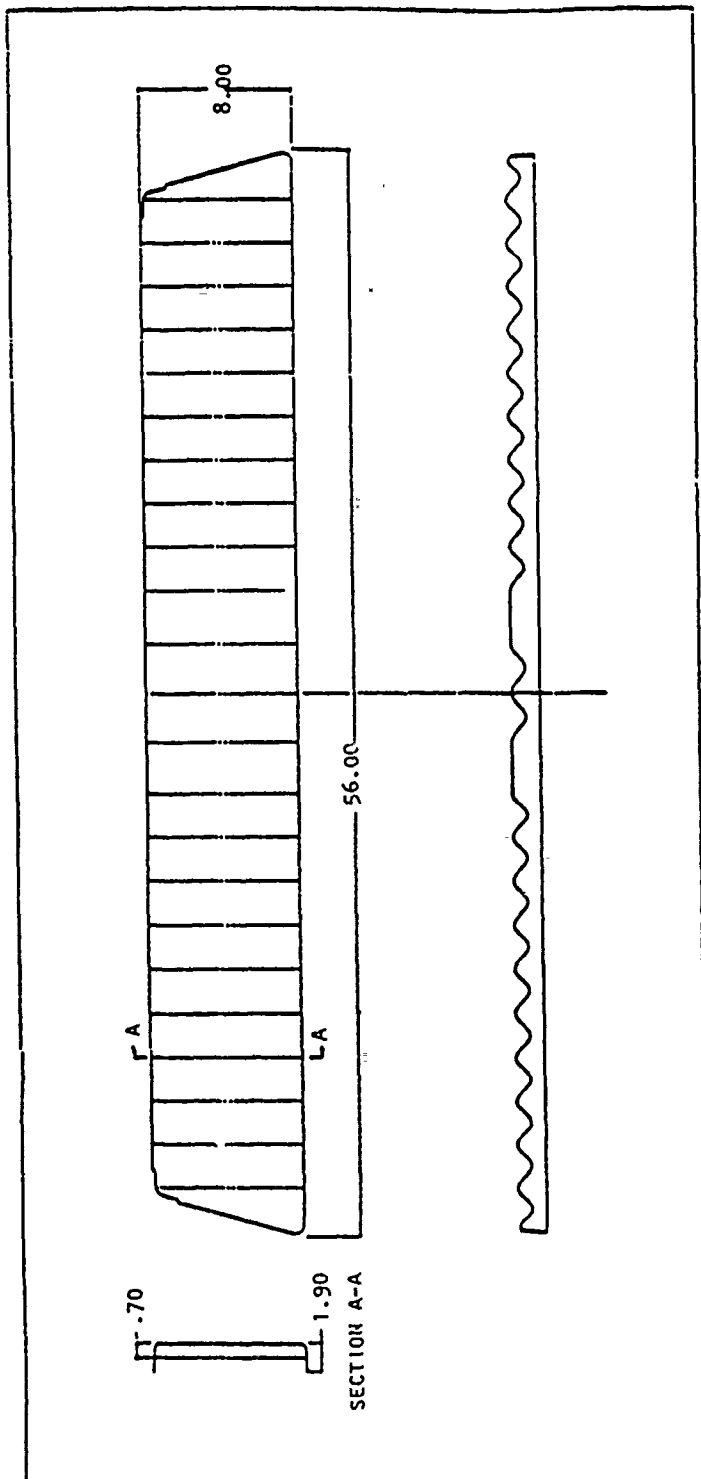
Figure 2-13. Superplastic Forming Concept 8 - ATF Floor Support; Provided by Lockheed Aeronautical Systems Company (Formerly Lockheed-California Company)

24 IN.

FLOOR
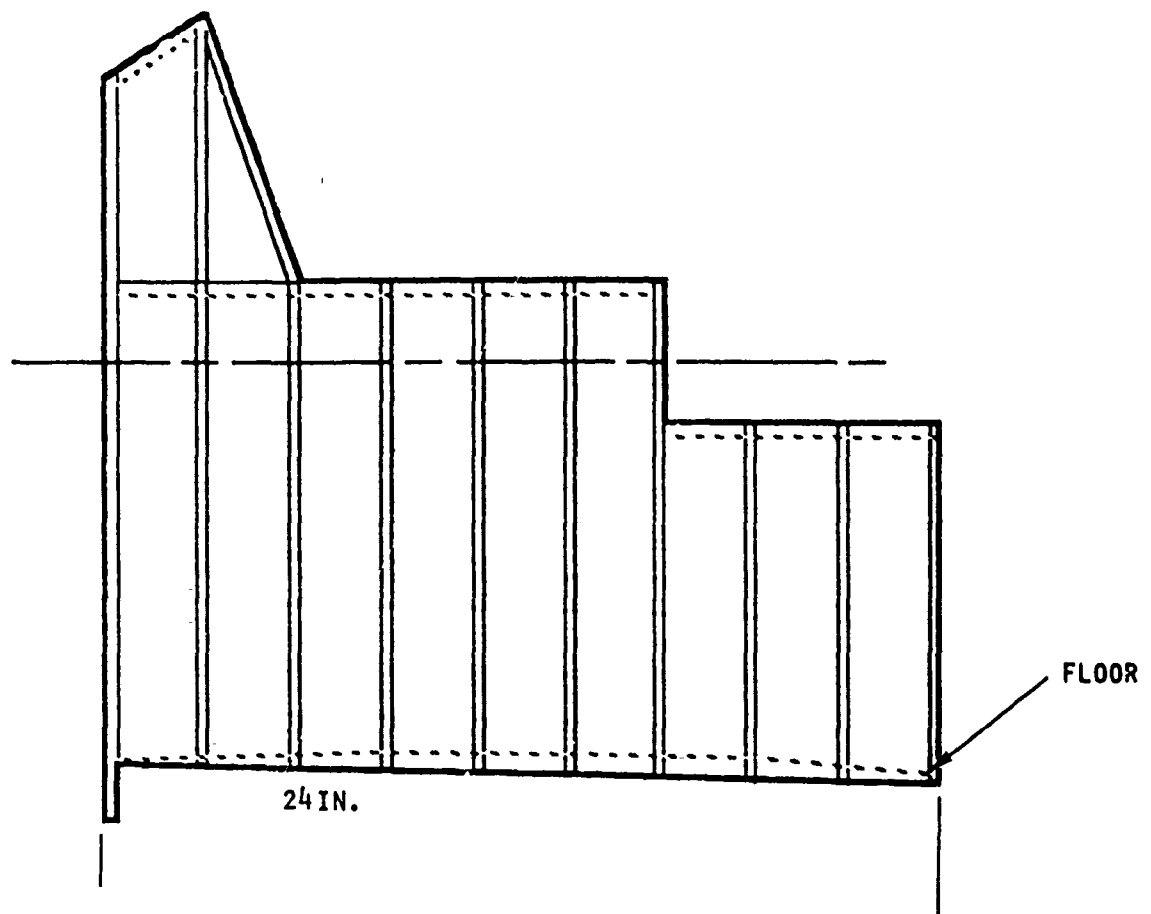
Figure 2-14. Conventional Concept 9 - ATF Center Keelson; Provided by
Lockheed Aeronautical Systems Company (Formerly Lockheed
California Company)
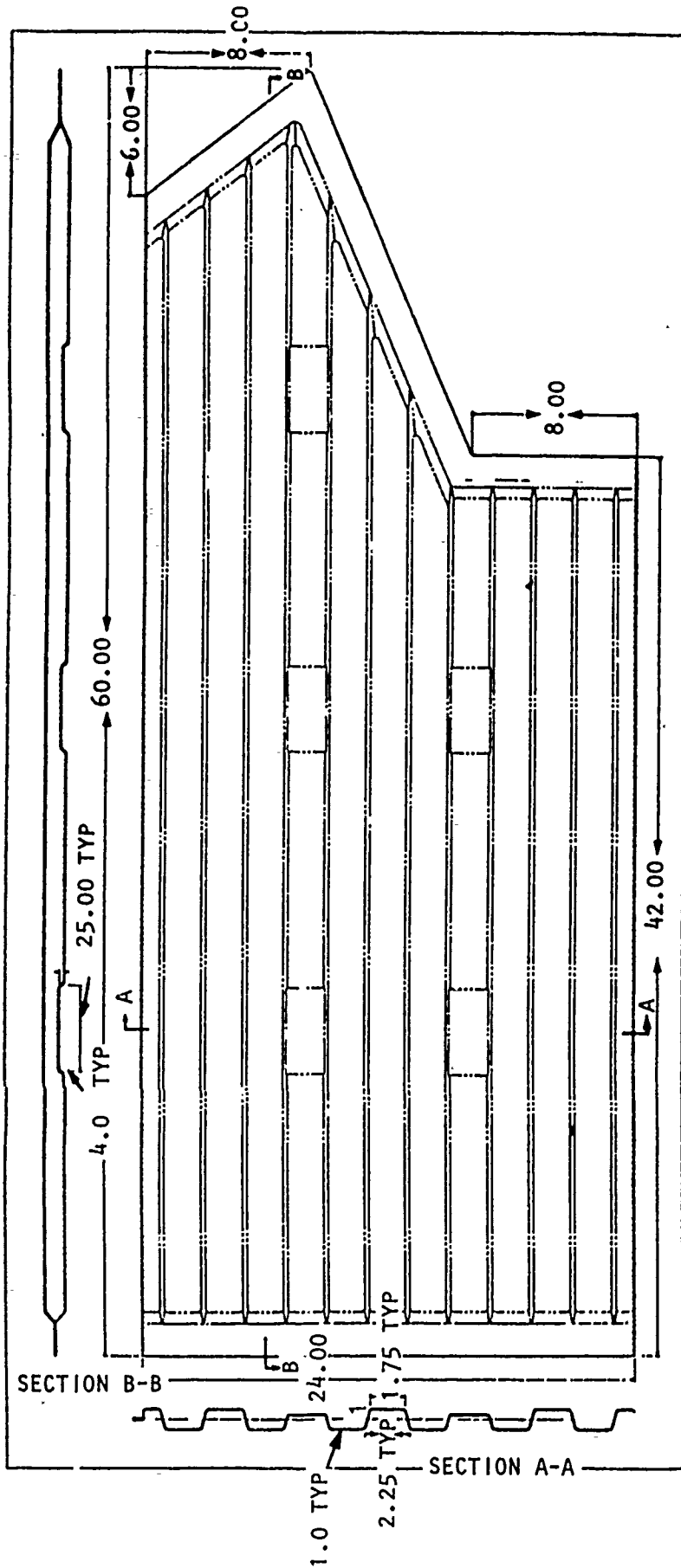
Figure 2-15. Superplastic Forming Concept 9 – ATF Center Keelson; Provided by Lockheed Aeronautical Systems Company (Formerly Lockheed-California Company)

selected parts will have a detailed design trade study conducted for each SPF configuration after which, as a minimum, one part will be selected as the demonstration part for fabrication.

2.1.2.2 Qualitative Design Trade Study

A qualitative trade study using a rating and weighting system was developed. The objective of this system is to sort the relative position of an SPF design relative to comparative conventional designs which perform the same fit and function. This approach uses the part count, manufacturing tasks, fabrication confidence or risk, and several other factors to define the complexity of the design.

The qualitative study included six sections of analysis: part complexity, fastener or spot-weld count, confidence or risk in fabricating the part, inspection method, kind of tooling, and purchase factor of the material. Part complexity is defined part count multiplied labor intensity. Both the part count and labor intensity are weighted factors. The weighting configuration is included as Table 2-1.

An example of part complexity is as follows: A single component (part count = 1) multiplied by a labor intensity of 2 (16 manufacturing steps) creates a complexity of 2. The value of complexity is also assigned a weighting factor appropriate to its importance in the qualitative study. The weighting factor for complexity is defined as 5 (a major cost driver) which drove the complexity to 2 x 5 = 10. The weighting factors for each stage of the study are:

Complexity	= 5	
Fastener count	= 3	
Confidence or risk	= 3	Multiplied by the part
Inspection method	= 5	value or derived value
Tooling	= 3	
Purchase factor	= 1	

The purchase price of the part is the value obtained when all six factors are added together.

The qualitative trade study was conducted by a team of both Lockheed and Rockwell personnel who represented Material and Process Engineering, Cost Estimating, Manufacturing Technology, Design, and Program Management. Each design (both conventional and SPF) was evaluated using the qualitative trade study, and a purchase price was obtained. The purchase price is a relative manufacturing indicator which can be used to compare the conventional design with the SPF concept.

TABLE 2-1

QUALITATIVE TRADE STUDY

Part Count - This value is dependent on the number of components in the subassembly.

1 = Single component part
2 = 2 to 5 component part
3 = 6 to 10 component part
4 = 11 to 15 component part
5 = 16 or more component part

Labor Intensity - This value is dependent on the number of different manufacturing steps required to fabricate the subassembly.

1 = 3 to 15 manufacturing steps
2 = 16 to 30 manufacturing steps
3 = 31 to 50 manufacturing steps
4 = 51 to 70 manufacturing steps
5 = 71 or more manufacturing steps

Manufacturing steps are defined as the number of different stations the part must go through to be completed (i.e., blank sheet, route edges, form, inspect, clean, heat treatment, check and straighten, chemically process, prime and paint, bond, cure, and final inspection). This simulation of a manufacturing process consists of 12 steps which breaks down into a labor intensity of 1.

Part Complexity = (Part count) x (labor intensity)

Fastener Count - (or spot-weld) - This value is dependent upon the number of fasteners used to create the subassembly.

0 = 0 fasteners
1 = 1 to 10 fasteners
2 = 11 to 20 fasteners
3 = 21 to 30 fasteners
4 = 31 to 50 fasteners
5 = 51 or more fasteners (Note: The manufacturing method has switched to automatic fastening at this point.)

Confidence or Risk - This value is strictly subjective. It is determined by the past experience of the contractor in fabricating parts similar to designs for the material being used.

1 = The part being examined is similar to parts that have been production-fabricated with scrap rates less than 10 percent.
2 = The part being examined is similar to parts that have been production-fabricated with scrap rates of 30 to 50 percent.
3 = The part being examined is similar to laboratory demonstration parts of similar size and complexity.

TABLE 2-1

QUALITATIVE TRADE STUDY (Concluded)

---

4 = The part being examined is similar to laboratory parts, but smaller and simpler in design.

5 = The part being evaluated is feasible, but the contractor has no experience in making this part.

Inspection Method - The values depend on the labor intensity and overall cost of the inspection method being examined.

1 = Production proven methods can be used, i.e., visual, dimensional drilling, fastener installation, configuration and identification.

2 = Production proven methods (high skill radiographic or ultrasonic tests)

3 = Limited experience methods (in production elsewhere)

4 = Limited experience methods II (experimental)

5 = No experience

Tooling - The weighting values depend upon the complexity of the required tooling and its normality.

1 = No special tooling is required

2 = No special tooling except drill jigs assembly jig, etc.

3 = Special tooling similar to that used with other production parts

4 = Special tooling similar to that used with smaller and simpler parts.

5 = Special tooling feasible but no history

Purchase Factor - This value is dependent upon the comparable material cost for the part with 7075 aluminum along with its scrap and mortality.

$$Fq: = \frac{\text{Total Material Cost}}{\text{Cost for same amount of 7075 aluminum}} + \text{Scrap} + \text{Mortality}$$

DEFINITION: Weighting Factor - These weighting factors apply to the overall weighting for each phase in the analysis.

1 = Little effect on cost

2 = Moderately low cost driver

3 = Moderate cost driver

4 = Moderately high cost driver

5 = Major cost driver

The results of the qualitative study are summarized in Figure 2-16. Four SPF configurations appeared to trade favorably with their conventional counterparts. The designs and results were transmitted to Wright-Patterson AFB for review and approval by the Air Force. Rockwell and the Air Force concurred on the selection of the three components for the next step in the design trade study; the components are the floor support beam, the forward fuselage bulkhead, and the Keelson shear panel.

2.1.3 DETAILED PART STUDY

The detailed design trade study and analysis have been initiated. Lockheed is currently developing the cost/weight data base for the three structural concepts to support the analysis. In addition, Lockheed is developing appropriate component load boundary conditions and load application concepts to support structural testing of the candidate component(s).

2.2 TASK 2 - MATERIAL EVALUATION AND SELECTION

An initial screening of available Al-Li alloys for application to the candidate parts is discussed in the following paragraphs. One of the screened alloys was recommended to the Air Force project engineer for approval after which detailed characterization of the alloy will form a data base for fabrication of the demonstration parts. This effort was a major in-house effort both of Rockwell Science Center and North American Aircraft.

2.2.1 CANDIDATE AL-LI ALLOYS

Candidate Al-Li alloys that were considered for this program are near-term "production" alloys from major aluminum producers. No experimental or laboratory-scale alloys were considered. Particular attention was given to those alloys that were capable of heat treatment to required strengths, durability (corrosion and fatigue resistance), and fracture toughness from the as-superplastically formed condition (without stretch) to satisfy the requirements identified in Task 1. Other essential requirements for the alloy were high values of superplastic ductility, which were reasonably isotropic relative to the sheet-rolling direction and where intergranular cavitation could be controlled with back pressure to prevent the dependance of design on the level of superplastic strain. The final evaluation criteria related to product availability and cost. It was imperative that the alloy be available for immediate procurement in a quantity up to approximately 500 pounds.

WEIGHTING FACTOR								5
COMPONENT CONFIGURATION				LABOR PART COUNT	X	INTENSITY	=	COMP
① BULKHEAD COCKPIT FOOT SUPPORT	Al-Li	CONV	SHEET METAL & LIGHT EXTRUSION	9	3	13	1	3
	Al-Li	SPF		1	1	12	1	1
② INTERM FUSELAGE UPPER FRAME	7075		MACHINED SOLID BILLET	1	1	19	2	2
	Al-Li	SPF	2-PIECE ADHESIVE BONDED STRUCTURE	2	2	13	1	2
	Al-Li	SPF	1-PIECE ROLL BONDED SHEET	1	1	18	2	2
	Al-Li	SPF	1-PIECE DIFFUSION BONDED SHEET	1	1	14	1	1
③ BULKHEAD FORWARD FUSELAGE	Al-Li	CONV	SHEET METAL & LIGHT EXTRUSION	16	5	18	2	10
	Al-Li	SPF	2-PIECE ADHESIVE BONDED SHEET	2	2	13	1	2
	Al-Li	SPF	1-PIECE ROLL BONDED SHEET	1	1	18	2	2
	Al-Li	SPF	1-PIECE DIFFUSION BONDED SHEET	1	1	14	1	1
④ VERTICAL STABILIZER	7075	CONV	SHEET METAL & LIGHT EXTRUSION	24	5	13	1	5
	Al-Li	SPF	SHEET	5	2	13	1	2
⑤ ANTENNA BOX	6061	CONV	SHEET METAL & LIGHT EXTRUSION	17	5	23	2	10
	Al-Li	SPF	1-PIECE SHEET	1	1	15	1	1
⑥ NOSE WHEEL KEEL BEAM	7075	CONV	SHEET METAL & LIGHT EXTRUSION	10	3	9	1	3
	Al-Li	SPF	2-SHEET DIFFUSION BONDED	2	2	15	1	2
	Al-Li	SPF	1-SHEET CONTINUOUS BEADS	r	1	14	1	1
⑦ GUN TROUGH	6061	CONV	SHEET METAL & LIGHT EXTRUSION	11	5	13	1	5
	Al-Li	SPF	SPF-SHEET + HYDROFORMED SHEET	2	2	25	2	4
⑧ FLOOR SUPPORT	Al-Li	CONV	BUILDUP SHEET METAL & EXTRUSION	10	3	16	2	6
	Al-Li	SPF	SHEET	1	1	15	1	1
⑨ CENTER KEELSON	7075	CONV	BUILTUP SHEET & EXTRUSION	6	3	9	1	3
	6061	SPF	SHEET	1	1	10	1	1

NOTES: 1. SHADED NUMBER IS MULTIPLIED BY ITS WEIGHTING FACTOR TO RESULT IN ITS WEIGHTED VALUE.
2. PURCHASE PRICE IS TOTAL OF ALL WEIGHTED VALUES FOR THE SELECTED FABRICATION METHOD.

Figure 2-16. Matr

5		3		3		5		3		1			
COMPLEXITY		FASTENER COUNT		CONFIDENCE/ RISK		INSPECTION		TOOLING		PURCHASE FACTOR		PURCHASE PRICE	
3	15	SPOT WELD 5	15	1	3	1	5	3	9	6	6	53	
1	5	0	0	4	12	1.5	7.5	4	12	4	4	40.5	
2	10	0	0	1	3	1	5	1	3	20	20	41	
2	10	0	0	3	9	2	10	3	9	4	4	42	
2	10	0	0	5	15	2	10	3	9	4	4	48	
1	5	0	0	4	12	2	10	3	9	4	4	40	
10	50	5	15	1	3	1	5	3	9	6	6	88	POSSIBLE PAYOFFS
2	10	0	0	3	9	2	10	3	9	4	4	42	
2	10	0	0	5	15	2	10	3	9	4	4	48	
1	5	0	0	4	12	2	10	3	9	4	4	40	
5	25	5	15	1	3	1	5	3	9	4	4	61	
2	10	5	15	4	12	1.5	7.5	5	15	4	4	63.5	
10	50	5	15	1	3	1	5	3	9	2	2	84	POSSIBLE PAYOFFS
1	53	0	0	5	15	1.5	7.5	4	12	4	4	43.5	
3	15	5	15	1	3	1	5	2	6	2	2	46	
2	10	0	0	4	12	2	10	3	9	4	4	45	
1	5	0	0	3	9	1.5	7.5	3	9	4	4	34.5	
5	25	SPOT WELD 5	15	1	3	2	10	3	9	4	4	66	
4	20		0	5	15	2	10	3	9	4	4	58	
6	30	5	15	1	3	1	5	2	6	6	6	65	POSSIBLE PAYOFFS
1	5	0	0	5	15	1.5	7.5	3	9	4	4	40.5	
3	15	5	15	1	3	1	5	2	6	2	2	46	POSSIBLE PAYOFFS
1	5	0	0	3	9	1.5	7.5	3	9	4	4	34.5	

Matrix of Weighting Factors for Candidate ATF Component Configurations

2 of 2

2.2.2 CANDIDATE ALLOY SCREENING

This subtask was carried out by the Rockwell Science Center. Previous work had narrowed down the selection of the best alloy for program application. Five criteria were used for the selection process:

1. The alloy must be in "production-ready" or "near production-ready" condition.

2. The alloy in the superplastic condition, should not exhibit flow stress levels much greater than 500 psi since this leads to greater difficulty in suppressing cavitation.

3. With a superimposed hydrostatic pressure of approximately 400-500 psi, the alloy should exhibit an elongation of at least 800-900 percent over a 0.5-inch gauge length. A material exhibiting elongations of this magnitude is capable of distributing strain in the part to maintain good thinning uniformity. Although in most production parts, such high strains are not actually realized, the tensile elongation value serves as an important indirect yardstick which combines strain uniformity, cavitation tendency, and an overall superplastic forming performance. Excessive nonuniformity in the thickness distribution and associated cavitation could be a structural problem source in a part which visually appears to be sound.

4. Cavitation should be completely suppressible up to true strains of at least 1.5 using a superimposed hydrostatic pressure of 400-500 psi.

5. The alloy should be heat-treatable so that the post-formed strength by thermal aging alone (no stretching is possible in superplastic formed parts) would be approximately 50,000 psi.

Almost all I/M Al-Li alloys responded well to SPF processing using the overaging practice. The overaging practice was implemented at Alcan plants in England (and was readily usable by Alcoa and Reynolds), thus reducing the thermomechanical processing issue from a critical one in terms of determining the alloy selection process. All alloys studied in the as-rolled condition exhibited dynamic recrystallization and high elongations. To provide isotropy of superplastic as well as room-temperature properties, the alloy was procured in cross-rolled condition.

Based on results obtained in 1986-1987 (refer to Table 2-2) and considering all criteria previously discussed, Alcan 8091-SP and Alcoa 2090-SP are the best candidate alloys for the screening. The Reynold's alloys are not

TABLE 2-2

SUPERPLASTIC ELONGATION IN Al-Li ALLOYS

Alloy Designation	Temp/Press. ($^\circ$F/psi)	Superplastic Test (S^{-1})	Elongation (%)	Room Temperature Test*		
				Yield Strength (ksi)	UTS (ksi)	Elongation (%)
8090-T3	950/400	10^{-3}/ 2×10^{-4}	1040(L) 560(T)	45.6	60.5	5.5
8090-SP	950/400	10^{-3}/ 2×10^{-4}	934(L) 309(T)	42.3	49.8	3.5
8091-CP	950/600	5×10^{-4}/ 2×10^{-4}	1450(L)			
8091-K	950/600	10^{-3}/ 2×10^{-4}	1275			
8091-SP	950/400	10^{-3}/ 2×10^{-4}	1015(L)	49.4	64.7	5.5
8091-2C	950/600	2×10^{-3}/ 2×10^{-4}	963(L)	40.0	48.7	7.6
2090-R1	950/600	2×10^{-3}/ 2×10^{-4}	1065(L)	39.5	48.5	5.4
2090-SP	950/600	2×10^{-3}/ 2×10^{-4}	980(L)	44.4	54.2	4.3
2090-R2	950/600	10^{-3}/ 2×10^{-4}	345(A)			
8090-R6	950/600	10^{-3}/ 2×10^{-4}	278 359			
2090-R8	950/600	10^{-3}/ 2×10^{-4}	996(C)			
2090-R27	950/600	10^{-3}/ 2×10^{-4}	680(L)			
8090-R96	950/600	10^{-3}/ 2×10^{-4}	598(L)			

Available in 48-inch wide production-grade material to support the program. Although some Reynolds Laboratory superpure base alloys exhibited good superplasticity, they suffered from two major problems: 1) if scaled-up, the cost could be very high and 2) since they were of the 2090 composition, their post-formed strength would be low. This last problem also eliminated Alcoa's 2090-SP alloy. The 8091 Al-Li alloy was selected for this program because of its high strength at room temperature, low flow stress at the superplastic temperature, and its availability as a fine-grain sheet material from the manufacturer. All data related to alloy screening were in place prior to contract award and at the start of the program Rockwell recommended 8091-SP to the Air Force project engineer. Rockwell procured large amounts of this alloy (in several gauges) from Alcan International.

2.2.3 DETAILED ALLOY EVALUATION

2.2.3.1 Superplastic Forming Evaluation of 8091 Al-Li Alloy

Thermomechanically processed 8091 alloy in the as-rolled condition was supplied in three gauge thicknesses (0.060, 0.090 and 0.125 inch). The microstructural evaluation of the alloy indicates that the as-received material was cross-rolled and in the unrecrystallized condition. The grain sizes of the as-received alloy were measured from optical micrographs of the solution-treated materials (950°F for 1 hour and aged at 374°F for 3 hours). Figure 2-17 is a representative micrograph. A number of undissolved precipitates (2-6 μm) were present in this alloy after 1 hour of solution treatment at 950°F. A solution treatment for 2-5 hours at 1022°F or above can dissolve all of these precipitates; however, slight grain growth was observed at this (1022°F) solution temperature (Figure 2-18). Earlier studies indicated that these undissolved precipitates at 1022 and 986°F did not cause any deterioration in the superplastic formability of the alloy. In addition, any prior solution treatment was found to be detrimental to the superplastic formability of these alloys. For these reasons, the as- received materials were directly tested for superplasticity without any other thermal treatments.

Superplastic tensile tests were performed in 0.5-inch gauge length samples with an Instron testing machine at constant strain rates. The samples were heated in a 5-zone split furnace with independent proportional temperature controllers. The uniform temperature zone extended over 10 inches. The tensile tests were performed in air as well as under back pressure. The back pressure was produced with a high-pressure retort which could be operated up to a maximum back pressure of 800 psi. Typically, back-pressure levels of 200, 400, and 600 psi were used in the tests. The strain-rate sensitivity (m) of the alloy was also evaluated by stepped strain

GRAIN SIZE: 7.2 μm x 4.4 μm
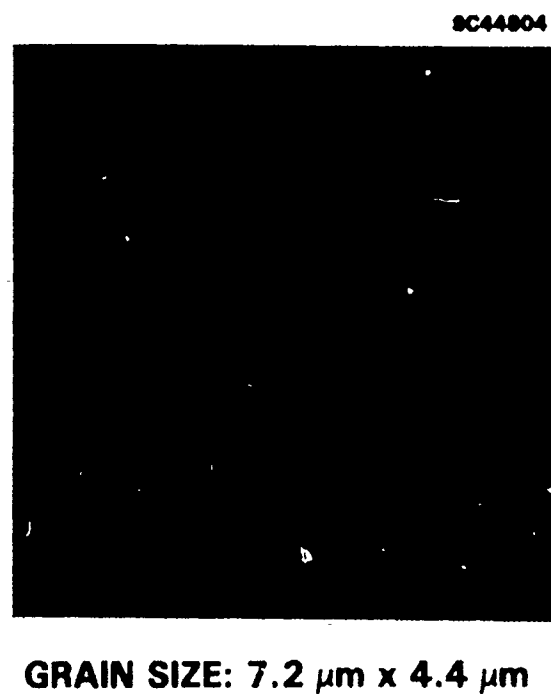
Figure 2-17. Microstructure of 8091 Al-Li
(950°F, 1 Hour)
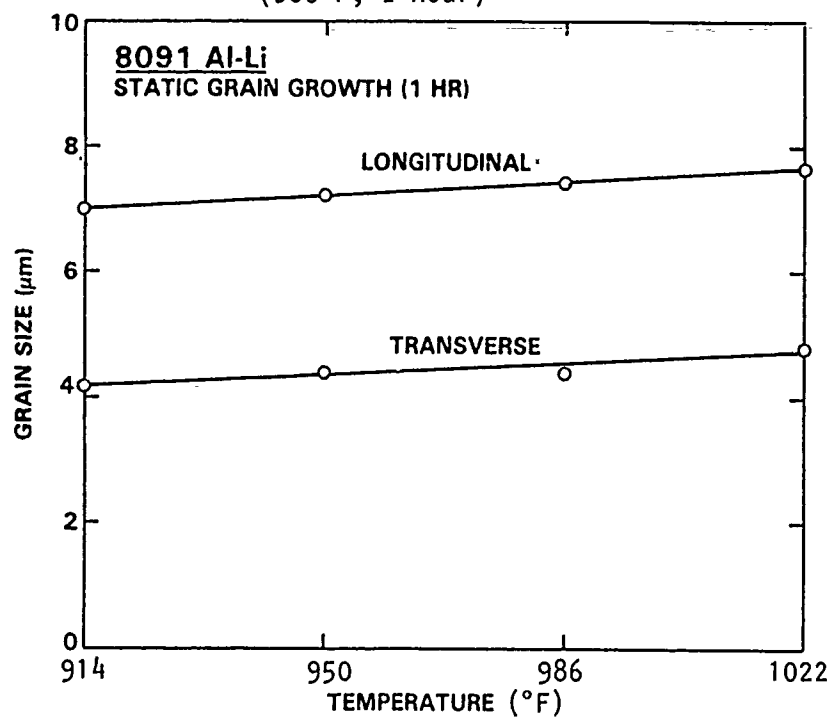
Figure 2-18. Static Grain Growth in 8091 Al-Li

rate tests in which the strain rate was increased periodically on a rising stress-strain curve. A few tests were performed to evaluate the effect of superplastic strain on strain-rate sensitivity. Strain rate sensitivity testing uses small changes in the strain rate (40 percent above the constant strain rate) several times during a constant strain-rate tensile test. The results from the strain-rate sensitivity tests are discussed in Subsection 2.2.3.1.7.

Previous research work on 8091 Al-Li alloy showed that superplastic elongations were higher in two-stage strain-rate tests than in single strain-rate tests. In two-stage strain-rate tests, the tensile sample is first deformed at a higher strain rate ($\dot{\epsilon}$ 1) to a predetermined strain level, then the strain rate is decreased by a decade ($\dot{\epsilon}$ 2), and the test is continued to failure of the sample. Some advantages of two strain-rate tests are that the initial high strain-rate deformation in the first stage causes rapid microstructural changes. These changes include the conversion of many low-angle to high-angle grain boundaries which maximize boundary strain in the material. This tends to lower the flow stress in the second stage of deformation thus delaying the macroscopic necking in the specimen. Other advantages are that superplastic cavitation (internal void formation) is reduced at lower flow stress levels and superplastic forming time can be reduced under two-stage strain-rate tests which often leads to more uniform deformation in the specimen.

2.2.3.1.1 Optimization of Superplastic Forming Test Temperatures

Superplastic tensile tests were performed under two strain rates (2×10^{-3} s^{-1} and 2×10^{-4} s^{-1}) at 950, 986 and 1022°F on all three gauge samples in air. Both longitudinal and transverse samples, to the rolling direction, were examined (Table 2-3). Figure 2-19 shows the effect of test temperature on superplastic elongations. The superplastic data show a peak in elongation at 986°F in three gauges of the alloy in the longitudinal samples.

TABLE 2-3

SUPERPLASTIC ELONGATION DATA FOR AL-LI ALLOY

Alloy	TMT	Temp. (°F)	Pressure (psi)	Strain Rates (S^{-1})	Elongation (%)	Thickness (in.)
8091	AR	950	Air	2×10^{-3} & 2×10^{-4}	418	0.060
8091	AR	986	Air	2×10^{-3} & 2×10^{-4}	458	0.060
8091	AR	1022	Air	2×10^{-3} & 2×10^{-4}	353	0.060
8091	AR	950	Air	2×10^{-3} & 2×10^{-4}	449	0.090
8091	AR	986	Air	2×10^{-3} & 2×10^{-4}	563	0.090
8091	AR	1022	Air	2×10^{-3} & 2×10^{-4}	367	0.090
8091	AR	950	Air	2×10^{-3} & 2×10^{-4}	530	0.125
8091	AR	986	Air	2×10^{-3} & 2×10^{-4}	605	0.125
8091	AR	1022	Air	2×10^{-3} & 2×10^{-4}	485	0.125
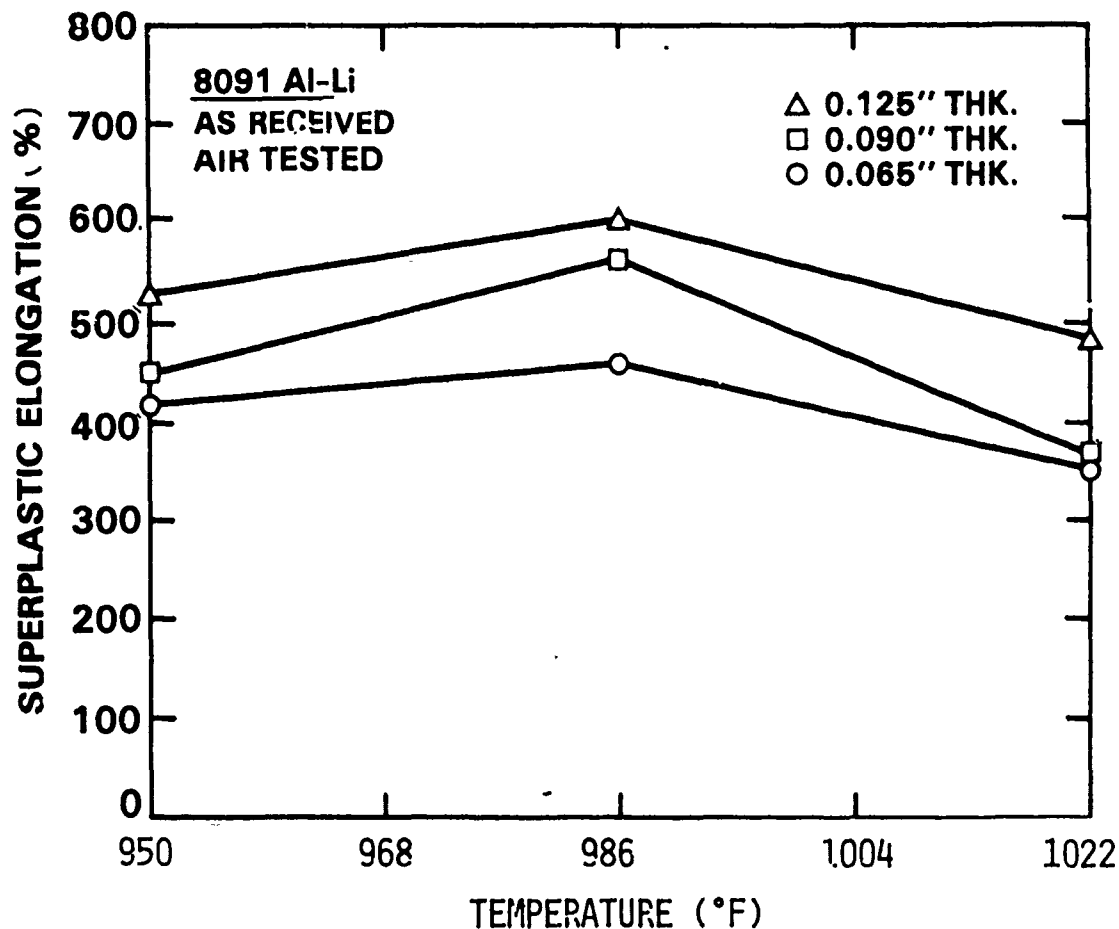
Figure 2-19. Superplastic Elongations in 8091 Aluminum-Lithium
Alloy as a Function of Test Temperature

2.2.3.1.2 Optimization of Second Strain Rate

Tensile tests were performed to determine the effect of second strain rate on total superplastic elongation. The samples were pulled at an initial strain rate of $2 \times 10^{-3} s^{-1}$ for 6 minutes at which time the strain rate was decreased and the test was continued to failure of the sample. Four different second strain rates were examined: $2 \times 10^{-4} s^{-1}$, $5 \times 10^{-4} s^{-1}$, $8 \times 10^{-4} s^{-1}$ and $1 \times 10^{-3} s^{-1}$; the corresponding superplastic elongation data are shown in Table 2-4 and Figure 2-20. The maximum elongation was observed at a second strate rate of $2 \times 10^{-4} s^{-1}$. The superplastic elongations decreased when the secondary strain rate was increased above $2 \times 10^{-4} s^{-1}$ as a result of higher flow stresses, subsequent superplastic cavitation, and premature failure of the samples. All subsequent tests were conducted using $2 \times 10^{-4} s^{-1}$ as the second strain rate.

TABLE 2-4

SUPERPLASTIC ELONGATION DATA FOR AL-LI ALLOY
AT DIFFERENT SECOND STAGE STRAIN RATES

Alloy	TMT	Temp. (^{o}F)	Pressure (psi)	Strain Rates (S^{-1})	Elongation (%)	Thickness (in.)
8091	AR	986	200	2×10^{-3} & 2×10^{-4}	984	0.090
8091	AR	986	200	2×10^{-3} & 5×10^{-4}	670	0.090
8091	AR	986	200	2×10^{-3} & 8×10^{-4}	567	0.090
8091	AR	986	200	2×10^{-3} & 10×10^{-4}	553	0.090
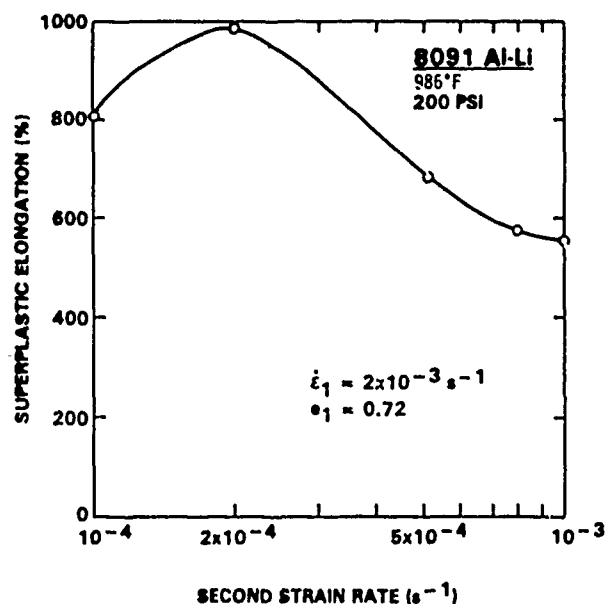
Figure 2-20. Superplastic Elongations in 8091 Al-Li Alloys as a
Function of Second Strain Rate

2.2.3.1.3 Optimization of First Strain Rate

Tensile tests were performed to determine the effect of the initial strain rate on total superplastic elongation. The samples were pulled at an initial strain rate from 0 strain to 0.72 after which the second strain rate (constant for all tests) was used until failure of the coupon. The four different initial strain rates used (1×10^{-3} to 10×10^{-3} S^{-1}) and the results from the initial strain rate optimization study are shown in Figure 2-21 and Table 2-5. At higher initial strain rates ($4 \times 10^{-3} s^{-1}$ and $1 \times 10^{-2} s^{-1}$), the total superplastic elongations were reduced as a result of higher flow stress levels and premature necking of the material. At lower initial strain rate ($1 \times 10^{-3} s^{-1}$), the elongation was reduced as a result of grain growth. The optimum strain-rate for the first stage of deformation was observed to be $2 \times 10^{-3}/S^{-1}$.

2-29
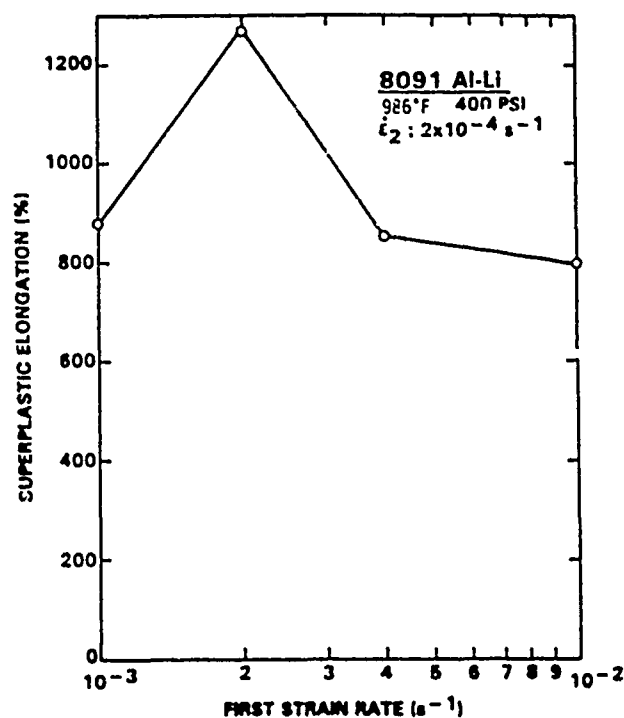
Figure 2-21. Superplastic Elongations in 8091 Al-Li Alloy
as a Function of First Strain Rate

TABLE 2-5

SUPERPLASTIC ELONGATION DATA FOR AL-LI ALLOY
AT DIFFERENT FIRST STAGE STRAIN RATES

Alloy	TMT	Temp. ($^{\circ}F$)	Pressure (psi)	Strain Rates (S^{-1})	Elongation (%)	Thickness (in.)
8091	AR	986	400	1×10^{-3} & 2×10^{-4}	880	0.090
8091	AR	986	400	2×10^{-3} & 2×10^{-4}	1275	0.090
8091	AR	986	400	4×10^{-3} & 2×10^{-4}	855	0.090
8091	AR	986	400	10×10^{-3} & 2×10^{-3}	795	0.090

2.2.3.1.4 Optimization of First-Stage Strain

The optimization of the SPF elongation continued with two-stage tensile tests performed at the optimum forming temperature (986°F) with varying amounts of strain in the first stage of the pull. The strain rates were kept constant (2 x $10^{-3}s^{-1}$ and 2 x $10^{-4}s^{-1}$) and the initial strain was varied from 0 to 2.0. The results are shown in Figure 2-22 and Table 2-6. The total superplastic elongations at 986°F increased rapidly with an increase in the initial strain (from 0.36 to 1.44) and finally decreased. The sharp drop in elongations at high first-stage strains. (>1.5) was caused by premature necking and superplastic cavitation. A first-stage strain just below 1.5 appears to be the optimum amount of initial strain for highest elongation values. At the lowest initial strains, in the tests conducted at 986°F, the total superplastic elongation was low because of the large number of low-angle grain boundaries which allowed grain growth during subsequent deformation. Similar experiments (refer to Table 2-6) at 950°F indicated that the first-stage strain should be limited to 1.08 or less for maximum elongation. In the tensile tests that followed this study, samples were pulled to 2 x $10^{-3}s^{-1}$ to a strain of 0.72 after which the strain rate was reduced to 2 x $10^{-4}s^{-1}$.
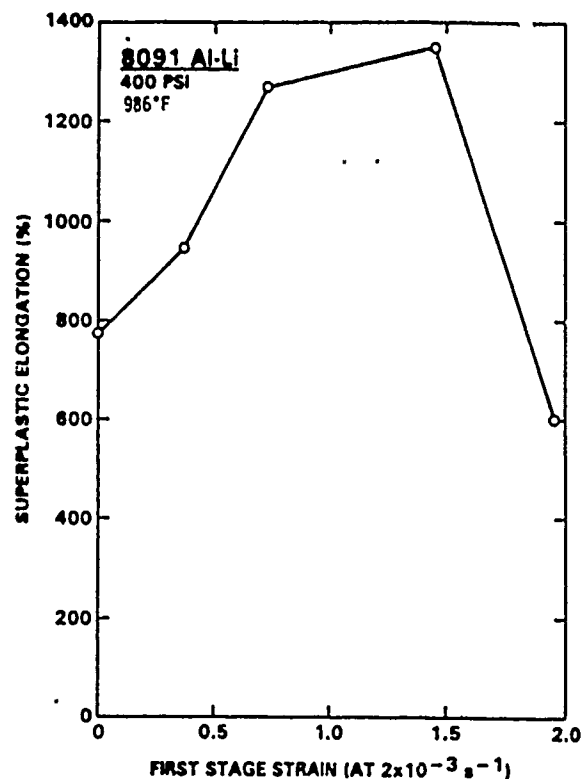
Figure 2-22.   Superplastic Elongation in 8091 Aluminum-Lithium
as a Function of Initial Strain

TABLE 2-6

OPTIMIZATION OF FIRST STAGE STRAIN FOR MAXIMUM
SUPERPLASTIC ELONGATION FOR AL-LI ALLOY

Alloy	TMT	Temp. (^{O}F)	Pressure (psi)	Strain Rates (s^{-1})	Strain	Elong. (%)	Thickness (In.)
8091	AR	986	400	2×10^{-3} & 2×10^{-4}	0.0	776	0.090L
8091	AR	986	400	2×10^{-3} & 2×10^{-4}	0.36	950	0.090L
8091	AR	986	400	2×10^{-3} & 2×10^{-4}	0.72	1275	0.090L
8091	AR	986	400	2×10^{-3} & 2×10^{-4}	1.08	1125	0.090L
8091	AR	986	400	2×10^{-3} & 2×10^{-4}	1.44	1350	0.090L
8091	AR	950	400	2×10^{-3} & 2×10^{-4}	0.36	636	0.090L
8091	AR	950	400	2×10^{-3} & 2×10^{-4}	0.72	792	0.090L
8091	AR	950	400	2×10^{-3} & 2×10^{-4}	1.08	784	0.090L
8091	AR	950	400	2×10^{-3} & 2×10^{-4}	1.44	524	0.090L

NOTE: TMT = Thermal Mechanical Treatment
       AR = As-Received

2.2.3.1.5 Effect of Back Pressure on Superplastic Elongations

Tensile tests were performed on 8091 Al-Li under back pressure to improve
the superplastic elongations and to reduce or eliminate cavitation. Tests
were conducted on both longitudinal and transverse samples at the optimum test
temperature (986°F) and under two strain-rate test conditions (2 x
$10^{-3}s^{-1}$ and 2 x $10^{-4}s^{-1}$). The first-stage strain was kept constant at
0.72. Back pressures of 200, 400 and 600 psi were used. The test data shown
in Tables 2-7 through 2-9 suggest that superplastic elongations for 8091 Al-Li
are dramatically improved for back pressures of 400 to 600 psi (Figure 2-23)
compared with those tested in air. Superplastic elongations for 8091-SP
exceed 1000 percent at the back pressure of 400 psi. A maximum elongation of
1350 percent was observed at 950°F in a transverse sample tested under 600
psi back pressure (Figure 2-24).

TABLE 2-7

OPTIMIZATION OF FIRST STAGE STRAIN FOR MAXIMIZING
SUPERPLASTIC ELONGATION DATA FOR AL-LI ALLOY

Alloy	TMT	Temp. (^{o}F)	Pressure (psi)	Strain Rates (S^{-1})	Elongation (%)	Thickness (in.)
8091	AR	950	Air	2×10^{-3} & 2×10^{-4}	530	0.125L
8091	AR	950	Air	2×10^{-3} & 2×10^{-4}	522	0.125T
8091	AR	950	200	2×10^{-3} & 2×10^{-4}	877	0.125L
8091	AR	950	200	2×10^{-3} & 2×10^{-4}	992	0.125T
8091	AR	950	400	2×10^{-3} & 2×10^{-4}	1250	0.125L
8091	AR	950	400	2×10^{-3} & 2×10^{-4}	1038	0.125T
8091	AR	950	600	2×10^{-3} & 2×10^{-4}	1138	0.125L
8091	AR	950	600	2×10^{-3} & 2×10^{-4}	1300	0.125T
8091	AR	986	Air	2×10^{-3} & 2×10^{-4}	605	0.125L
8091	AR	986	Air	2×10^{-3} & 2×10^{-4}	490	0.125T
8091	AR	986	200	2×10^{-3} & 2×10^{-4}	979	0.125L
8091	AR	986	200	2×10^{-3} & 2×10^{-4}	903	0.125T
8091	AR	986	400	2×10^{-3} & 2×10^{-4}	1275	0.125L
8091	AR	986	400	2×10^{-3} & 2×10^{-4}	1045	0.125T
8091	AR	986	600	2×10^{-3} & 2×10^{-4}	1200	0.125L
8091	AR	986	600	2×10^{-3} & 2×10^{-4}	1200	0.125T
8091	AR	1022	Air	2×10^{-3} & 2×10^{-4}	485	0.125L
8091	AR	1022	Air	2×10^{-3} & 2×10^{-4}	447	0.125T
8091	AR	1022	400	2×10^{-3} & 2×10^{-4}	869	0.125L
8091	AR	1022	400	2×10^{-3} & 2×10^{-4}	905	0.125T

NOTE: TMT = Thermal Mechanical Treatment
       AR = As-Received

TABLE 2-8

OPTIMIZATION OF BACK PRESSURE TO MAXIMIZE
SUPERPLASTIC ELONGATION DATA FOR AL-LI ALLOY
(THICKNESS = 0.090-IN.)

Alloy	TMT	Temp. ($^{\circ}$F)	Pressure (psi)	Strain Rates (S^{-1})	Elongation (%)	Thickness (in.)
8091	AR	950	Air	2×10^{-3} & 2×10^{-4}	449	0.090L
8091	AR	950	Air	2×10^{-3} & 2×10^{-4}	555	0.090T
8091	AR	950	200	2×10^{-3} & 2×10^{-4}	770	0.090L
8091	AR	950	200	2×10^{-3} & 2×10^{-4}	932	0.090T
8091	AR	950	400	2×10^{-3} & 2×10^{-4}	1051	0.090L
8091	AR	950	400	2×10^{-3} & 2×10^{-4}	982	0.090T
8091	AR	950	600	2×10^{-3} & 2×10^{-4}	950	0.090L
8091	AR	950	600	2×10^{-3} & 2×10^{-4}	1350	0.090T
8091	AR	986	Air	2×10^{-3} & 2×10^{-4}	563	0.090L
8091	AR	986	Air	2×10^{-3} & 2×10^{-4}	572	0.090T
8091	AR	986	200	2×10^{-3} & 2×10^{-4}	984	0.090L
8091	AR	986	200	2×10^{-3} & 2×10^{-4}	912	0.090T
8091	AR	986	400	2×10^{-3} & 2×10^{-4}	1275	0.090L
8091	AR	986	400	2×10^{-3} & 2×10^{-4}	1250	0.090T
8091	AR	986	600	2×10^{-3} & 2×10^{-4}	1018	0.090L
8091	AR	986	600	2×10^{-3} & 2×10^{-4}	1175	0.090T
8091	AR	986	Air	2×10^{-3} & 2×10^{-4}	367	0.090L
8091	AR	1022	Air	2×10^{-3} & 2×10^{-4}	477	0.090T
8091	AR	1022	400	2×10^{-3} & 2×10^{-4}	479	0.090L
8091	AR	1022	400	2×10^{-3} & 2×10^{-4}	766	0.090T

NOTE: TMT = Thermal Mechanical Treatment
      AR = As-Received

TABLE 2-9

OPTIMIZATION OF BACK PRESSURE TO MAXIMIZE
SUPERPLASTIC ELONGATION DATA FOR AL-LI ALLOY
(THICKNESS = 0.060-IN.)

Alloy	TMT	Temp. ($^{\circ}$F)	Pressure (psi)	Strain Rates (S^{-1})		Elongation (%)	Thickness (in.)
8091	AR	950	Air	2×10^{-3} & 2×10^{-4}		418	0.060L
8091	AR	950	Air	2×10^{-3} & 2×10^{-4}		479	0.060T
8091	AR	950	200	2×10^{-3} & 2×10^{-4}		694	0.060L
8091	AR	950	200	2×10^{-3} & 2×10^{-4}		889	0.060T
8091	AR	950	400	2×10^{-3} & 2×10^{-4}		835	0.060L
8091	AR	950	400	2×10^{-3} & 2×10^{-4}		972	0.060T
8091	AR	950	600	2×10^{-3} & 2×10^{-4}		731	0.060L
8091	AR	950	600	2×10^{-3} & 2×10^{-4}		1113	0.060T
8091	AR	986	Air	2×10^{-3} & 2×10^{-4}		458	0.060L
8091	AR	986	Air	2×10^{-3} & 2×10^{-4}		572	0.060T
8091	AR	986	200	2×10^{-3} & 2×10^{-4}		943	0.060L
8091	AR	986	200	2×10^{-3} & 2×10^{-4}		912	0.060T
8091	AR	986	400	2×10^{-3} & 2×10^{-4}		976	0.060L
8091	AR	986	400	2×10^{-3} & 2×10^{-4}		1078	0.060T
8091	AR	986	600	2×10^{-3} & 2×10^{-4}		990	0.060L
8091	AR	986	600	2×10^{-3} & 2×10^{-4}		1125	0.060T
8091	AR	1022	Air	2×10^{-3} & 2×10^{-4}		353	0.060L
8091	AR	1022	Air	2×10^{-3} & 2×10^{-4}		345	0.060T
8091	AR	1022	400	2×10^{-3} & 2×10^{-4}		623	0.060L
8091	AR	1022	400	2×10^{-3} & 2×10^{-4}		864	0.060T

NOTE: TMT = Thermal Mechanical Treatment
      AR = As-Received
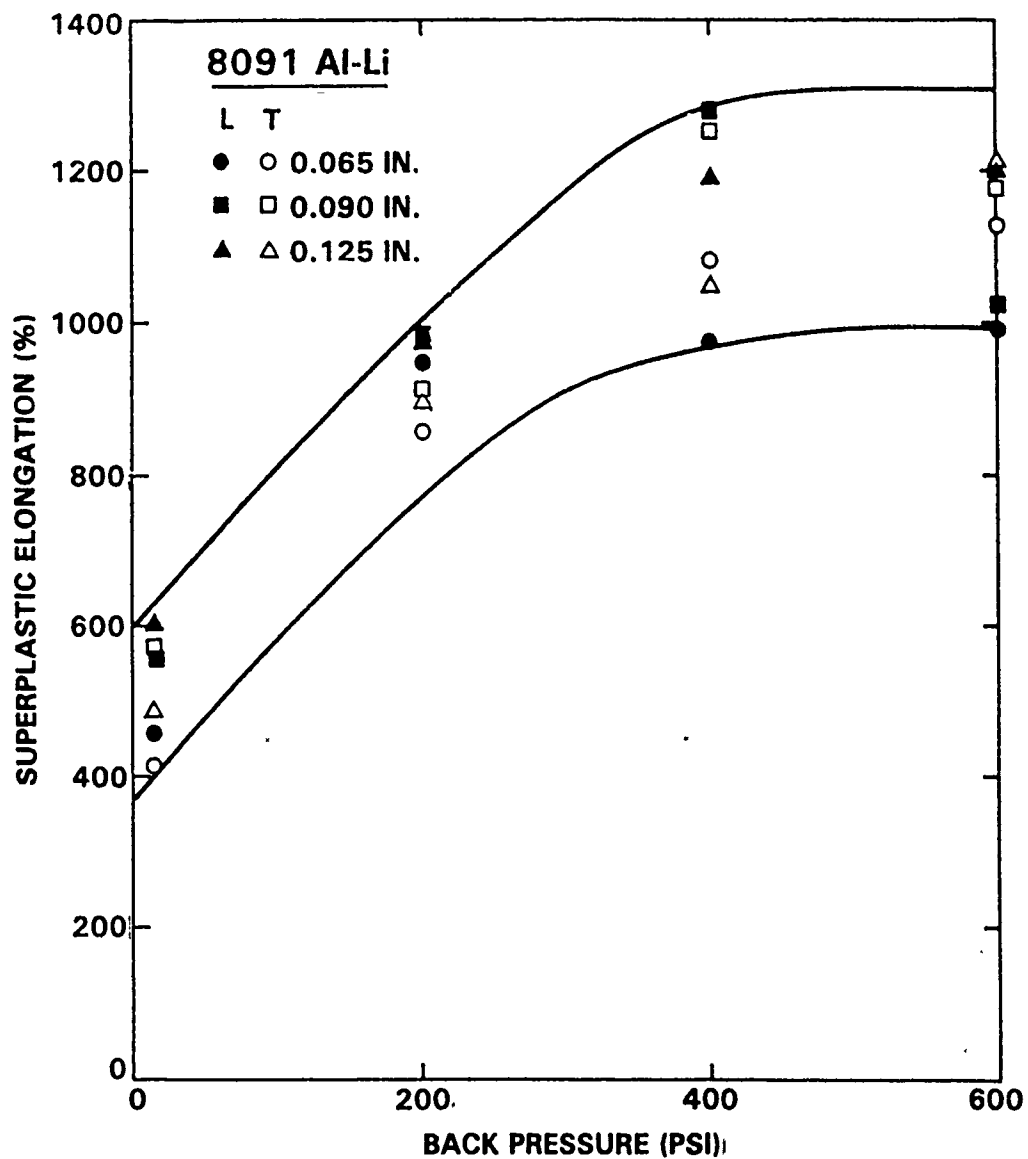
Figure 2-23. Superplastic Elongations in 8091 Al-Li Alloy as a Function
of Back Pressure

1350%
600 PSI

555%
AIR

UNTESTED
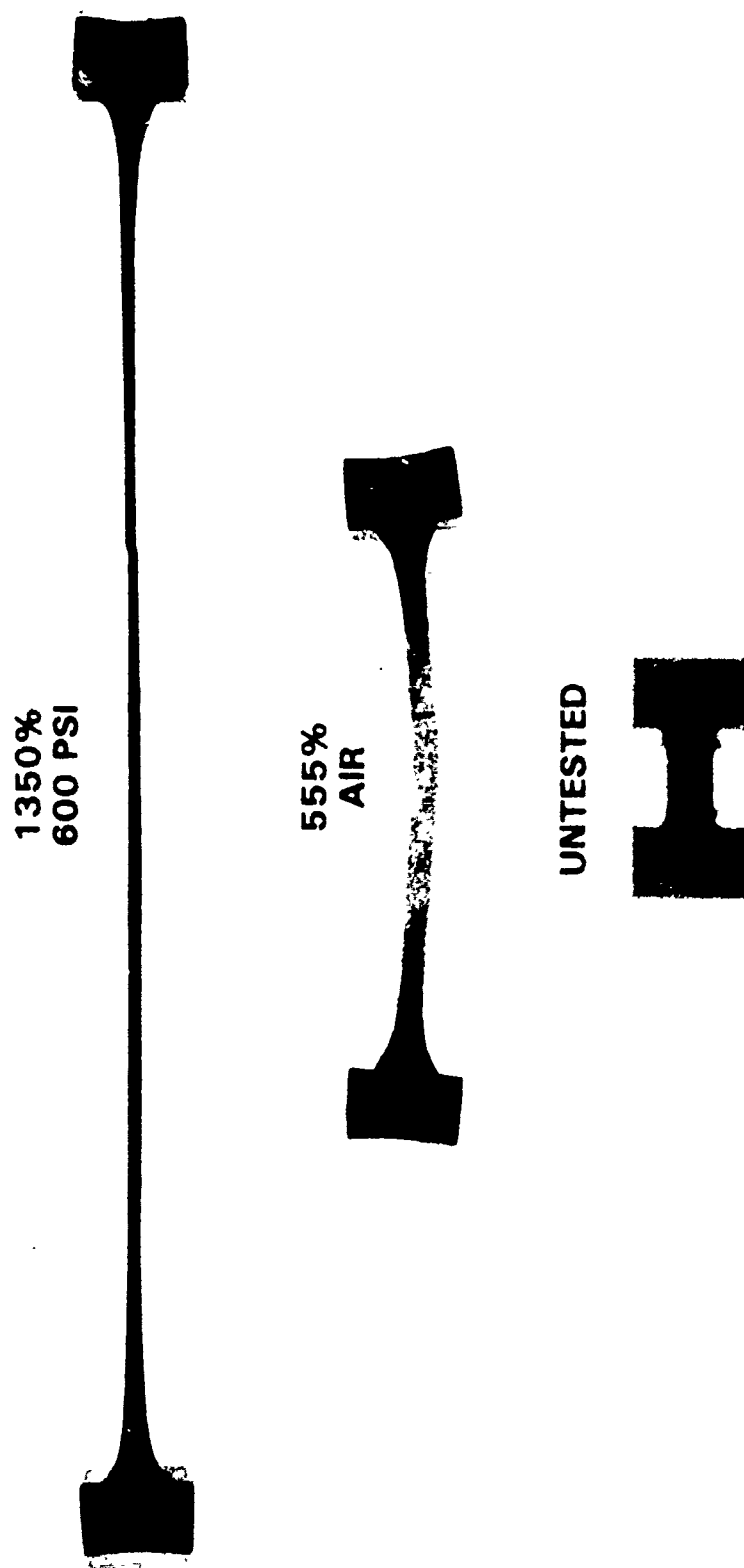
(950°F, 2 x 10^{-3} and 2 x 10^{-4} S^{-1})

Figure 2-24. Superplastic Elongations in 2091 Aluminum-Lithium Alloy

2.2.3.1.6 Effect of Gauge Thickness on Superplastic Elongation

The grain sizes in three-gauge thicknesses differed slightly from one another. The thicker gauge (0.125-inch) material had a finer grain size than the thinner gauge although the difference was very small. The superplastic elongations in 8091 Al-Li as a function of thickness are shown in Figure 2-25. The thicker gauge material (0.125-inch) showed higher elongations than the thinner gauge material. This may be related to surface oxidation and early failure of the thin gauge material. A significant increase in superplastic elongation was noted (Figure 2-25) at 400 psi back pressure for thicknesses of 0.060 to 0.090-inch.

2.2.3.1.7 Flow Stresses and Strain-Rate Sensitivity (m)

The flow stress levels in 8091 Al-Li as a function of strain are shown in Figure 2-26. At the beginning of the test the material showed considerable strain hardening; in the second phase of the test an apparent steady-state condition was established for each temperature. The flow stress levels were higher at low temperature (950°F) compared with those at 1022°F. The static grain growth in 8091 Al-Li alloy caused higher flow stress levels and strain hardening in the initial stage of testing.

The strain-rate sensitivity of the material was evaluated by the stepped strain rate tests (Figure 2-27) as a function of strain rate. The strain-rate sensitivity was highest for the range 2×10^{-4} to 5×10^{-4} s^{-1}. The maximum strain sensitivity value was relatively low (0.5) and decreased with increasing strain rate. The flow stress curves at 950 and 986°F were very close to each other thus reflecting similar superplastic behavior. Figure 2-28 shows the variation of m with superplastic strain at 986°F. The strain-rate sensitivity decreased with strain in a monotonic way and a small improvement in m at the beginning of the tests (strain < 0.2) is expected.

2.2.3.1.8 Superplastic Cavitation in 8091 Al-Li Alloy

Superplastic cavitation in 8091 Al-Li alloy was evaluated by metallographic examination and density measurements. The metallographic examinations of the tensile-tested samples in both air and back pressure showed a marked contrast in the superplastic cavitation (Figure 2-29). Air-tested samples showed extensive cavitation, while cavitation was suppressed by the back pressure of 400 psi. The density measurement (Figures 2-30 and 2-31) also indicated high superplastic cavitation in air-tested samples which gradually decreased at 200, 400 and 600 psi back pressures. The fracture strains were higher in samples tested under back pressure ($\epsilon > 2.8$) compared with those tested in air ($\epsilon = 2.0$). Density measurements of the superplastically deformed materials also indicated that cavitation was
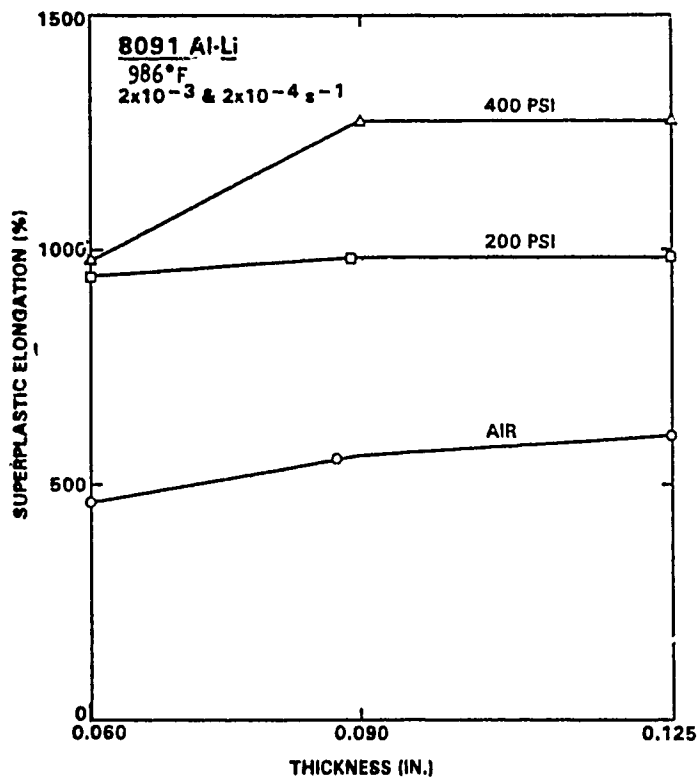
Figure 2-25.   Superplastic Elongations in 8091 Al-Li as a Function of
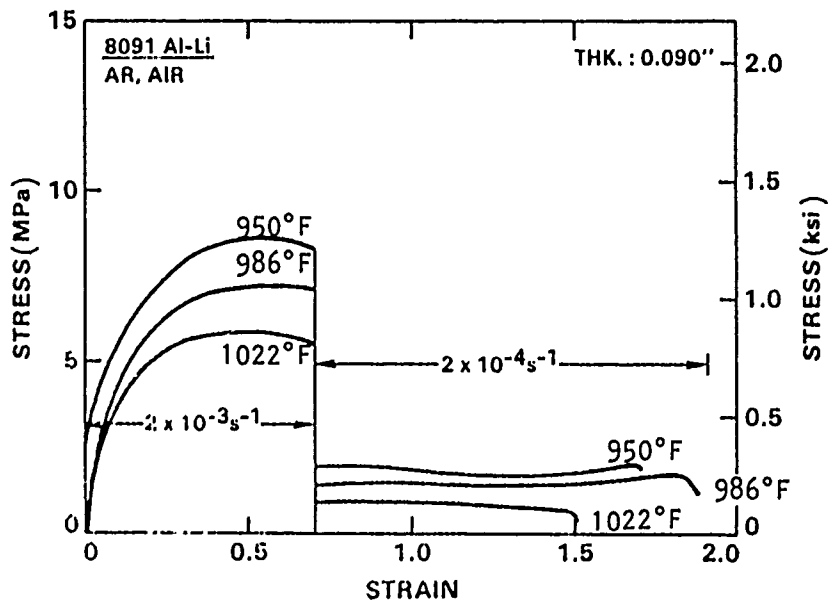Thickness

Figure 2-26.   Flow Stress Versus Strain for 8091 Al-Li at Different Test
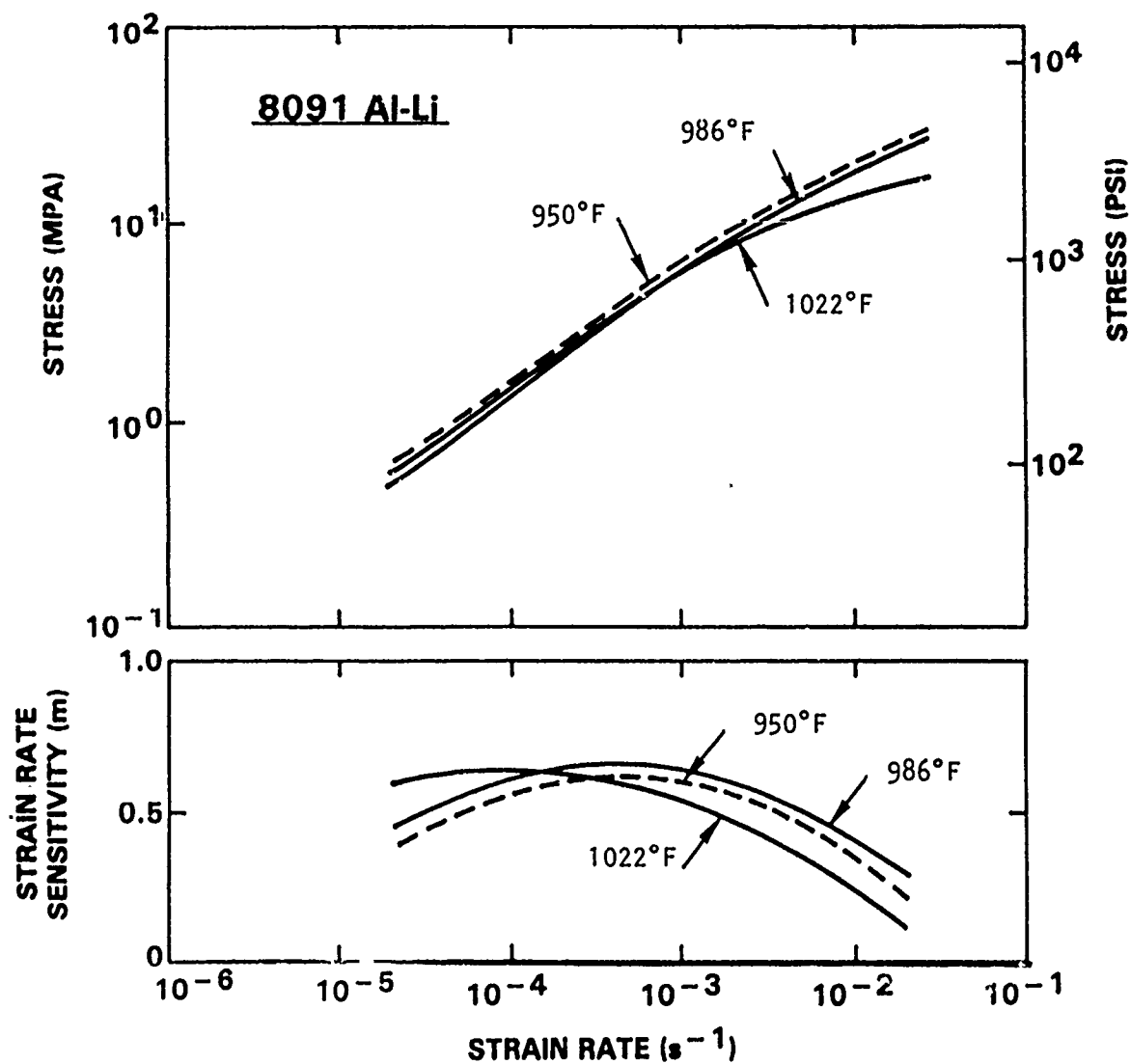Temperatures

Figure 2-27. Flow Stress and Strain Rate Sensitivity as a
Function of Strain Rate
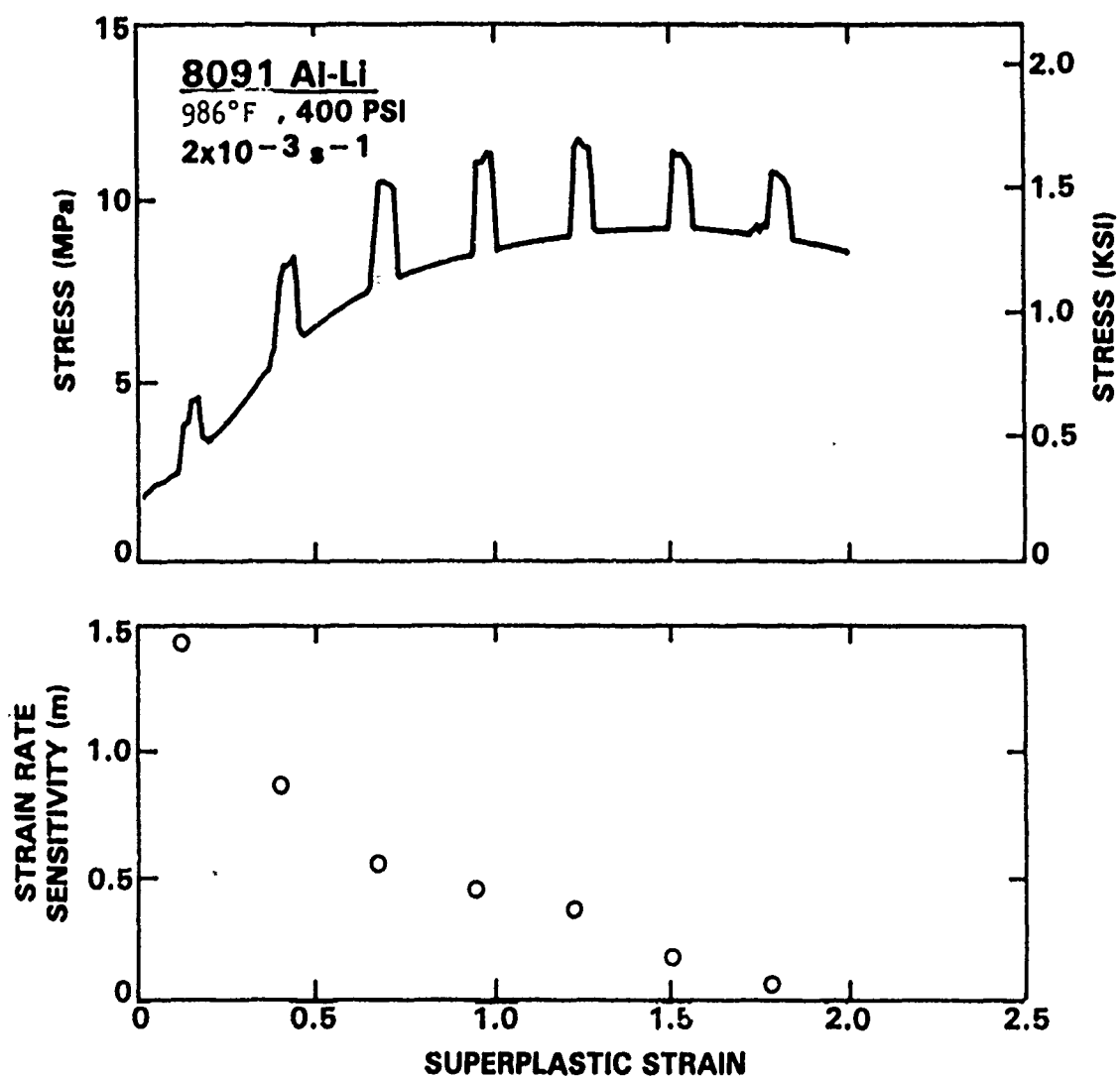
Figure 2-28. Variation of Strain Rate Sensitivity With Superplastic Strain

ε = 1.9

AIR

0.5 mm

ε = 3.5

400 psi

(986°F, 2×10^{-3} and 2×10^{-4} S^{-1})

0.5 mm

Figure 2-29. Optical Micrographs Showing Superplastic Cavitation in 8091 Al-Li Alloy in air and 400 psi Back Pressure

Figure 2-30. Superplastic Cavitation (As-measured from Density Change) as a Function of Superplastic Strain

Figure 2-31. Comparison of Superplastic Cavitation in Air and With Back Pressure

initiated as early as 0.5 strain in the air-tested samples and was postponed to a strain of 1.5 under a back pressure of 400 psi (refer to Figure 2-31). The cavitation was n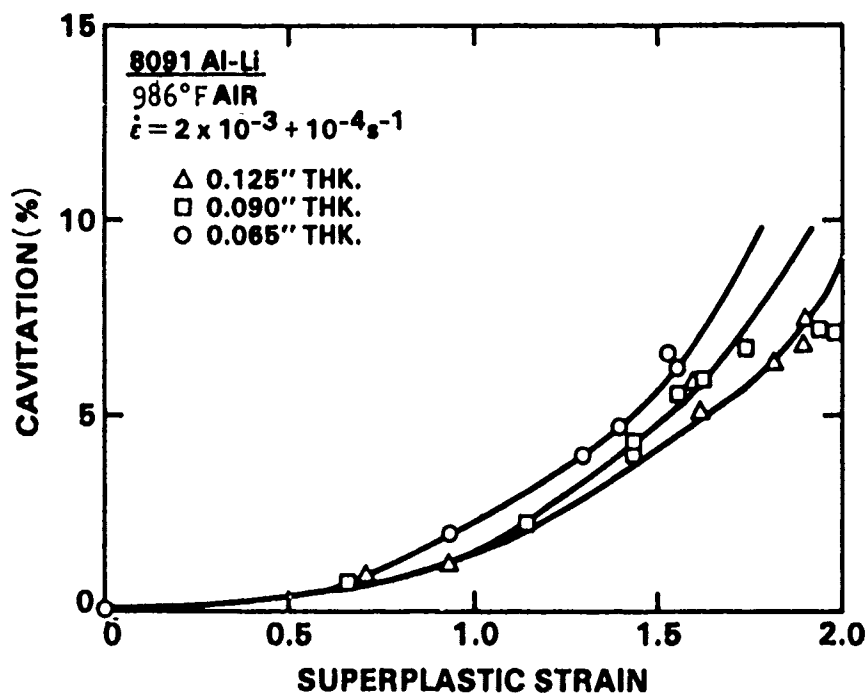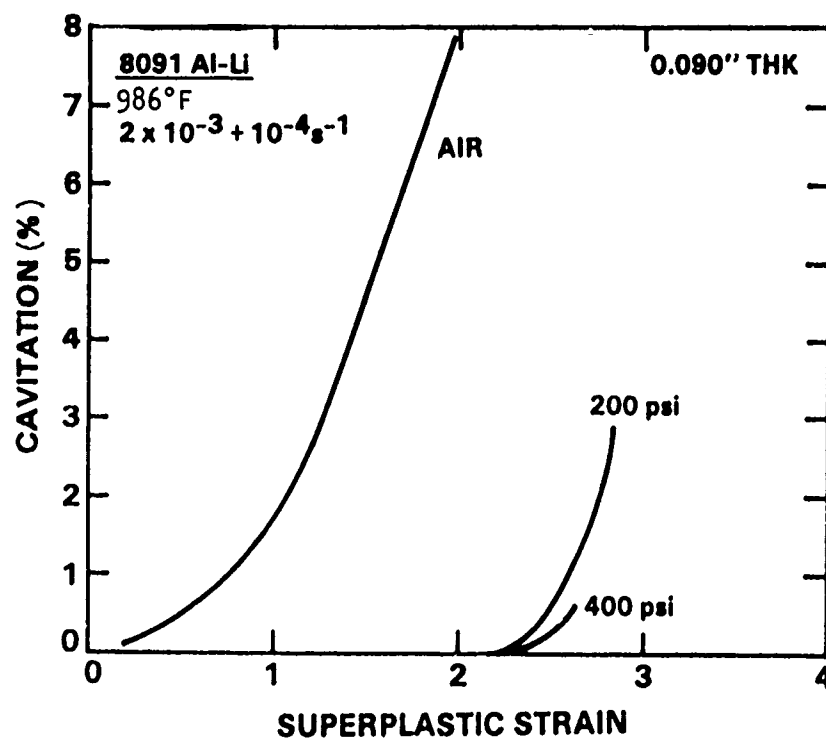egligible in samples tested with a back pressure of 600 psi. Superplastic cavitation in thin gauge samples was slightly higher than in thick gauge samples (refer to Figure 2-30).

2.2.3.1.9 Dynamic Grain Growth

The 8091 Al-Li alloy showed considerable dynamic grain growth at all test temperatures. Figure 2-32 presents the data at three test temperatures ranging from 950 to 1022°F. At the lowest test temperature, the grain size in the grip section was relatively small compared with the grain size at 1022°F; however, the average grain size increased linearly with superplastic strain at all three test temperatures. The grain growth behavior at 950 and 986°F were very close to each other compared with grain growth at 1022°F. The rate of dynamic grain growth was higher at 1022°F.

2.2.3.1.10 Formability Studies in 8091 Al-Li Alloy

Two kinds of subscale parts (Figure 2-33) were superplastically formed using gas-forming techniques. The sheet materials were cleaned with a wire brush and circular grid patterns were printed onto the surface. Rectangular pans of 6- by 6- by 1-inch and hemispherical domes (2.5-inch diameter) were fabricated using the pressure-time cycles shown in Figures 2-34 and 2-35. The parts were fabricated with a back pressure of 400 psi to suppress cavitation. The dimensions of the grid circles were measured at 10X, and the major and minor strains were calculated for each circle along the longitudinal and transverse sections of the pans. Figures 2-36 and 2-37 show the variation of strains in the pans. The thickness variations along the length and width of the pans are shown in Figures 2-38 and 2-39. Clearly, the maximum strains are seen near the corners and edges, and the thinning is small at the middle of the pan. Similar measurements of strains were made in the hemispherical dome along the meridian. Figures 2-40 and 2-41 show the strain and thickness variation along the meridian of the domes. There is considerable thinning of the material at the apex of the dome where the fracture occurred. The fracture strain is about 2.36 percent which corresponds to 960 percent in the biaxial strain conditions.

Superplastic cavitation in the pans and domes were also evaluated by metallography (Figures 2-42 and 2-43). The superplastic cavitation was negligible in the pans as the material was less deformed. The cavitation was high at the apex of the dome as the material was strained to over 2.36 (960 percent).
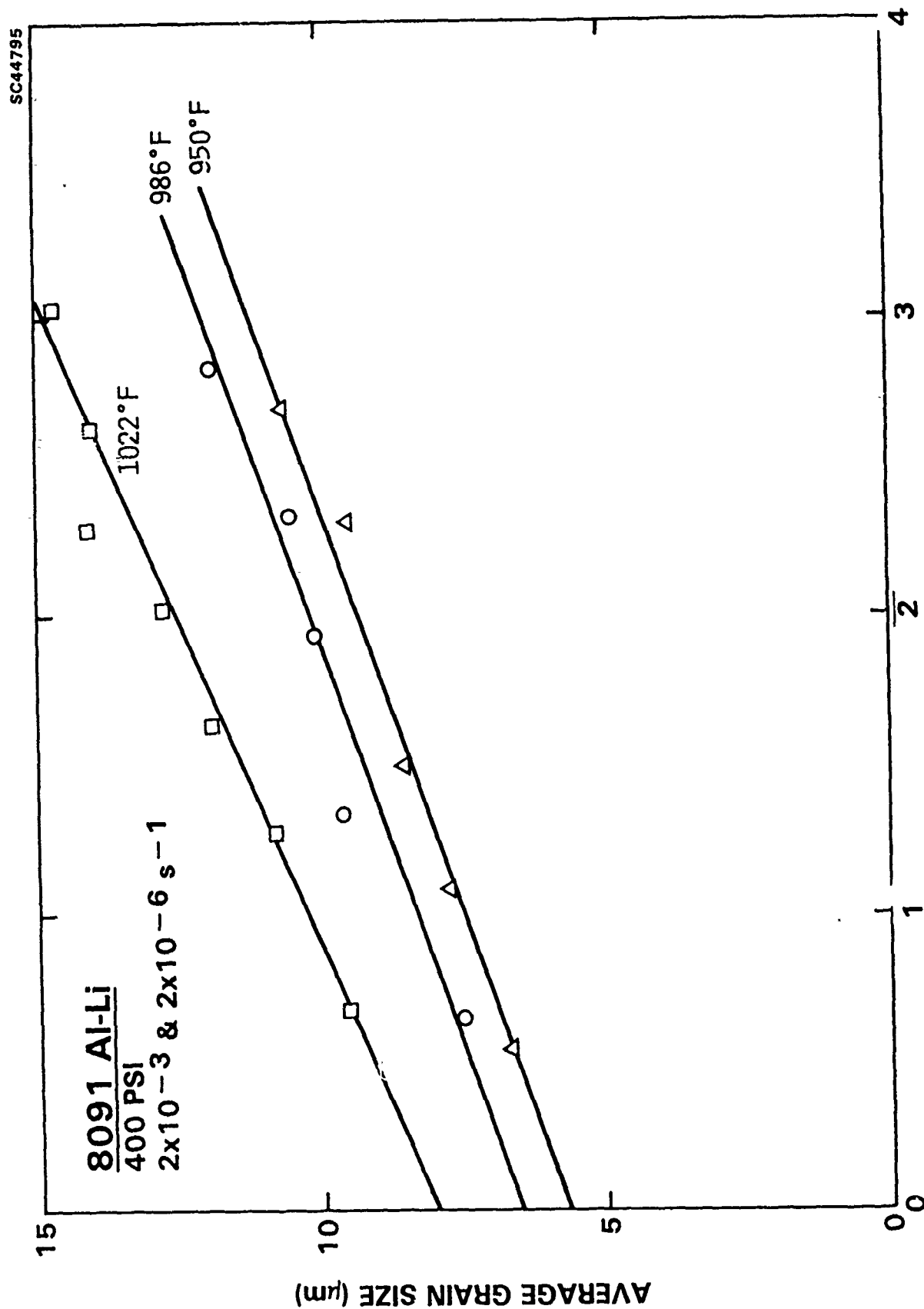
Figure 2-32. Comparison of Dynamic Grain Growth in 8091 Al-Li at Three Test Temperatures
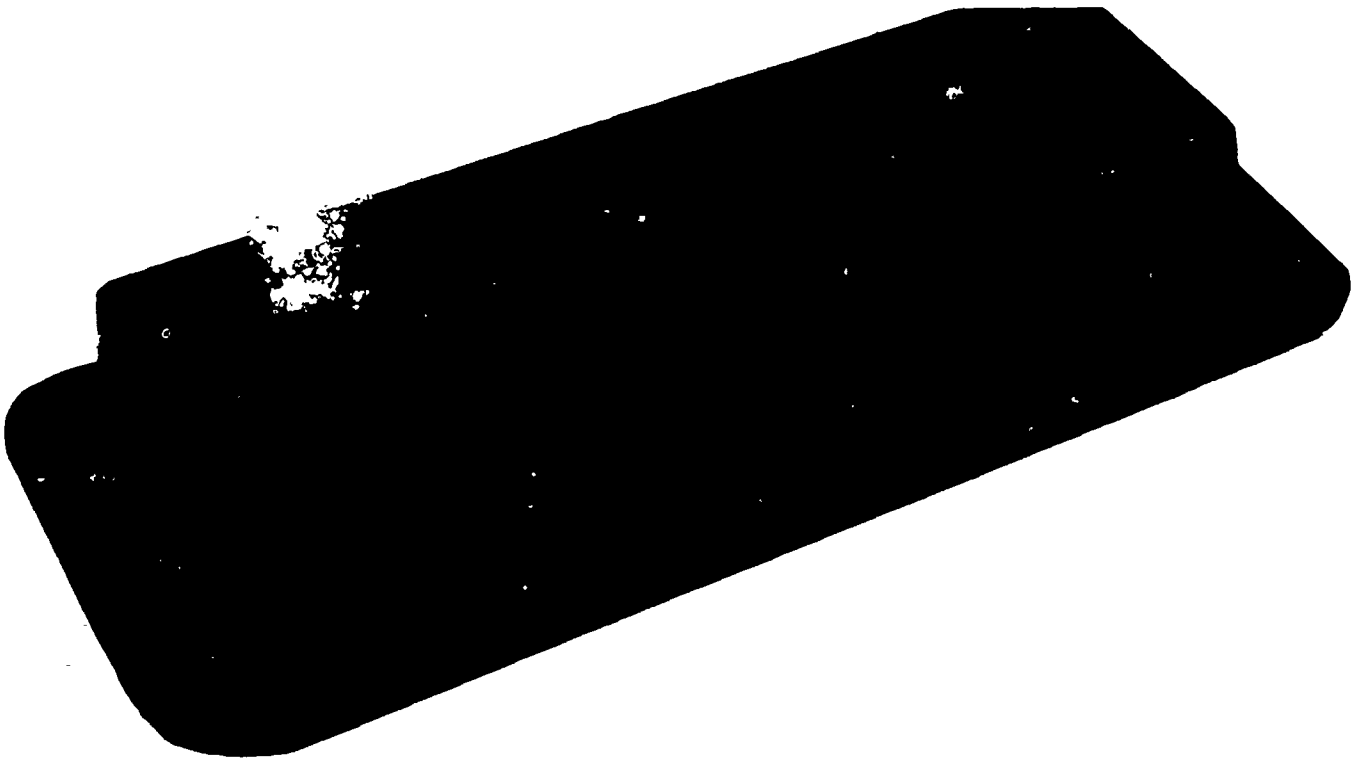
NOTE: SUPERPLASTICALLY FORMED 8091 AL-LI USING 2-STEP STRAIN RATES (2×10^{-3} S^{-1} + 2×10^{-4} S^{-1}); COMPONENT 1
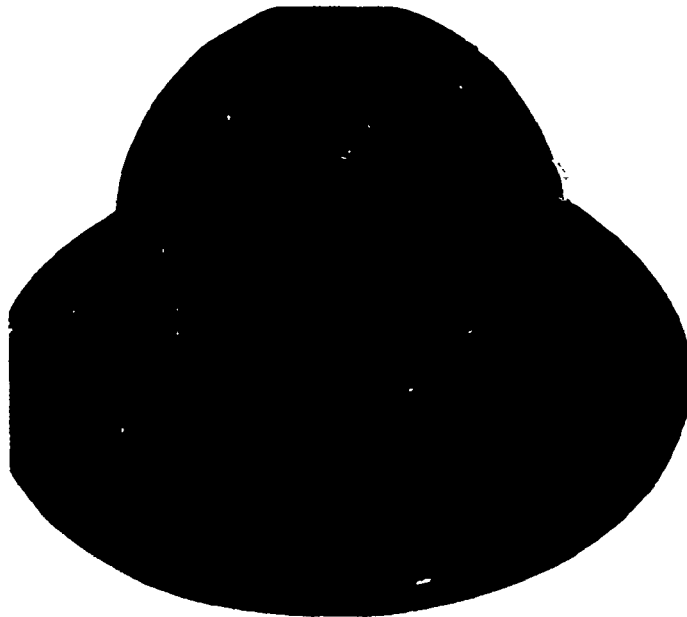
NOTE: SUPERPLASTICALLY FORMED 8091 AL-LI ALLOY USING 2-STEP STRAIN RATES (2×10^{-1} S^{-1} + 2×10^{-4} S^{-1}); COMPONENT 2

Figure 2-33. Subscale Components Fabricated from 8091 Aluminum-Lithium
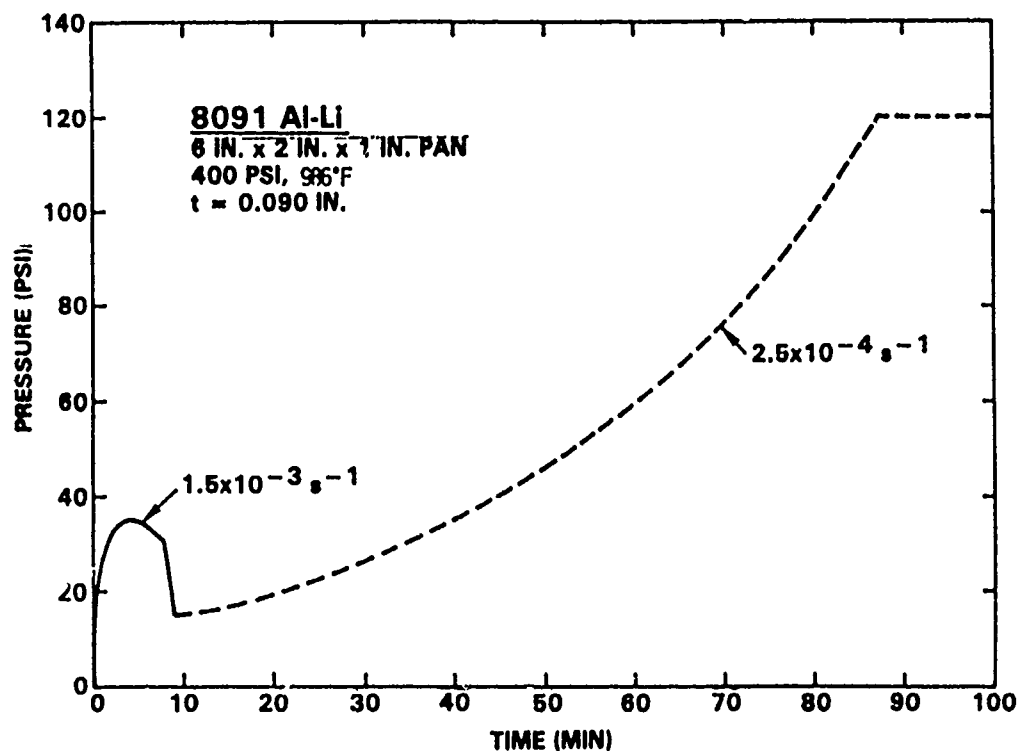
Figure 2-34.   Pressure-Time Cycle for 6- by 2- by 1-Inch Pan
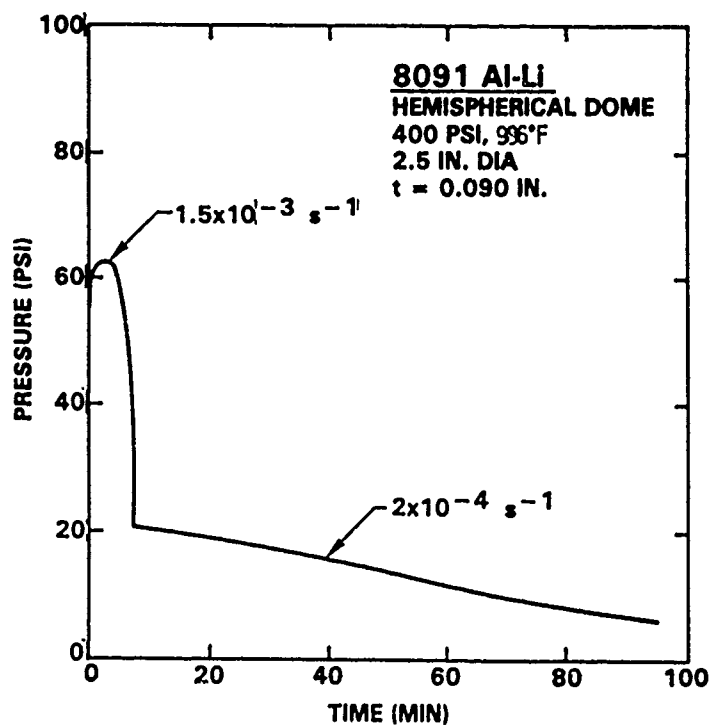
Figure 2-35.   Pressure-Time Cycle Used to Fabricate
Hemispherical Dome Pans
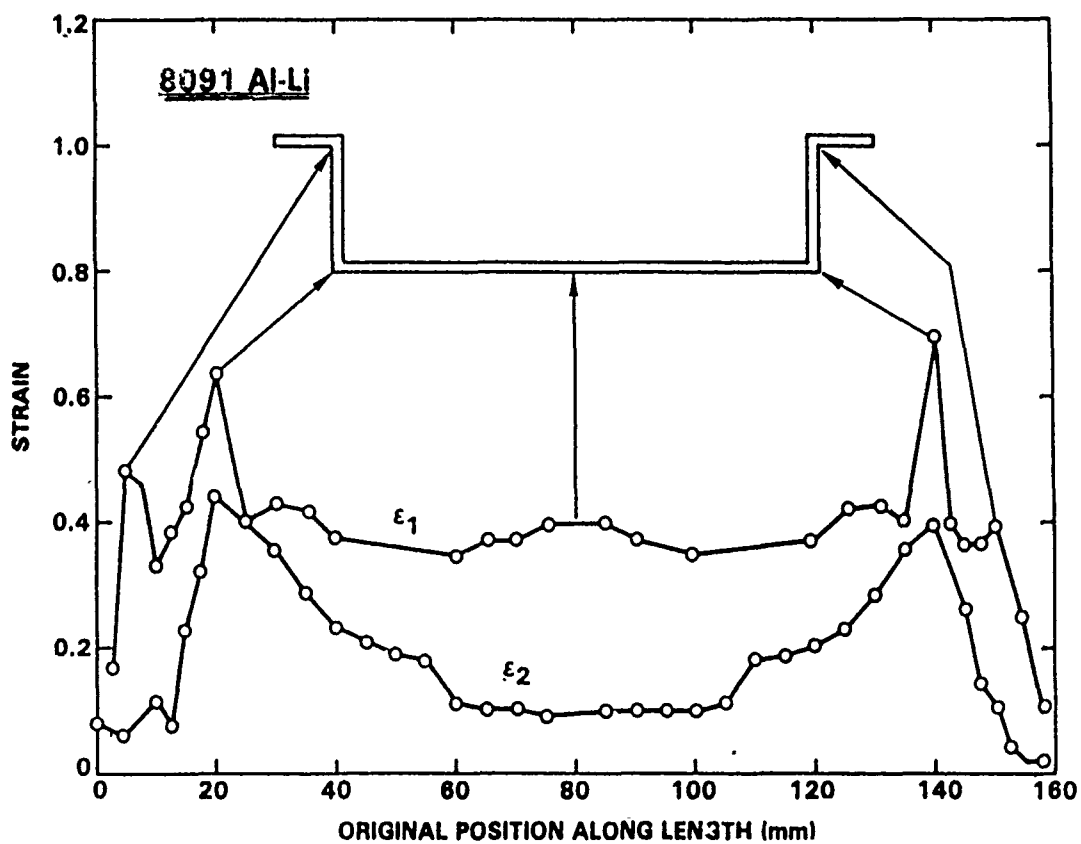
Figure 2-36. Strain Distributions Along the Length of 6- by 2- by 1-Inch Pan
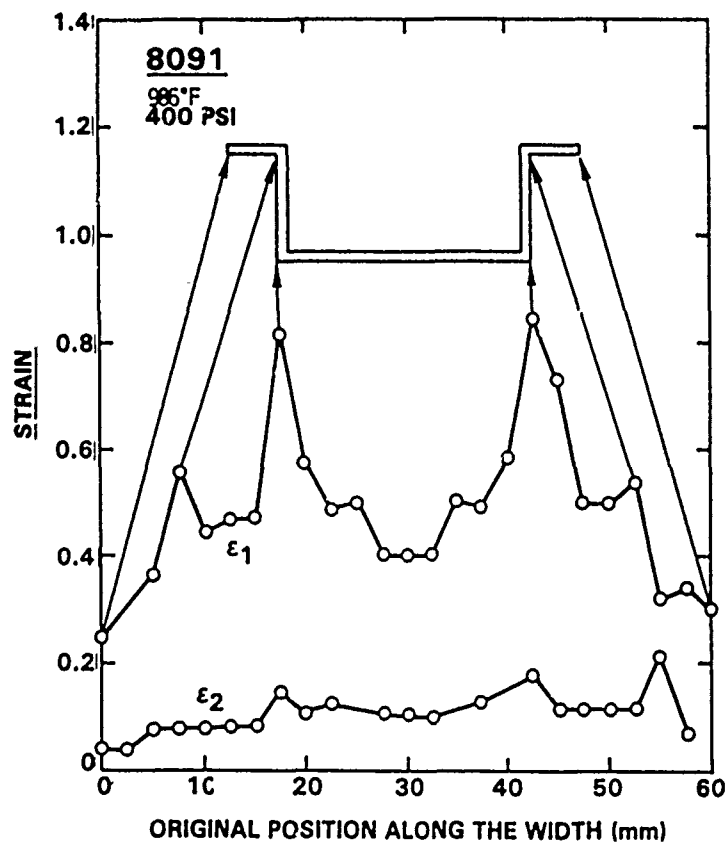
Figure 2-37. Strain Distribution Along the Width of 6- by 2- by 1-Inch Pan
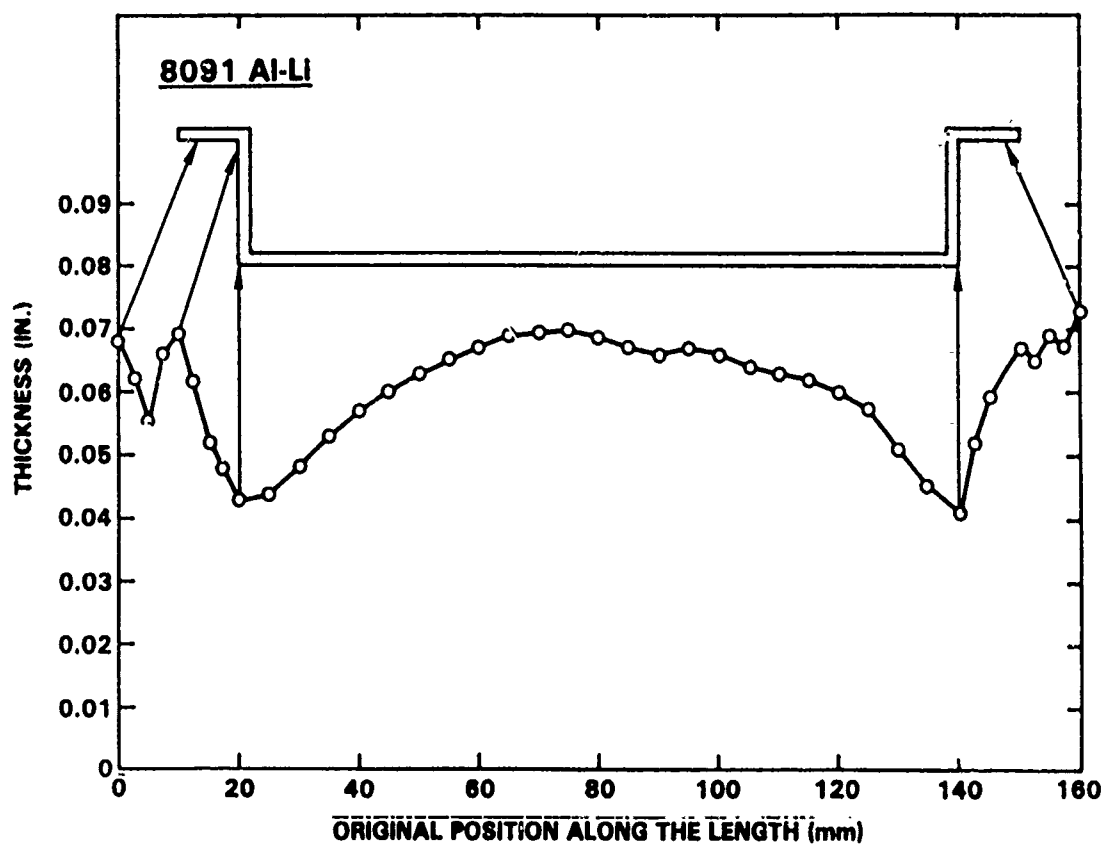
Figure 2-38. Thickness Variations Along Length of Pan
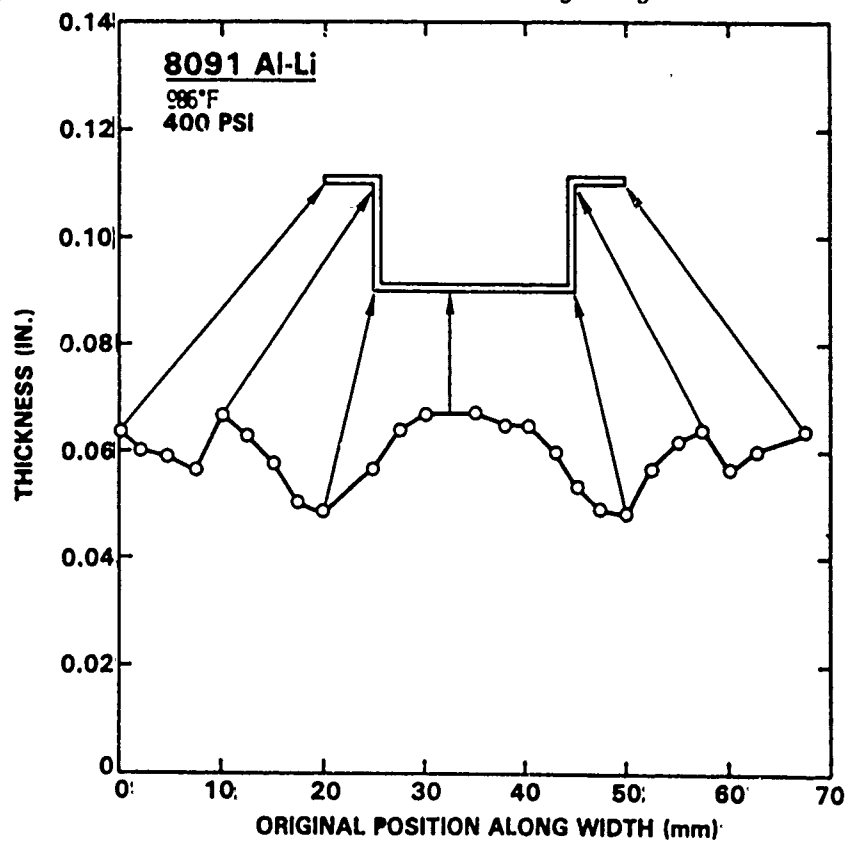
Figure 2-39. Thickness Distribution Along Width of Pan
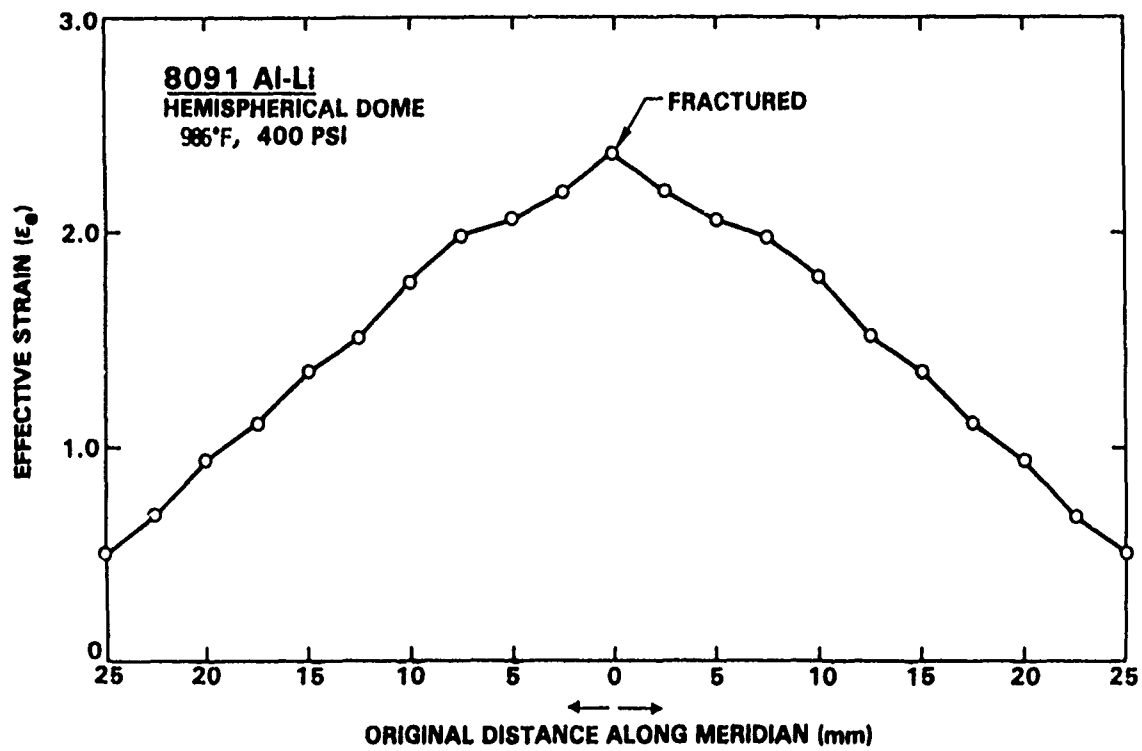
Figure 2-40. Strain Distribution on the Meridian of the Hemispherical Dome
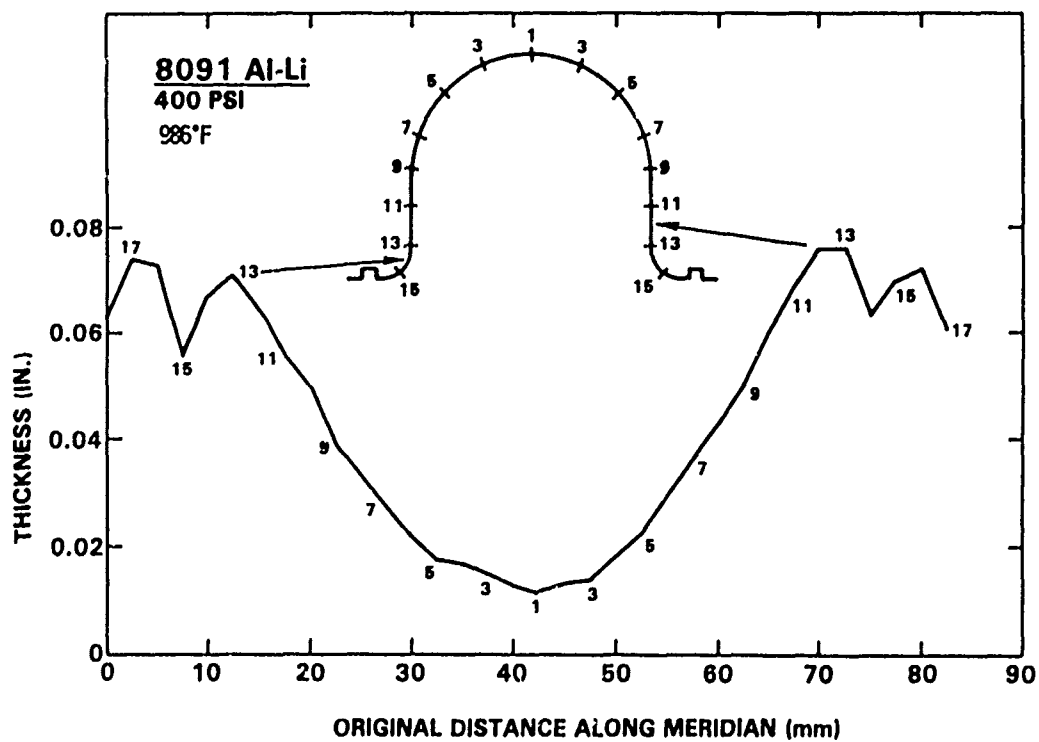
Figure 2-41. Thickness Distribution Along the Meridian of Hemispherical Dome
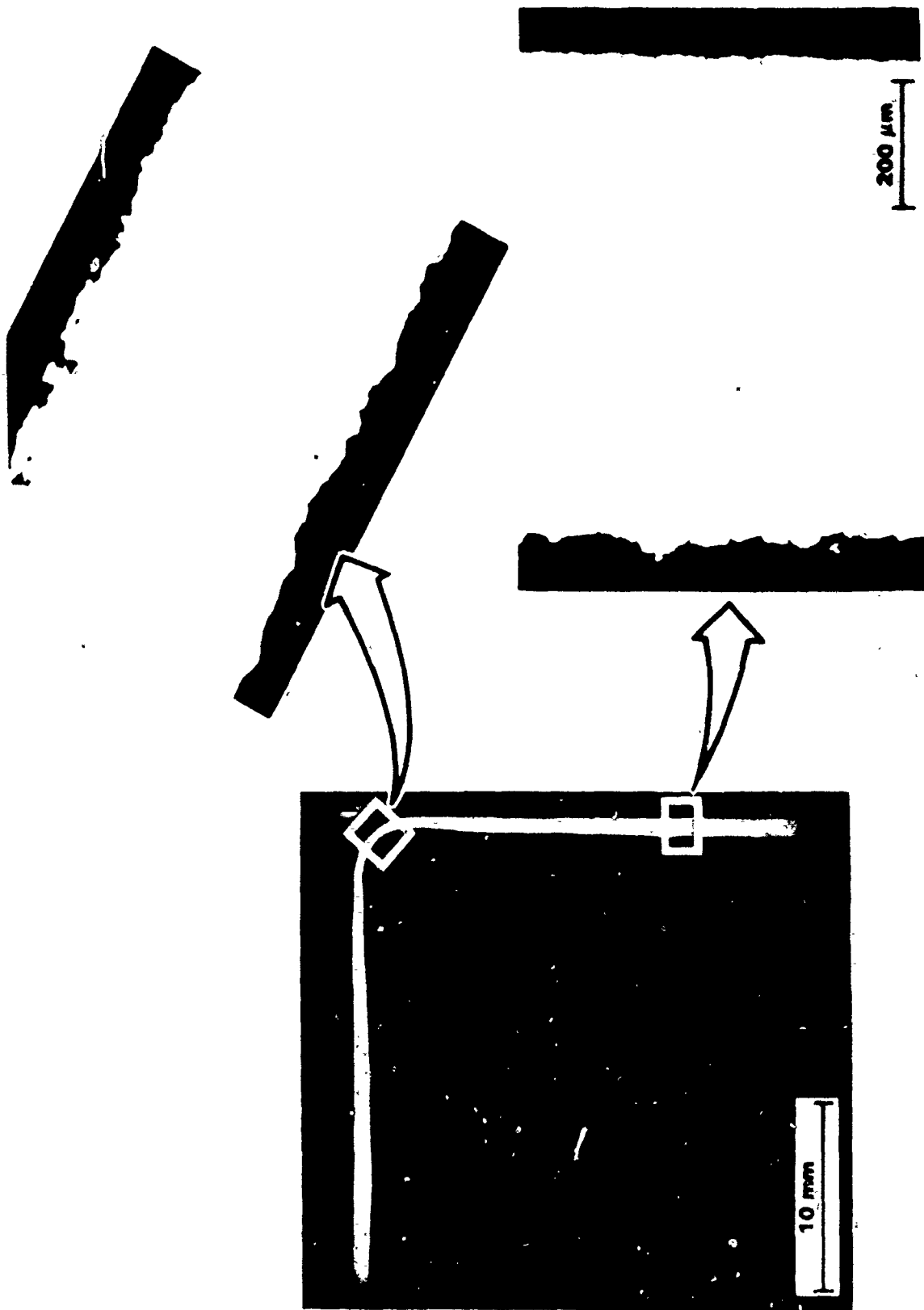
Figure 2-42. Metallographic Analysis of Cavitation in Rectangular Pan, 400 psi, 986°F
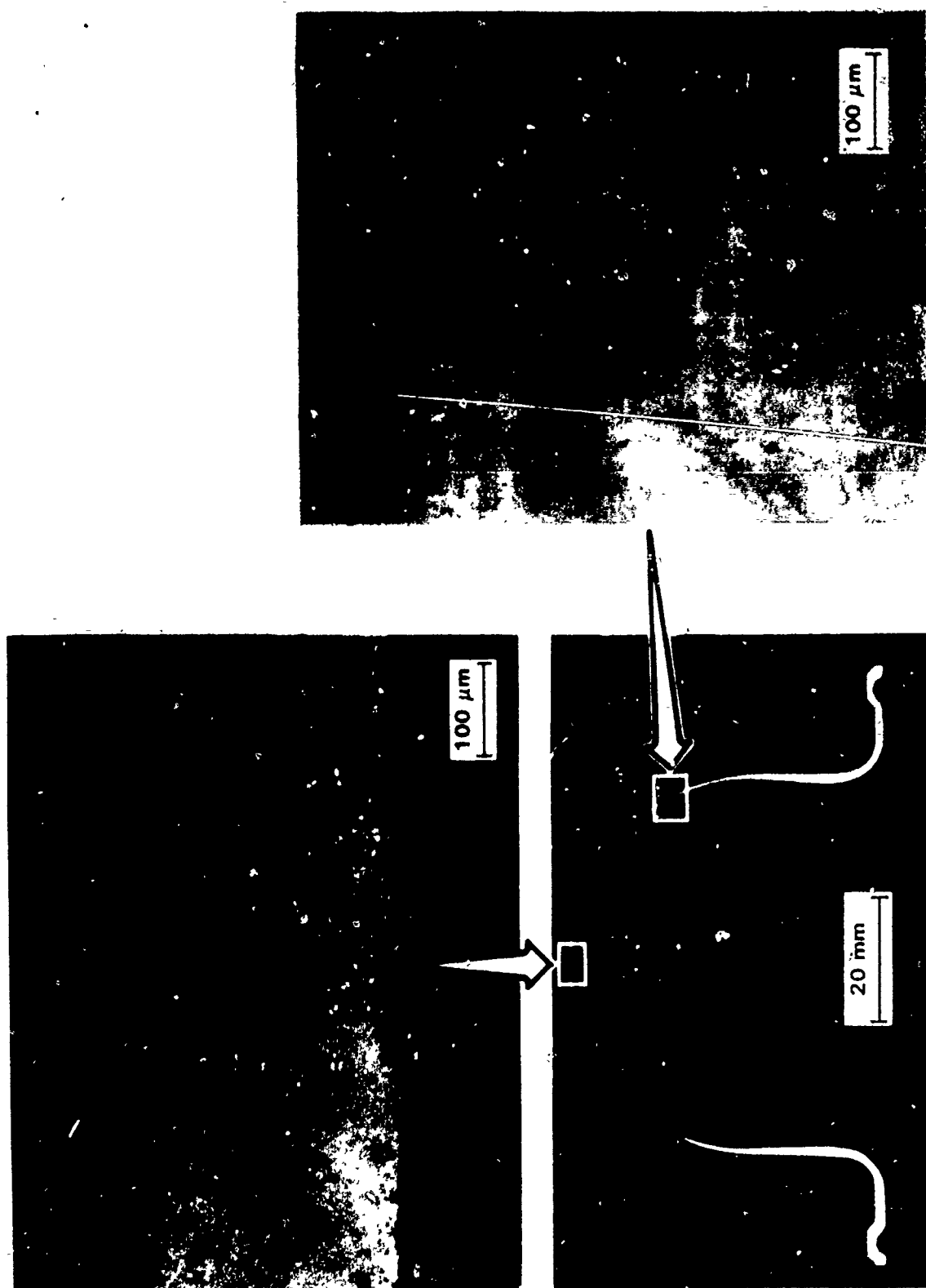
Figure 2-43. Metallographic Analysis of Cavitation in Hemispherical Pan, 400 psi, 986°F

2.2.3.2 DESIGN DATA GENERATION

SPF test material in the form of 6-by-18-by 18 inch has been fabricated to support the development of preliminary design allowables for the SPF 8091 Al-Li material. The fabricated pans contain varying amounts of strain which will permit a critical assessment of the mechanical property behavior of the material relative to SPF processing technology. The mechanical property test plan for the optimized SPF material property characterization task is delineated in Table 2-10. Individual tests requiring heat treatment will be solution treated at 1013°F, water quenched, and aged at 365°F. Machining of the individual test coupons for subsequent material property testing is currently in progress.

TABLE 2-10

ENGINEERING DESIGN DATA TEST MATRIX FOR SPF AL-LI SHEET

| TEST	NUMBER OF COUPONS	
	PRE-SPF	POST-SPF
Tensile Strength, (Smooth)	6	24
Tensile Strength, (Notched)	4	8
*Elevated Temp. Tensile (Smooth)	4	8
Fracture Toughness (Kc)	2	2
Smooth Fatigue Life	8	16
Notch Fatigue Life	8	16
Fatigue Crack Propagation	2	2
Compression Strength	4	4
Shear Strength	4	4
Bearing Strength	4	4
Exfoliation Corrosion	1	3
Stress Corrosion	3	3
Residual Tensile Strength (Post-SCC)	3	3
Chemical Analysis	1	3

* Elevated temperature tests are being conducted at 200 to 300°F.

2.2.4 HEAT TREATMENT EVALUATION

2.2.4.1 Post-SPF Heat Treatment Optimization Studies

Commercially available aluminum-lithium alloys rely on thermomechanical processing for property optimization. Such processing usually involves a solution heat-treatment, controlled stretch, and isothermal aging. Relative to superplastic formed material (i.e., parts) the intermediate step of controlled stretch is not practical if not impossible. Optimized properties in SPF-formed Al-Li components, therefore, must be approached through thermal processing (i.e., solution heat treatment, quenching and some combination of aging parameters). Thus, a task was developed and implemented with an objective of developing optimized post-SPF strength levels for the 8091 Al-Li alloy being characterized for this program.

2.2.4.2 Text Matrix for Optimization of 8091 Al-Li Heat Treatment

The optimization of the 8091 Al-Li heat treatment and corresponding property development was undertaken at Washington State University. The several test matrixes used in the optimization study examined three solution heat treatment (SHT) temperatures, the natural aging behavior, the artificial aging, the quench sensitivity of the material, and duplex aging cycles. The test matrixes are shown in Tables 2-11 and 2-12. The properties of the materials were initially characterized by hardness testing with property validation which was accomplished by tensile testing.

The test matrix was divided into two main sections: The first section describes the optimization of a heat treatment cycle for as-received (AR) material, while the second section describes the test matrix for superplastically formed 8091 material. Each of the two sections has two subtasks. The initial subtask features heat treatment evaluation using hardness data. The second subtask verifies the optimum thermal processing parameters using tensile testing.

To develop heat treatment parameters in a timely manner, it was decided to use as-received material, especially processed for SPF for the initial screening. Property validation would use SPF-processed material. This was necessary because the initial heat treatment studies were conducted concurrently with SPF material characterization studies.

2.2.4.3 Natural Aging Study

The initial testing at Washington State University used as-received 8091 Al-Li which was especially processed for SPF but was not formed. The material was sectioned into 1- by 6-inch strips and solution heat-treated. The solution heat treatment was conducted in an open air furnace for 1 hour and 15 minutes at the designated test temperature followed by immediate cold water

TABLE 2-11

ISOTHERMAL AGING TEMPERATURES TEST MATRIX; SOLUTION
HEAT TREATED FOR 1.25 HOURS

Solution Heat Treatment Temperature	959°F	986°F	1013°F
Natural Age	Ambient Temp	Ambient Temp	Ambient Temp.
Artificial Age	293°F	293°F	193°F
Artificial Age	311°F	311°F	311°F
Artificial Age	329°F	329°F	329°F
Artificial Age	338°F	338°F	338°F
Artificial Age	365°F	365°F	365°F
Artificial Age	383°F	383°F	383°F
Artificial Age	437°F	437°F	437°F

TABLE 2-12

DUPLEX AGING TEMPERATURE TEST MATRIX; SOLUTION HEAT TREATED
FOR 1.25 HOURS

Solution Heat Treatment Temperature	959°F	986°F	1013°F
Temp. 1	167°F	167°F	167°F
Temp. 2	212°F	212°F	212°F
Temp. 3	257°F	257°F	257°F
Temp. Final	Optimum	Optimum	Optimum

quench. The strips of 8091 (to be used for the natural aging study) were cut into hardness specimens with approximate 0.5- by 1-inch dimensions. The coupons were lightly ground prior to testing to assure accurate hardness readings. Hardness tests were conducted on a Rockwell superficial hardness tester with 45T scale.

The results of the natural aging study (up to 5000 hours duration) are summarized in Figure 2-44. The hardness of the material that was solution heat treated at all three temperatures did not change significantly for the first 10 hours of natural aging. Once the initial 10 hours of aging were complete, the material began to rapidly age. The coupon that was solution heat treated at 1013°F aged more rapidly than the coupons solution heat treated at 986°F or at 959°F and maintained higher hardness levels to the completion of the study at 5000 hours. The mechanism for natural aging appeared indicative of a nucleation and growth process which is not typical in conventional aluminum alloys.

The natural aging study branched into a low temperature aging study. The temperatures examined were 5, 35, 68°F (ambient temperature), and 113°F. All coupons were solution heat treated at 986°F for 1 hour and 15 minutes, immediately water quenched, and aged at the test temperatures listed above. The results of this study, seen in Figure 2-45, show that the 5 and 35°F aging temperatures delayed the onset of natural aging for up to 1000 hours. After the 1000 hour mark, the materials began to naturally age slowly. The aging temperature of 113°F hastened the natural aging response but did not increase the final hardness of the material.

2.2.4.4 Isothermal Aging

The next step in the study of the as-received 8091 Al-Li aging response was to artificially age the material after solution heat treatment. The hardness coupons were prepared as in the natural aging study but upon removal from the quench tank and following drying, the coupons were placed in various open air aging furnaces at different test temperatures. The temperatures examined were 311, 329, 338, 365, 383, and 437°F. The results for all three solution heat treatment temperatures are shown in Figures 2-46 through 2-52. The isothermal aging studies indicated a tendency for rapid overaging in coupons aged at 437°F at all three solution heat treatment temperatures. Aging temperatures of 311 and 329°F achieved the highest hardness values for aging times of 100 to 1000 hours. Aging times greater than approximately 48 hours are viewed as impractical for production use and will be avoided if possible. The temperatures which gave the best aging response for relatively short times were 365 and 338°F. The data in Figures 2-51 and 2-52 indicate that the aging response at 338°F was highest at the solution heat-treatment temperature of 1013°F, while the response at 365°F was highest at the 986°F solution heat treatment temperature. It appears from Figures 2-49 through 2-52 that the aging response has a dependence on the solution heat treatment temperature used. The "dependence affect" becomes more pronounced as the aging temperature increased from 311 to 365°F. Based on the hardness
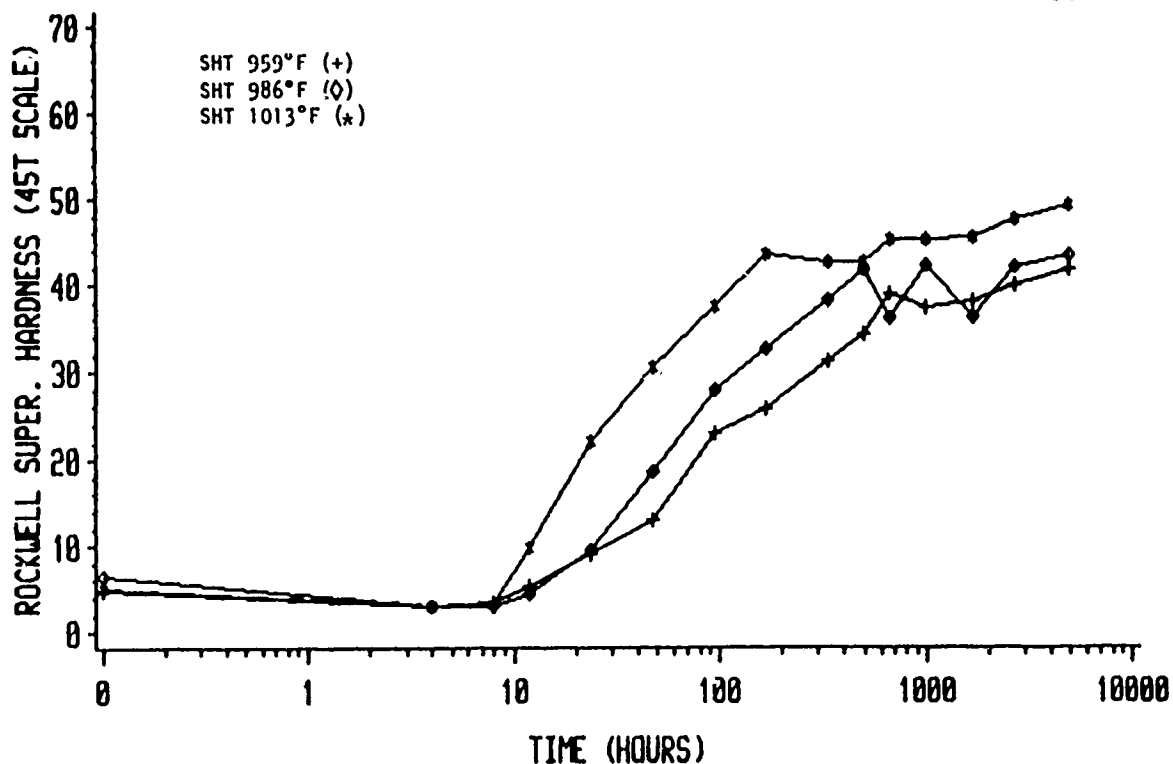
Figure 2-44. Data Curves Illustrating the Natural Aging Behavior Found in the As-rolled Condition of 8091 Al-Li Alloy Following Three Different Solution Heat Treatment Temperatures
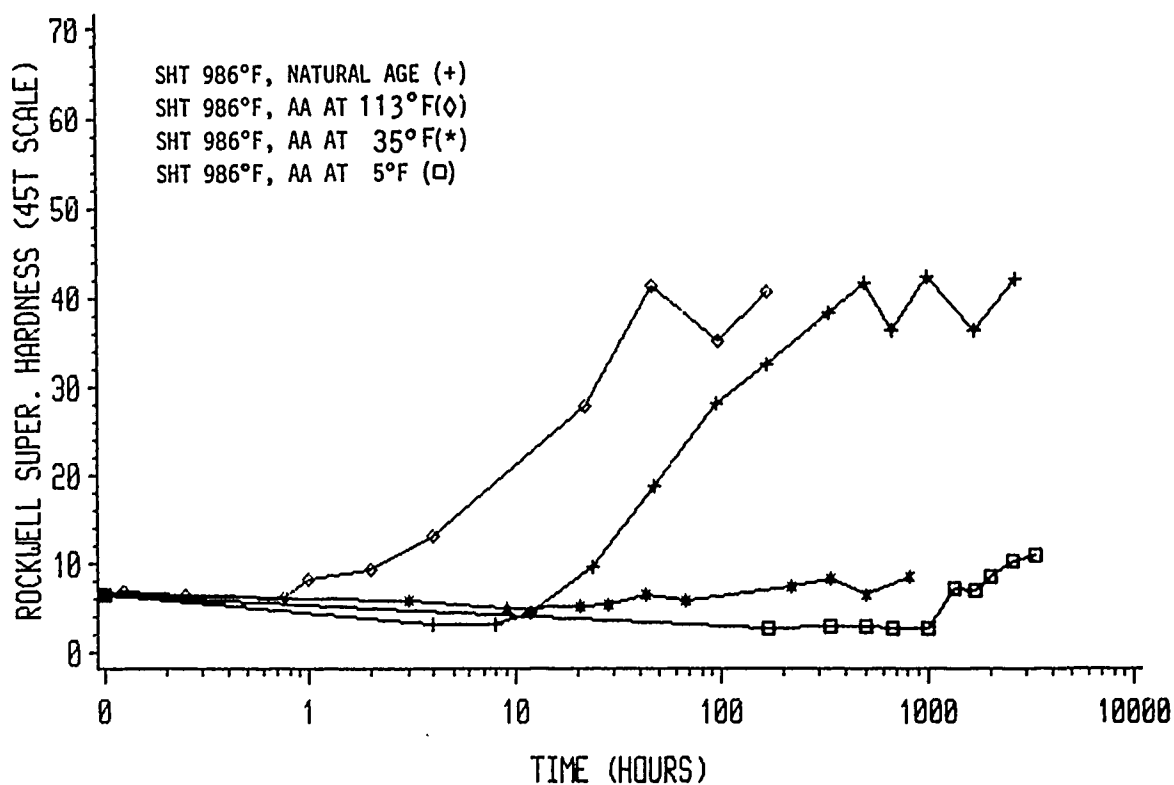
Figure 2-45. Comparison Between Natural and Artificial Aging Behavior of 8091 Al-Li; As-received Material was Solution Heat Treated at 986°F and Then Aged for Various Times
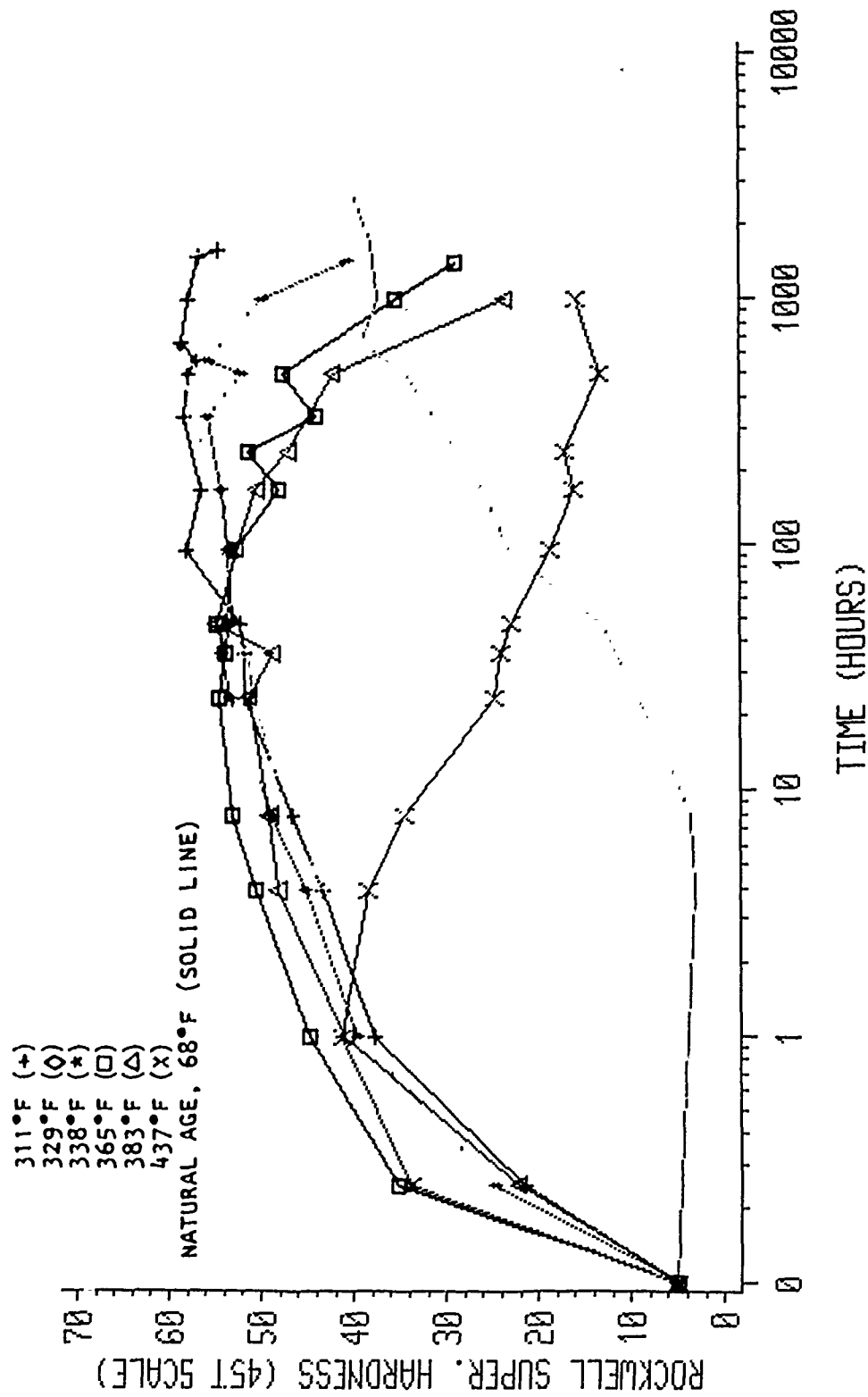
Figure 2-46. Composite Graph Illustrating Both Artificial and Natural Aging Behavior
Found in 8091 Al-Li Alloy After Solution Heat Treatment at 959°F
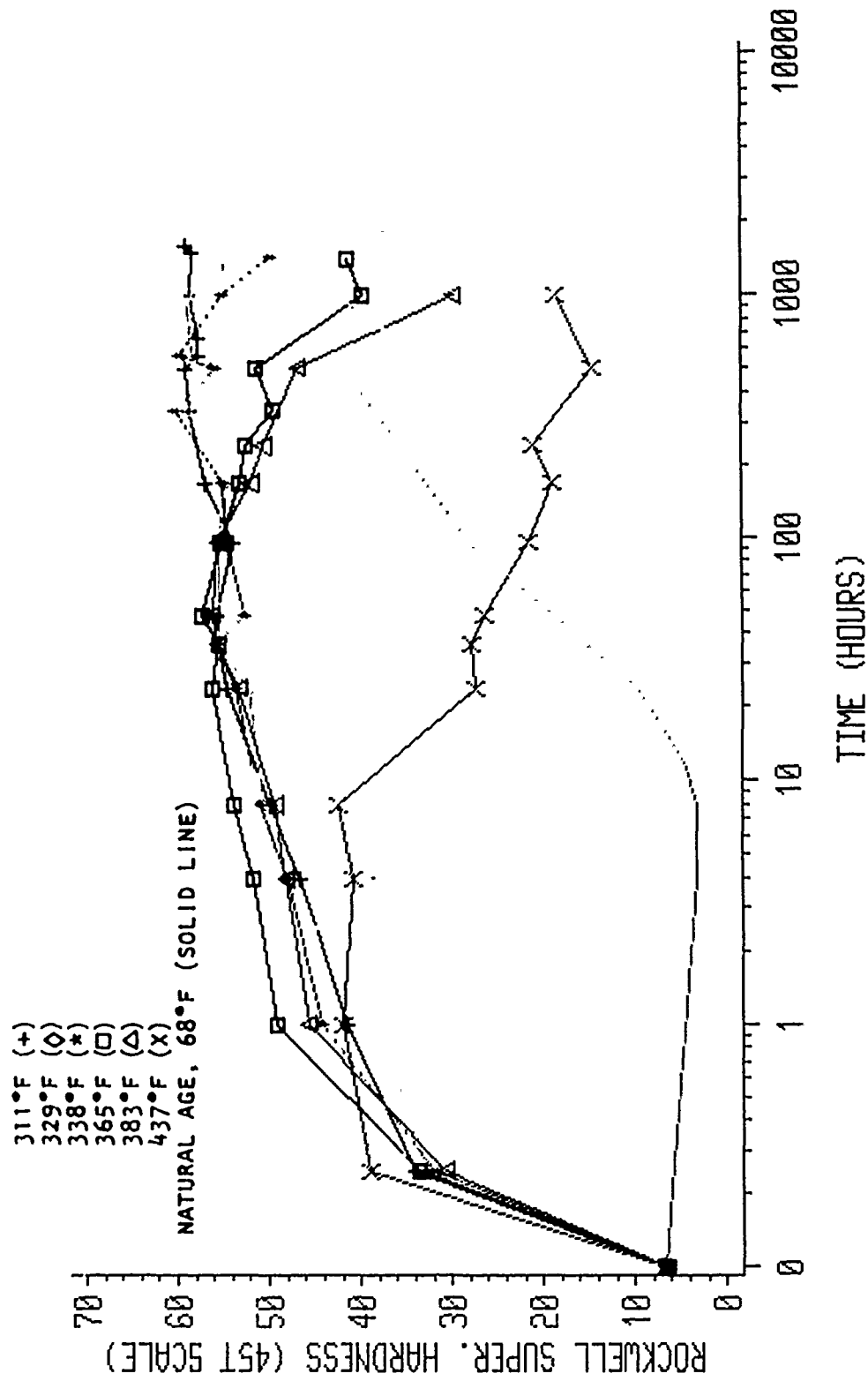
Figure 2-47. Composite Graph Illustrating Both Artificial and Natural Aging Behavior Found in 8091 Al-Li Alloy After Solution Heat Treatment at 986°F
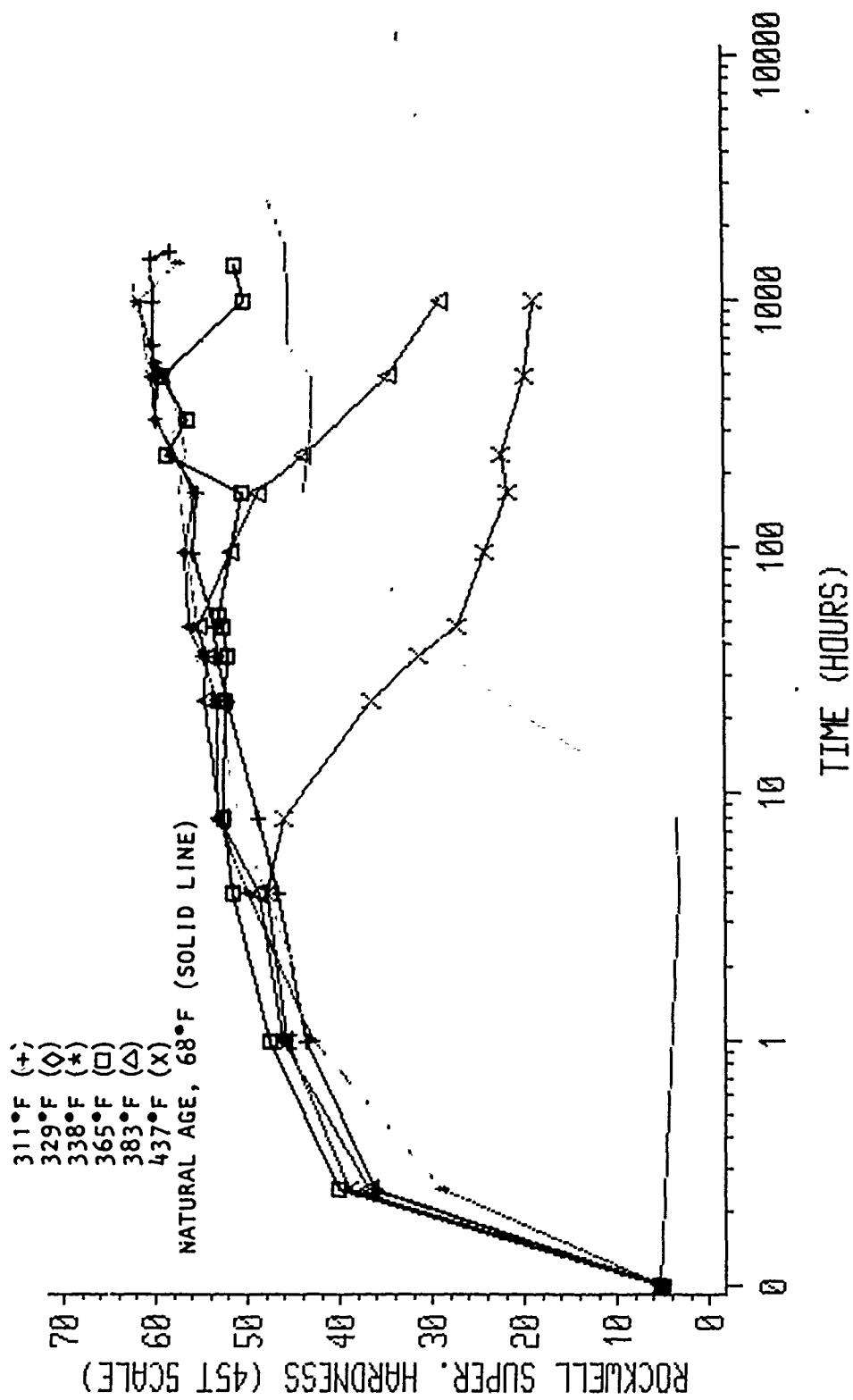
Figure 2-48. Composite Graph Illustrating Both Artificial and Natural Aging Behavior Found in 8091 Al-Li Alloy After Solution Heat Treatment at 1013°F

Figure 2-49. Data Curves Illustrating Artificial Aging Behavior Found in 8091 Al-Li Alloy at 311°F Following Three Different Solution Heat Treatment Temperatures

Figure 2-50. Data Curves Illustrating Artificial Aging Behavior Found in 8091 Al-Li Alloy at 329°F Following Three Different Solution Heat Treatment Temperatures

Figure 2-51. Data Curves Illustrating Artificial Aging Behavior Found in 8091 Al-Li
Alloy at 338°F Following Three Different Solution Heat Treatment
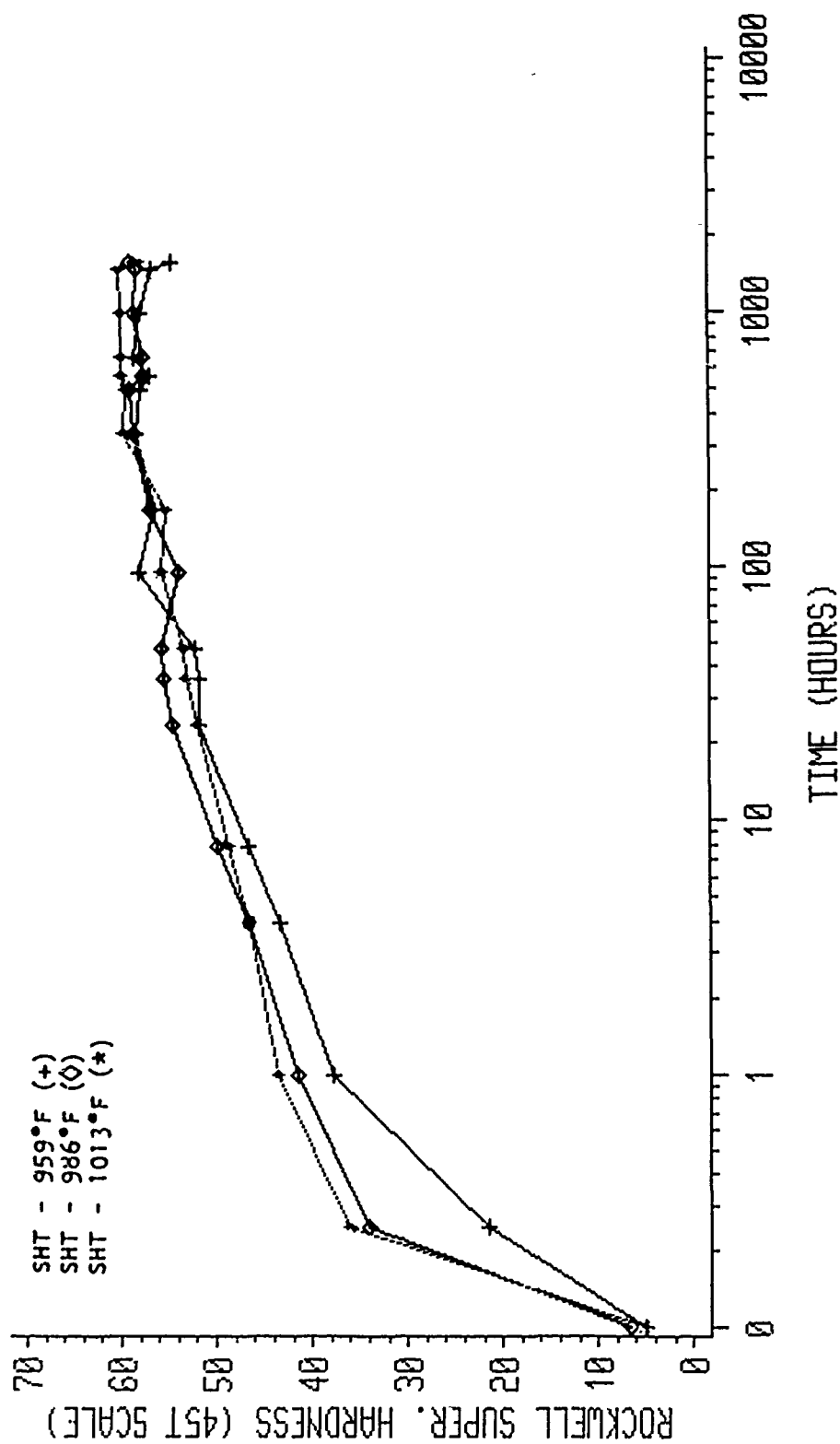Temperatures

Figure 2-52. Data Curves Illustrating Artificial Aging Behavior Found in 8091 Al-Li Alloy at 365°F Following Three Different Solution Heat Treatment Temperatures
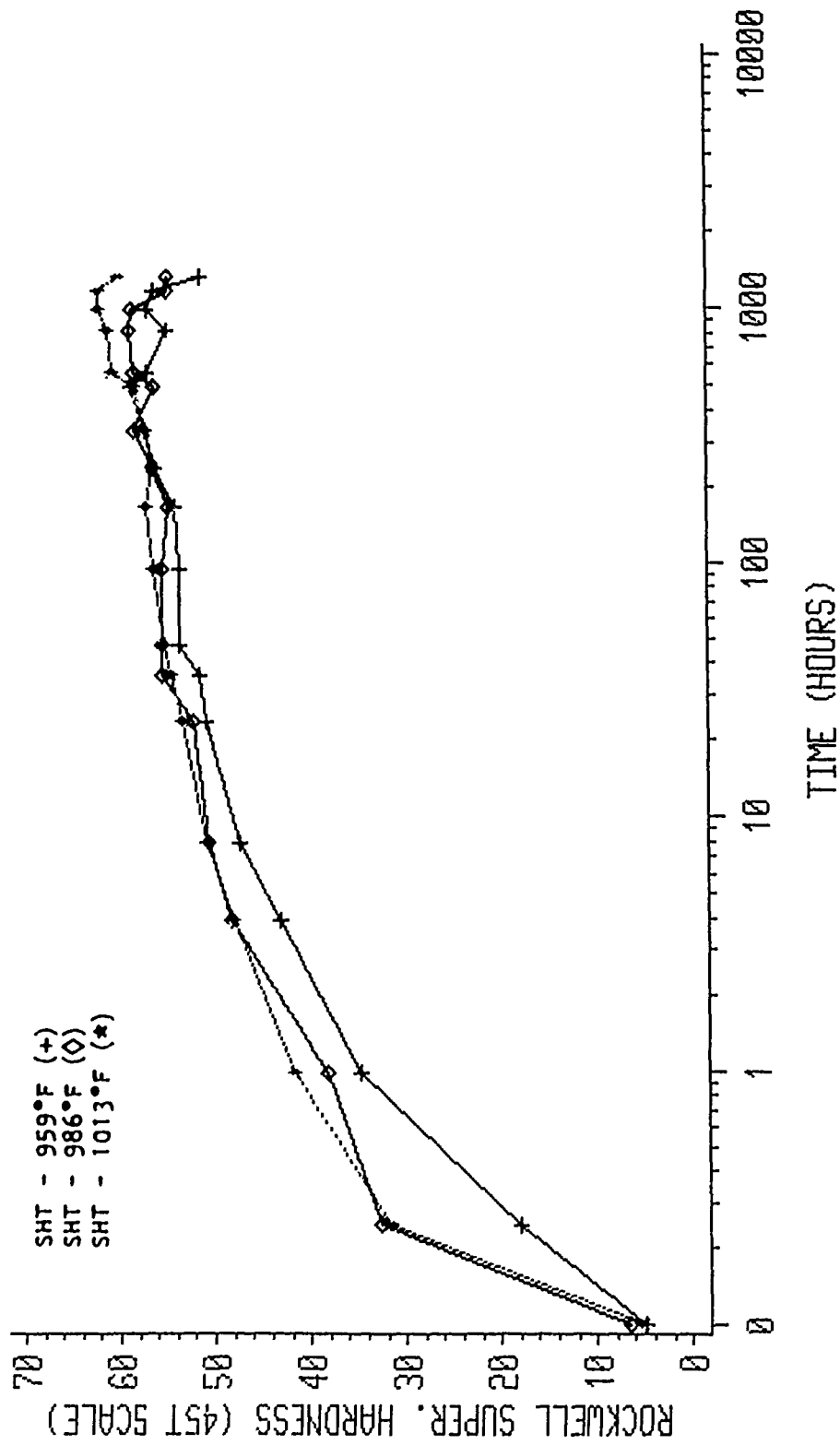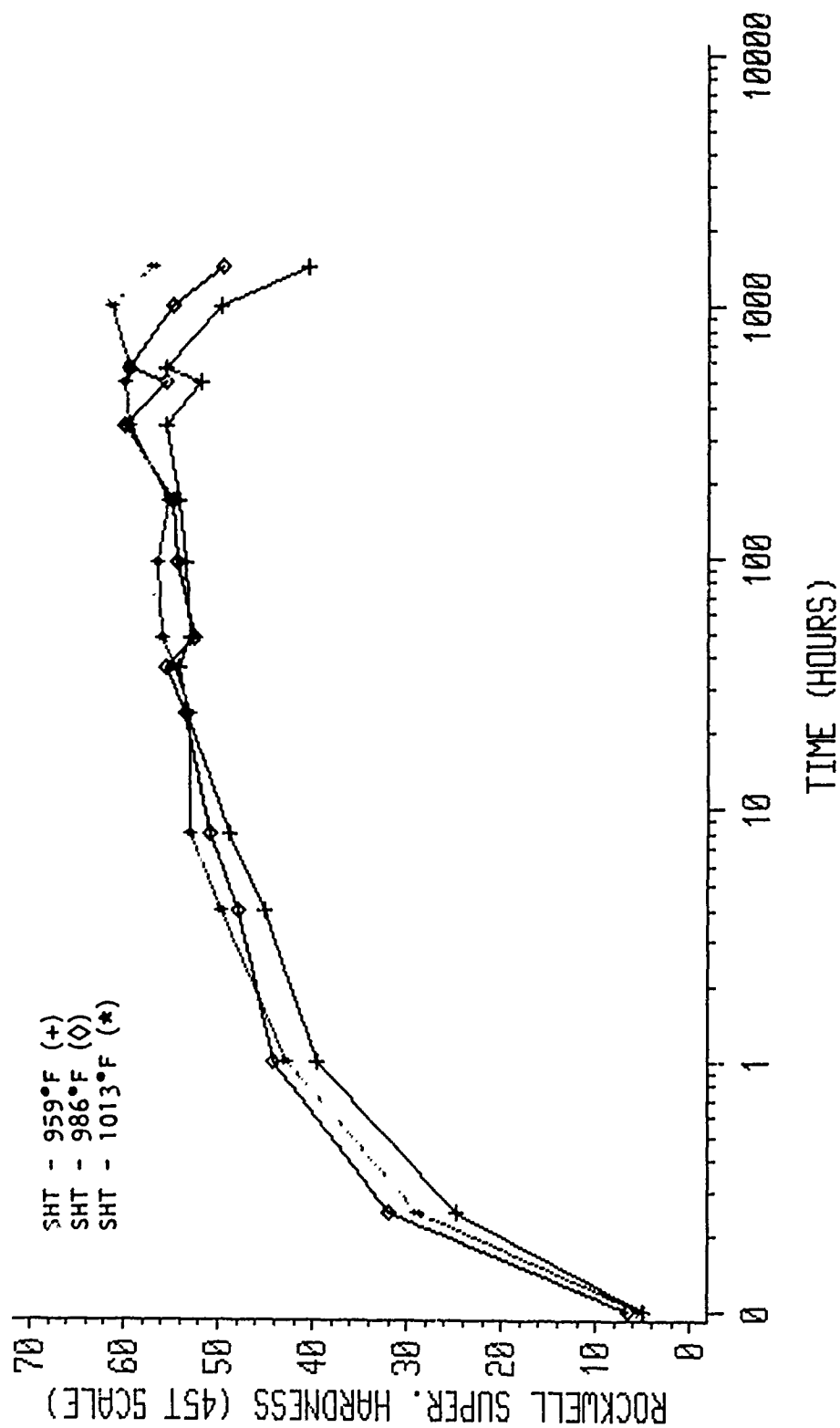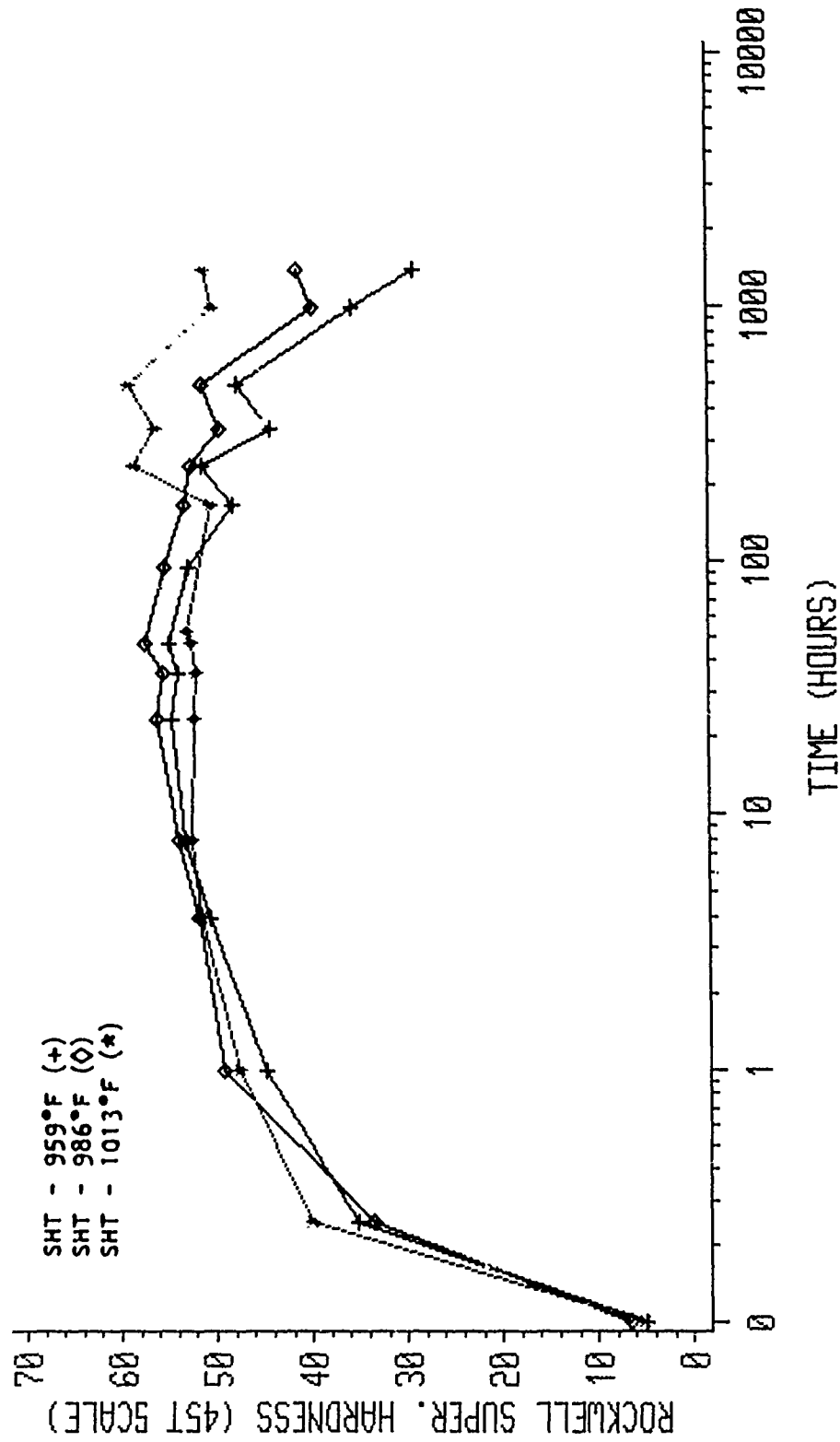
data for the artificial aging response of the 8091 Al-Li, the solution heat-treatment temperature of 1013°F resulted in the highest hardness values.

An examination was initiated to observe the effects that a natural aging interval would have on the artificial aging behavior of 8091. An important consideration in the design of the matrix for these tests was the strong, natural aging response a solution heat-treatment of 1013°F produced in the material. The objective of the study was to determine whether the precipitates found from different natural aging intervals would act as nucleation sites for the precipitates that appear at much higher artificial aging temperatures. A related consideration was whether or not low temperature precipitates would survive the higher temperatures without dissolving. The test coupons were prepared similarly to the natural aging study coupons. Figure 2-53 shows the naturally aged conditions of the material prior to aging at 365°F. Figure 2-54 shows the results from the subsequent aging at 365°F. Hardness data for the material that did not have a natural aging interval were included for comparison with materials naturally aged from 24 to 168 hours. The material that did have a natural aging interval appeared to reach a peak hardness sooner than the material without the natural aging. Washington State University believes that more tests are necessary to fully predict the behavior of the natural aging effect on the artificial aging response for 8091.

2.2.4.5 Ramp and Soak Profile

The objective of the duplex aging study is to evaluate the potential for increasing strength and/or reducing aging time by varying the aging temperature-time combinations. The aging response resulting from the test parameters listed in Table 2-12 was also determined from the hardness testing. Initial tests used solution heat-treatment temperatures of 1013°F for 1 hour and 15 minutes. The two additional solution heat-treatment temperatures (959 and 986°F) will be examined once the optimum duplex aging parameters for the 1013°F solution heat-treatment test are determined. Any reduction in solution heat-treatment time for the duplex aging studies will result from the quench sensitivity studies (Subsection 2.2.4.6) concerning as-received 8091 Al-Li.

The duplex aging treatment will occur in a ramp and soak environment. The final temperature will result in the peak hardness values discussed in Subsection 2.2.4.4. The three ramp and soak profiles used for the initial phase of this study are presented in Figures 2-55 through 2-57. The data in Figures 2-58 through 2-60 compared each ramp and soak profile with the isothermal aging curve for 365°F. The isothermal hardness being compared with the ramp and soak data were subjected to the identical solution heat-treatment parameters prior to aging. Profile 1's (Figure 2-59) hardness values were significantly less than the isothermal aging cycle until aging times of 125 hours had elapsed. The exceptionally long aging times required
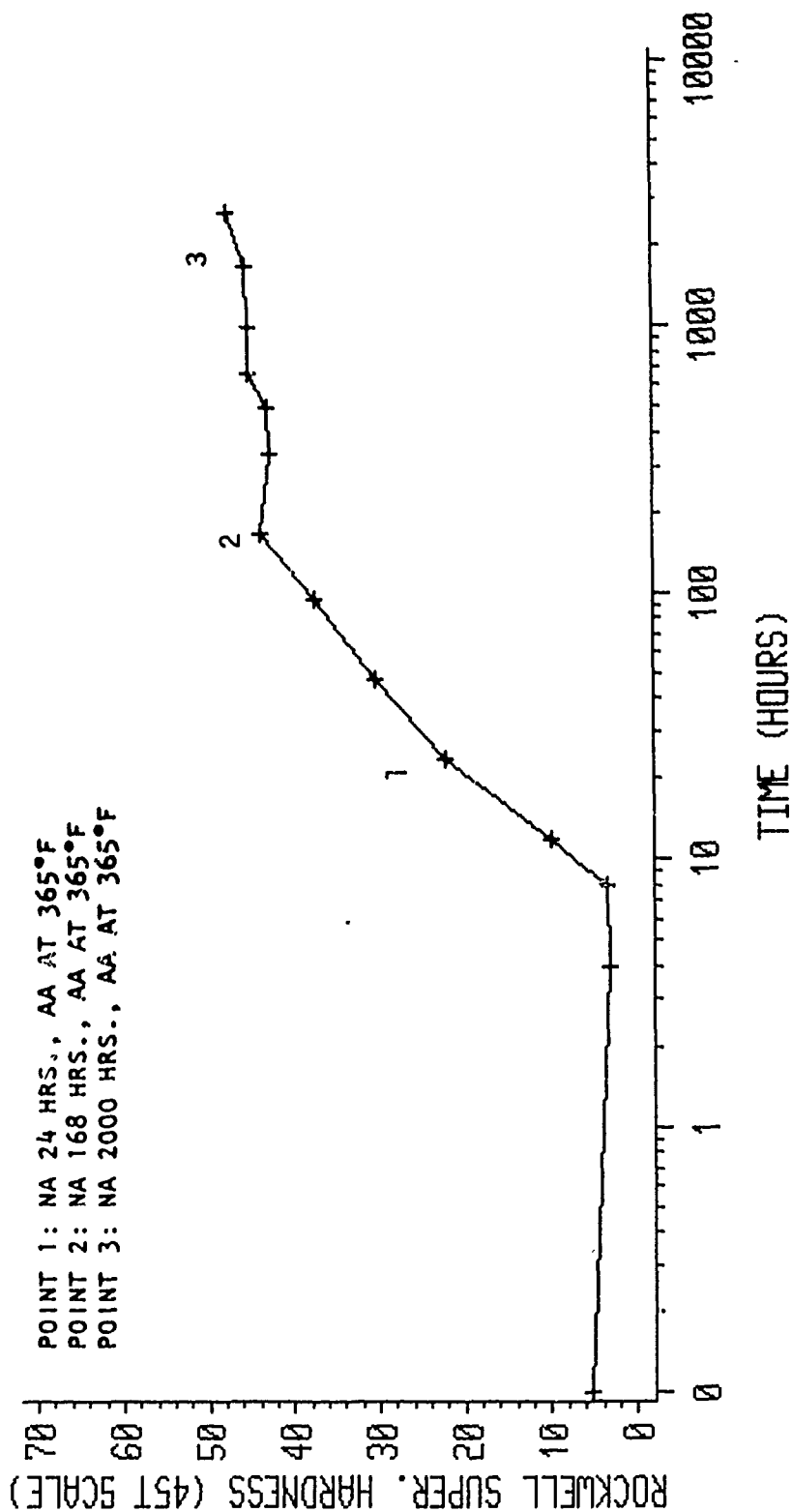
Figure 2-53. Data Curve Illustrating Natural Aging Behavior After Solution Heat Treatment at 1013°F. The Three Designated Points Indicate Starting Conditions of the Alloy for a Natural Age (24 Hours, 168 Hours and 2000 Hours)/ Artificial Age (365°F) Study
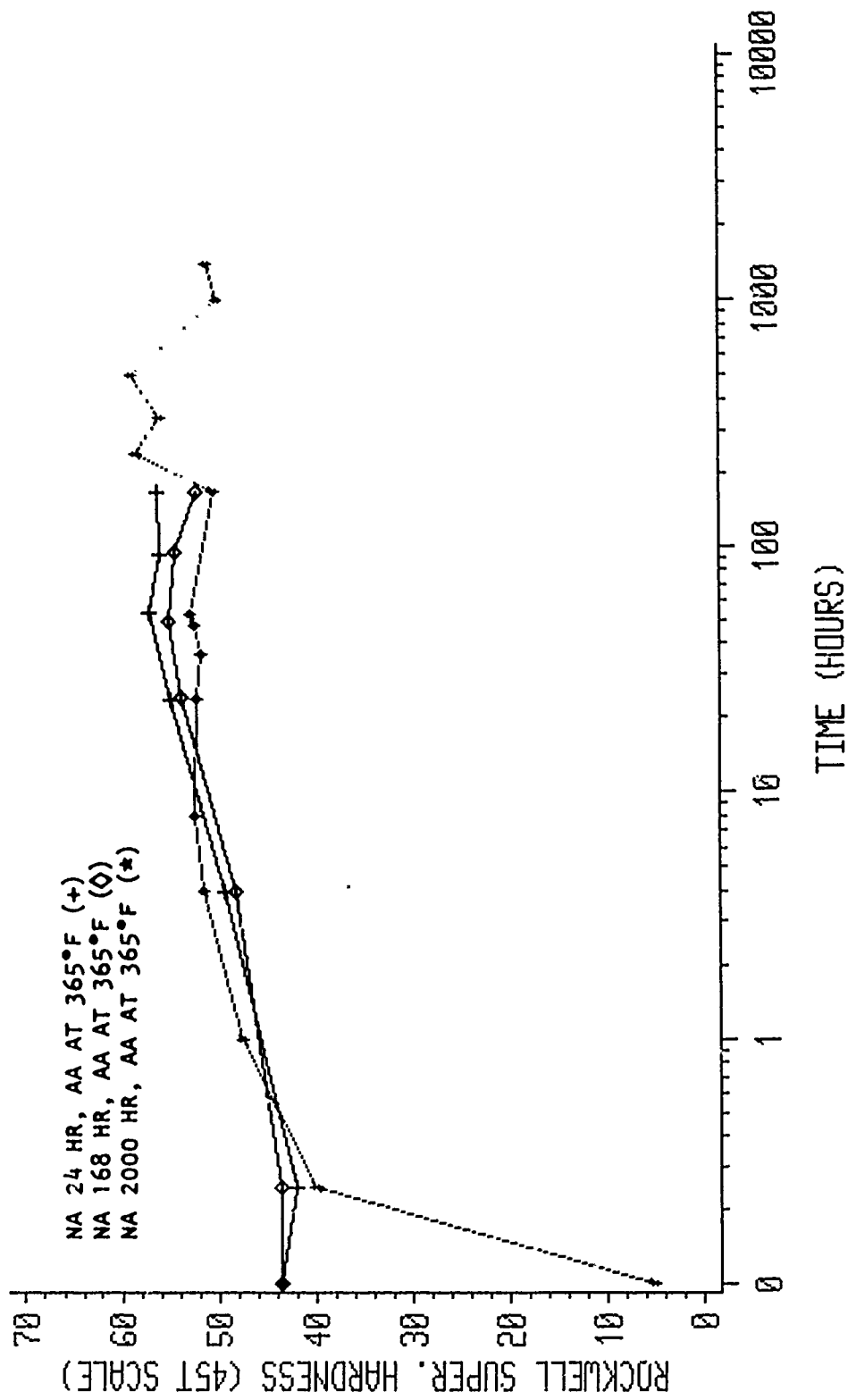
Figure 2-54. Graphic Illustration of the Behavior from Two Natural/Artificial Aging Studies Compared With an Artificial Aging Curve at 365°F. The As-received Material was Solution Heat Treated at 1013°F Prior to Aging.
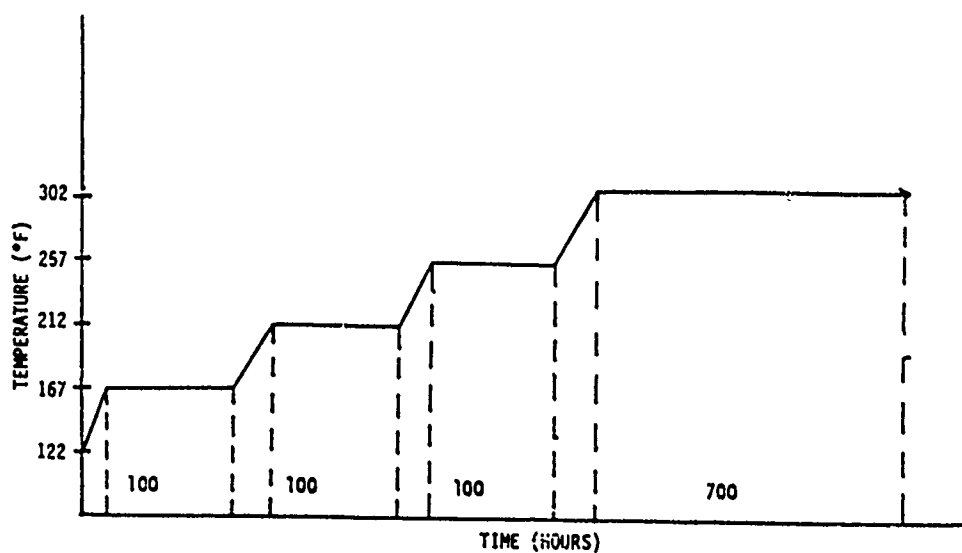
Figure 2-55. Ramp and Soak Profile 1; Material was Initially
Solution Heat Treated at 1013°F
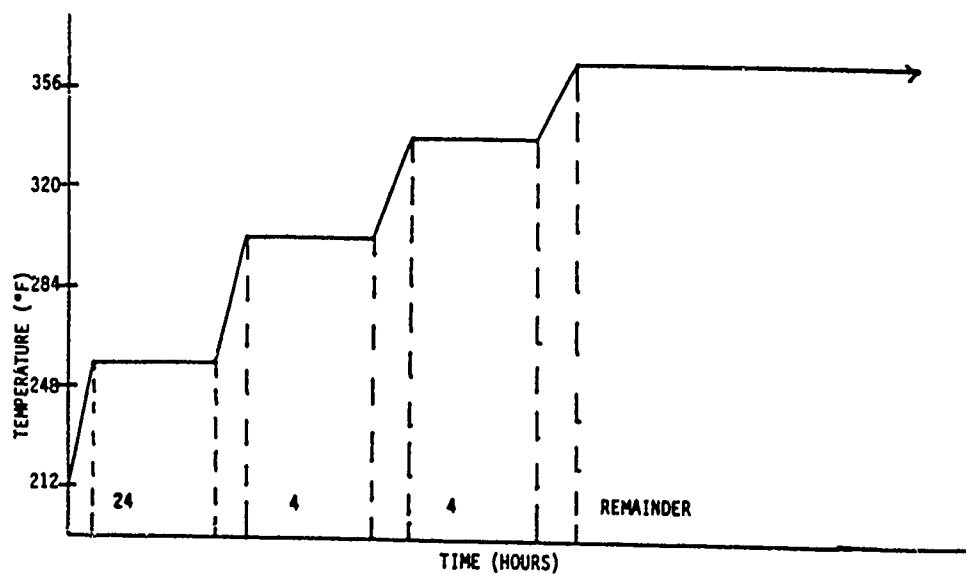
Figure 2-56. Ramp and Soak Profile 2; Material was Initially
Solution Heat Treated at 1013°F
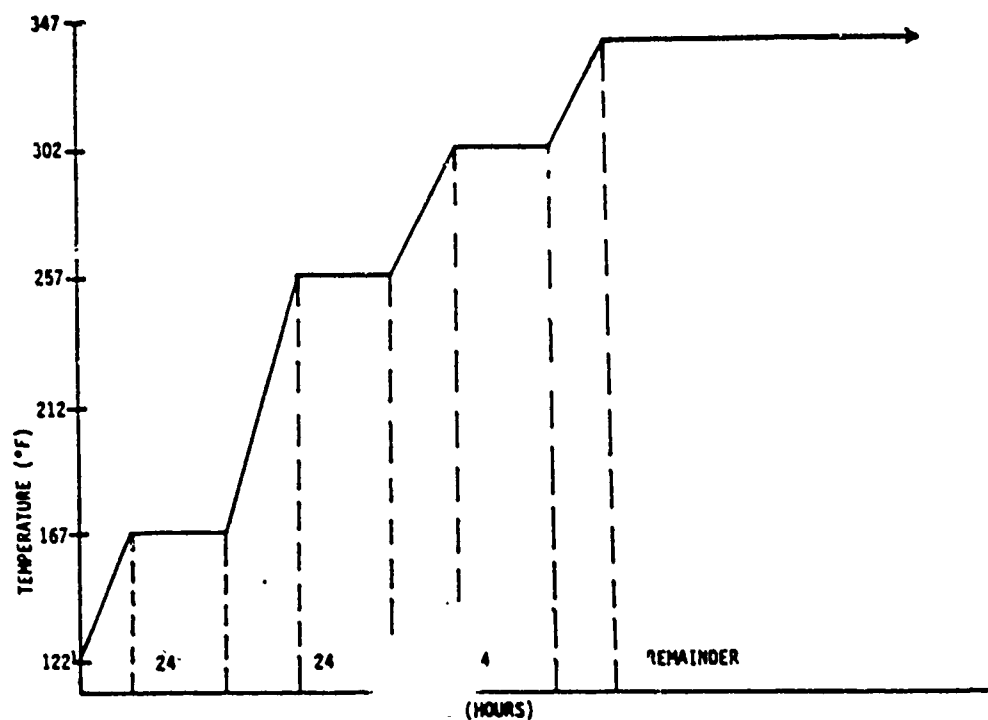
Figure 2-57. Ramp and Soak Profile 3; Material Initially Solution Heat Treated at 1013°F
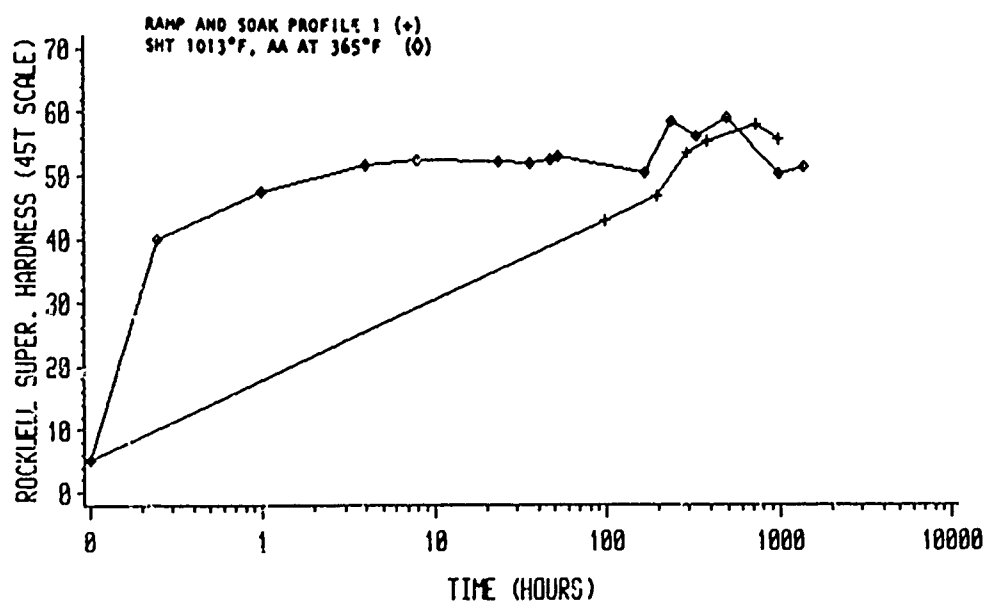
Figure 2-58. Hardness Results for Ramp and Soak Profile 1. The As-received Material was Solution Heat Treated at 1013°F for 1.25 Hours and Then Artificially Aged 100 Hours/167°F, 100 Hours/212°F, 100 Hours/257°F, and 700 Hours/311°F. Also Shown is AA/365°F
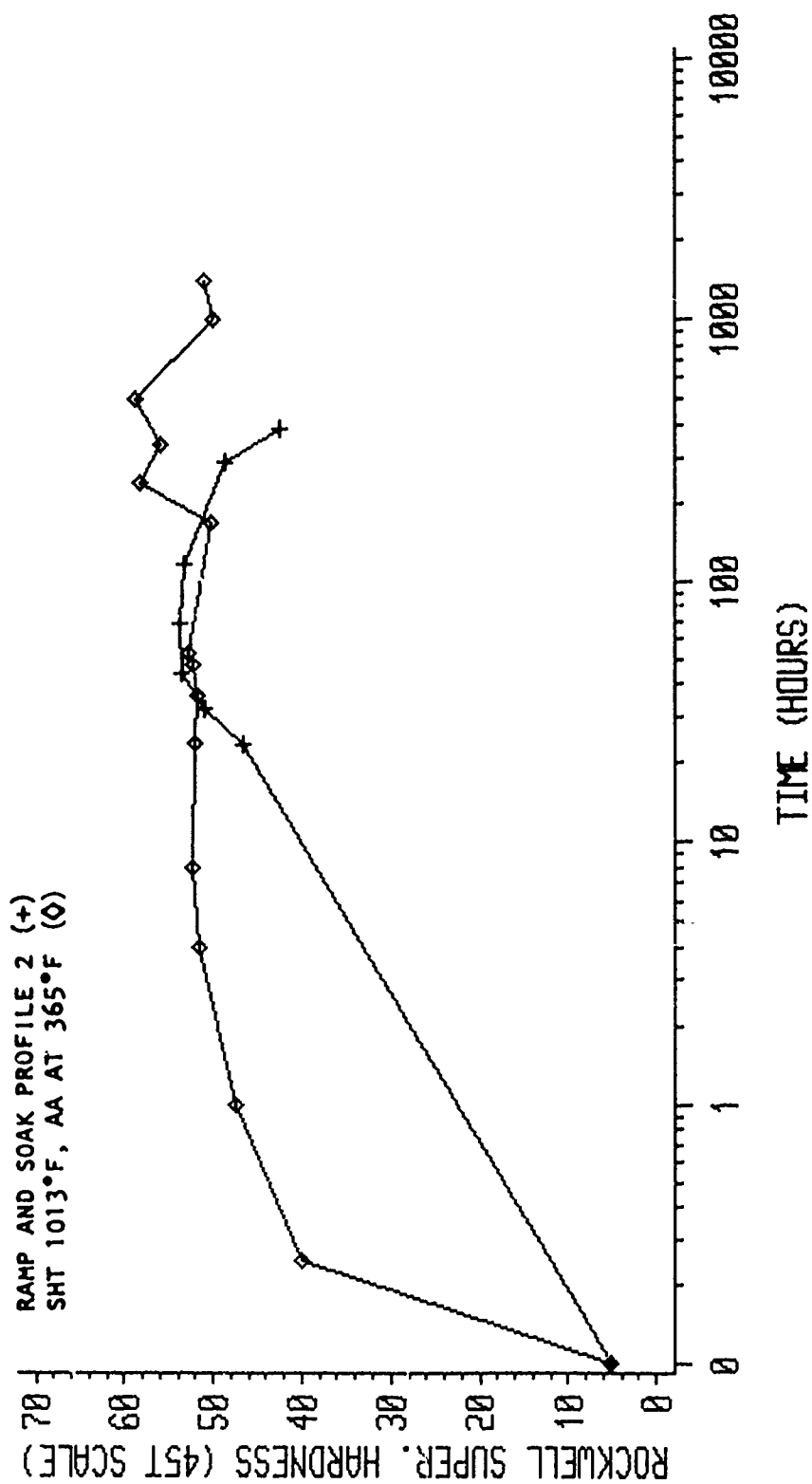
Figure 2-59. Hardness Results for Ramp and Soak Profile 2. The As-rolled Material was Solution Heat Treated at 1013°F for 1.25 Hour and Then Artificially Aged: 24 Hours/257°F, 4 Hours/302°F, 4 Hours/338°F, 350 Hours/365°F. Also Shown is AA at 365°F (Isothermal).
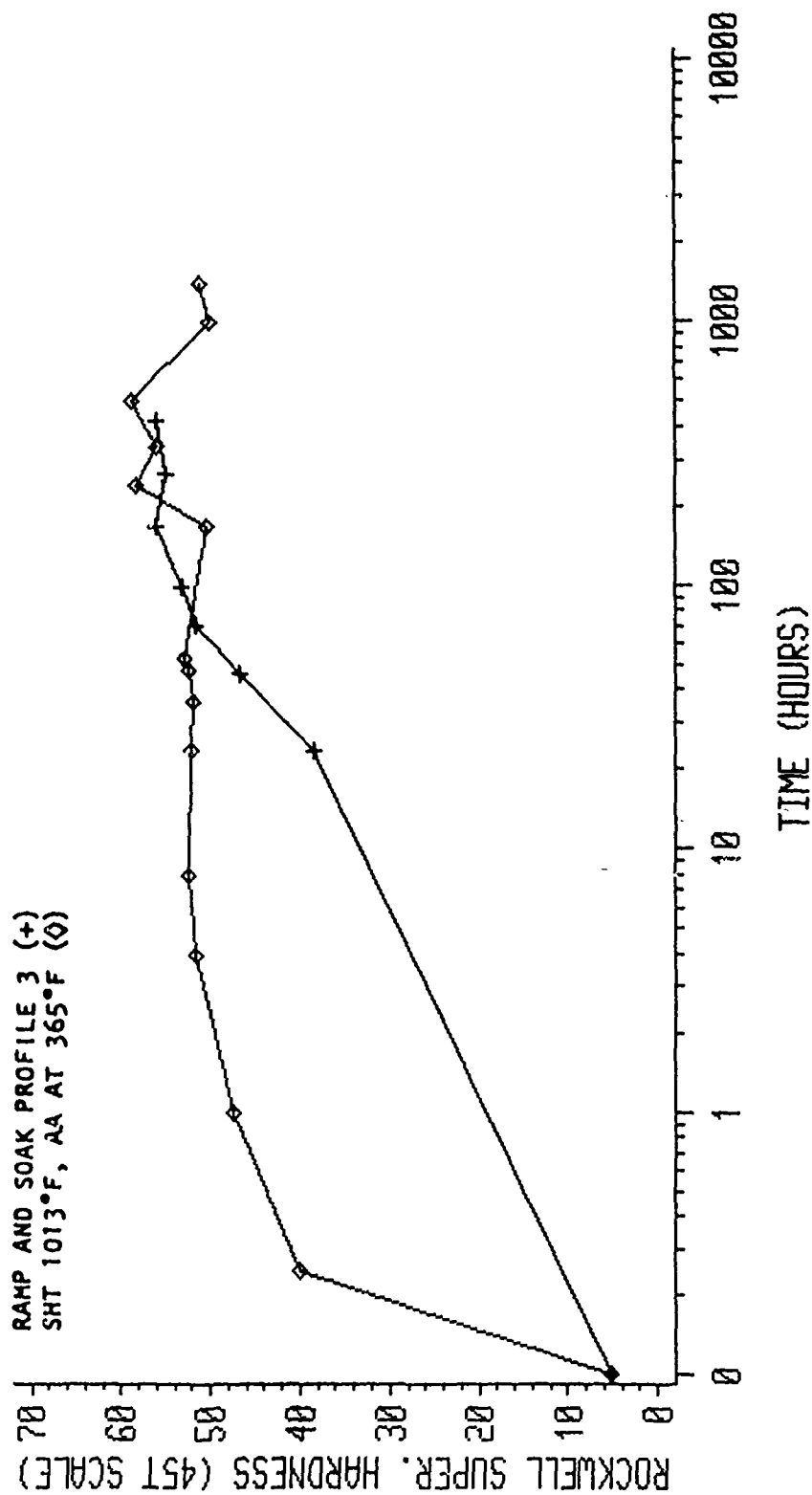
Figure 2-60. Hardness Results for Ramp and Soak Profile 3. The As-rolled Material was Solution Heat Treated at 1013°F for 1.25 Hours and Then Artificially Aged: 24 Hours/167°F, 24 Hours/257°F, 24 Hours/302°F, 348 Hours/338°F. Also Shown is AA at 365°F (Isothermal).

for Profile 1 made it an impractical choice for optimization. Profile 2 reached its maximum hardness (which was greater than the hardness of the 365°F cycle) after approximately 30 to 40 hours after which it overaged.

Profile 3 reached the hardness level of the isothermal age at approximately 80 hours and continued to increase with the aging time. The three ramp and soak profiles are graphed together in Figure 2-61. The relatively low initial aging temperatures used in all three profiles resulted in the lowest hardness values. Profile 2 resulted in the highest initial hardness, while Profile 1 resulted in the overall peak hardness. Continued modification to the profiles, which includes higher aging temperatures and shorter times, may produce a better aging response in the material for overall aging times of 24 to 48 hours.

2.2.4.6 Quench Sensitivity

The relatively high initial hardness values that resulted from isothermal aging at 365°F indicated that this temperature should be selected for optimization. The optimization procedure consisted of two parts: First, solution heat-treatment time was decreased from 1.25 to 0.5 hours. Second, three different quench rates were examined: a cold water quench, a cold air blast, and a still air cooling. The results of this optimization and the original 365°F isothermal aging curve are shown in Figure 2-62. These data revealed several factors: first, reduced solution heat-treatment time of 0.5 hours increased the hardness by two values greater than the 1.25 hour solution heat-treatment response. Second, the cold air blast quench resulted in lower initial hardness values through 8 hours of aging time. Once 8 hours of aging time had passed, the hardness values were nearly identical to those obtained from the cold water quench. Finally, as expected, the still air cooling resulted in lower hardness values at all aging times. These data suggest that optimal parameters for the as-received material are a solution heat-treatment at 1013°F for 0.5 hours followed by an immediate cold water quench and a 24 to 48 hour age at 365°F. If all other parameters are held constant, a cold air blast quench may also result in optimal parameters after 24 to 48 hours of aging. Mechanical testing will be conducted to verify these results.

2.2.4.7 Mechanical Properties of As-Received 8091 Al-Li

Once optimal parameters from the isothermal aging and quench sensitivity studies were established, tensile tests were conducted to determine the resulting mechanical properties. In accordance with the ASTM E8 standard, tensile tests were conducted on naturally aged material, and non-optimized isothermal aging studies. The results from the tensile tests gauged the hardness data to the strengthening response in the alloy. The isothermal aging parameters on either side of the aging temperatures which produce the maximum hardness values will be evaluated to determine whether or not they result in a better strength-ductility relationship.
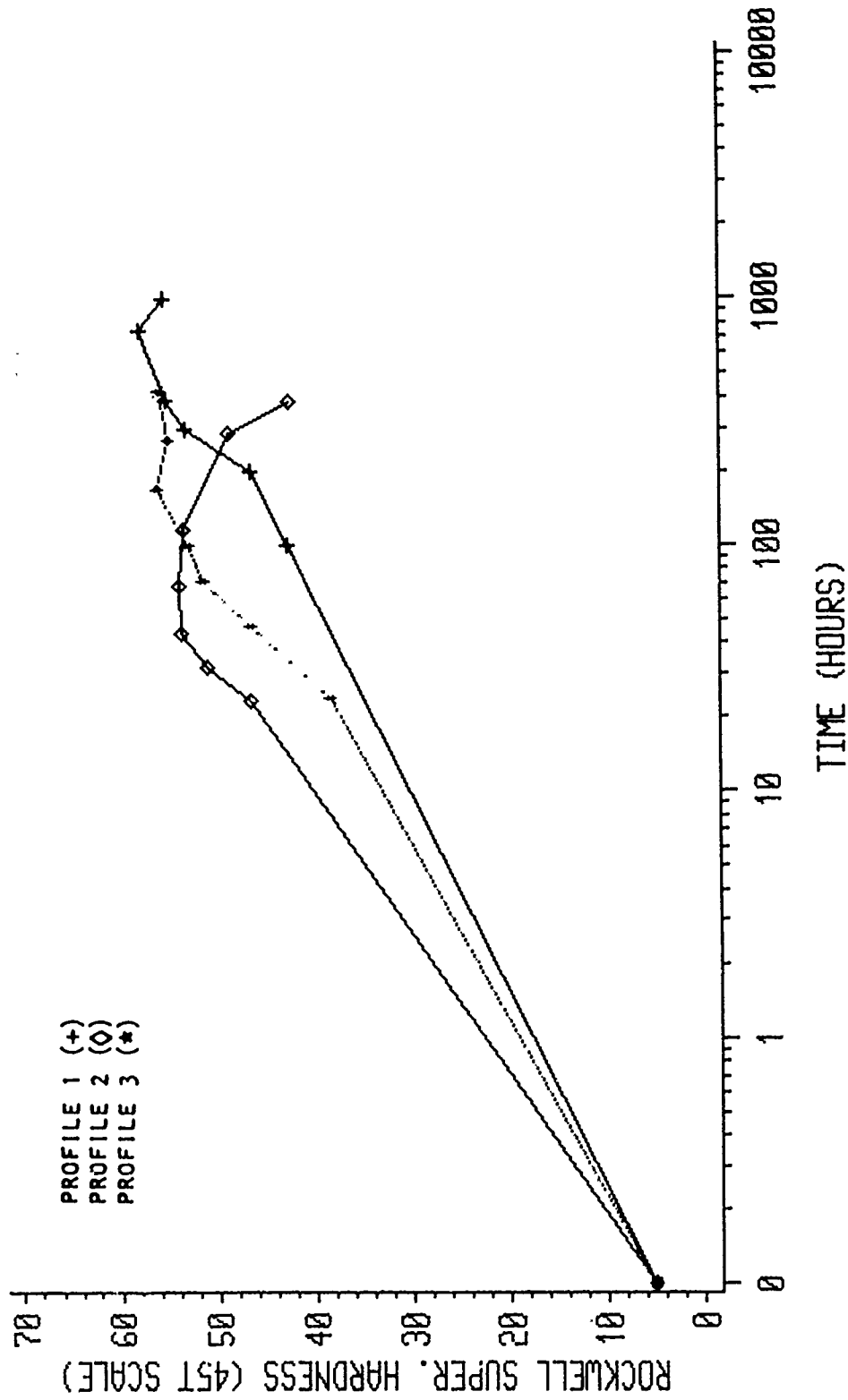
Figure 2-61. Graphic Comparison of Three Ramp and Soak Profiles (Tested Thus Far in the Program)
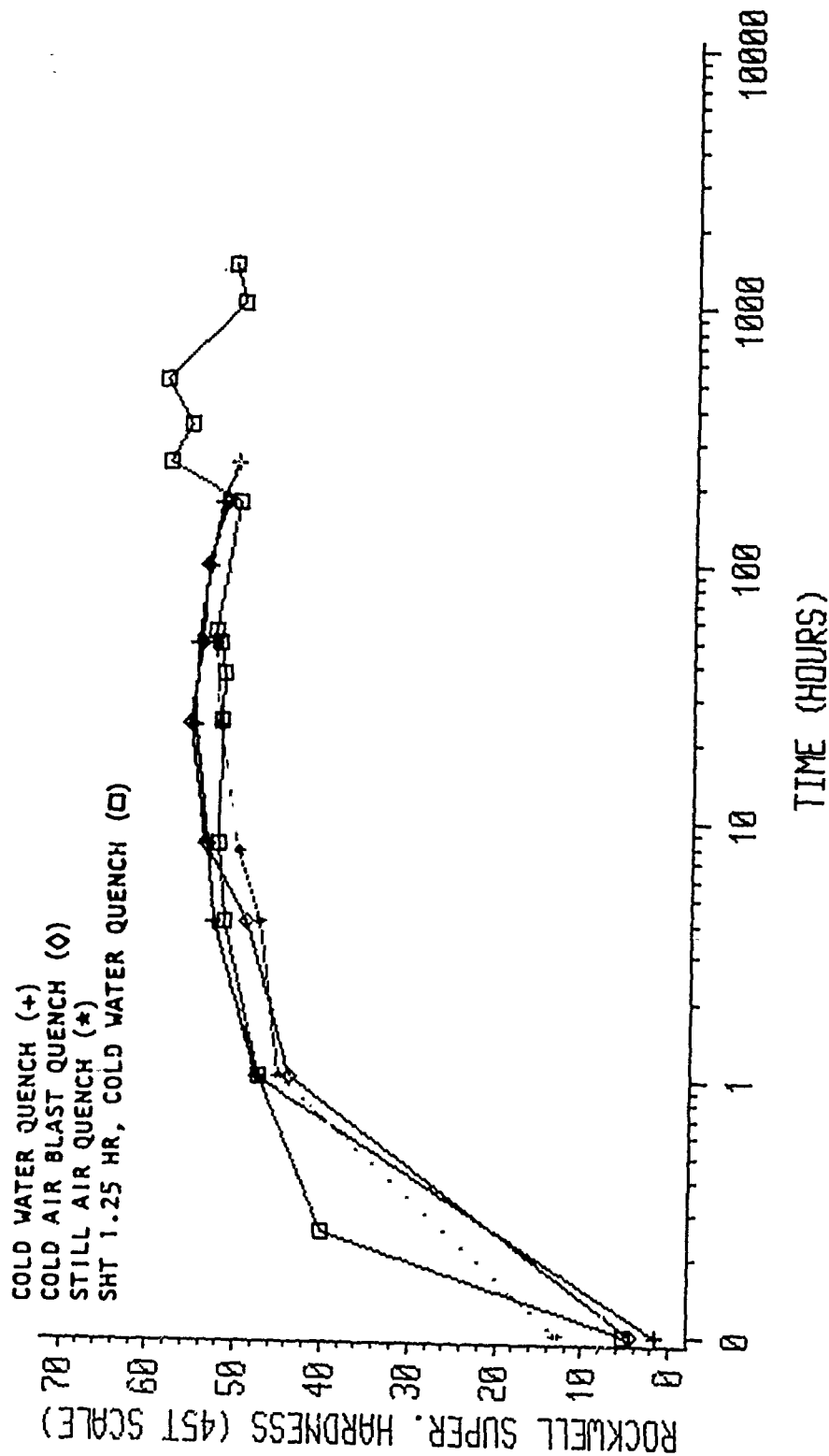
Figure 2-62. Hardness Data for Optimization of As-rolled Material. Material was Solution Heat Treated at 1013°F for 0.5 Hour, Quenched Using Three Different Quench Rates and Aged at 365°F. Also Shown are Data for 1.25 Hour Solution Heat Treatment and Quenching in Cold Water

The ultimate tensile strength, yield strength, and percentage of elongation values for the as-received natural aging study are shown in Figures 2-63 and 2-64. The strength data displayed the same general trends found in the hardness study. Increasing the solution heat-treatment temperatures resulted in a greater natural aging response. The strength increases from the material solution heat-treatment at 986 and 959°F were less than expected. In addition, the strengthening in relation to all three temperatures did not occur until natural aging of 150 to 5000 hours had elapsed. These data contrast with the hardness data which indicated that aging initiates at approximately 10 hours. The highest strength and hardness values were obtained after solution heat-treatment at 1013°F and natural aging for 5000 hours. The highest tensile values were an ultimate strength of 63.6 ksi and a yield strength of 44.5 ksi for the naturally aged material at 5000 hours. The elongation data (Figure 2-64) did not display an obvious overall trend except for a few isolated points where the values decreased with increasing solution heat treatment temperature and aging time.

The non-optimized isothermal aging tensile data are represented along with the natural aging data in Figures 2-65 and 2-66. The tensile data for the artificially aged material follow the same approximate trend as the hardness data. The strengths of the material aged at 329°F were less than the 365°F age until approximately 3 hours into the cycle. After 3 hours, the strengths at the two temperatures remained nearly identical up to 10 hours. The strength data for the 365°F age did not go beyond 10 hours. A projection indicates that if the strength data follow the hardness data, there will be a plateau in the strength until 100 hours followed by an increase. The artificial aging response, however, increased the strength for aging times between 20 and 40 hours to a significantly greater amount than the naturally aged strength.

The elongation data for the artificially aged material (refer to Figure 2-66) decreased with the increasing aging times and solution heat-treatment temperatures. The strength and elongation data for the material aged at 329°F appear to have slightly better tensile properties than the 365°F age and significantly better tensile properties than the naturally aged material. The optimization may change this plot slightly, allowing the 365°F age to surpass the tensile properties of the 329°F age for all aging times. These

Figure 2-63. Graphic Illustration of the Ultimate Tensile Strength and Yield Strength Values for the As-rolled Material After Solution Heat Treatment at 1013°F, 1.25 Hours, and Natural Aging Through 5000 Hours.

Figure 2-64. Percentage Elongation Values for Strength Data Shown in Figure 2-63.

ULTIMATE, AA AT 365°F (+)
YIELD, AA AT 365°F (+)
ULTIMATE, AA AT 329°F (◇)
YIELD, AA AT 329°F (◇)
ULTIMATE, NA AT 68°F (∗)
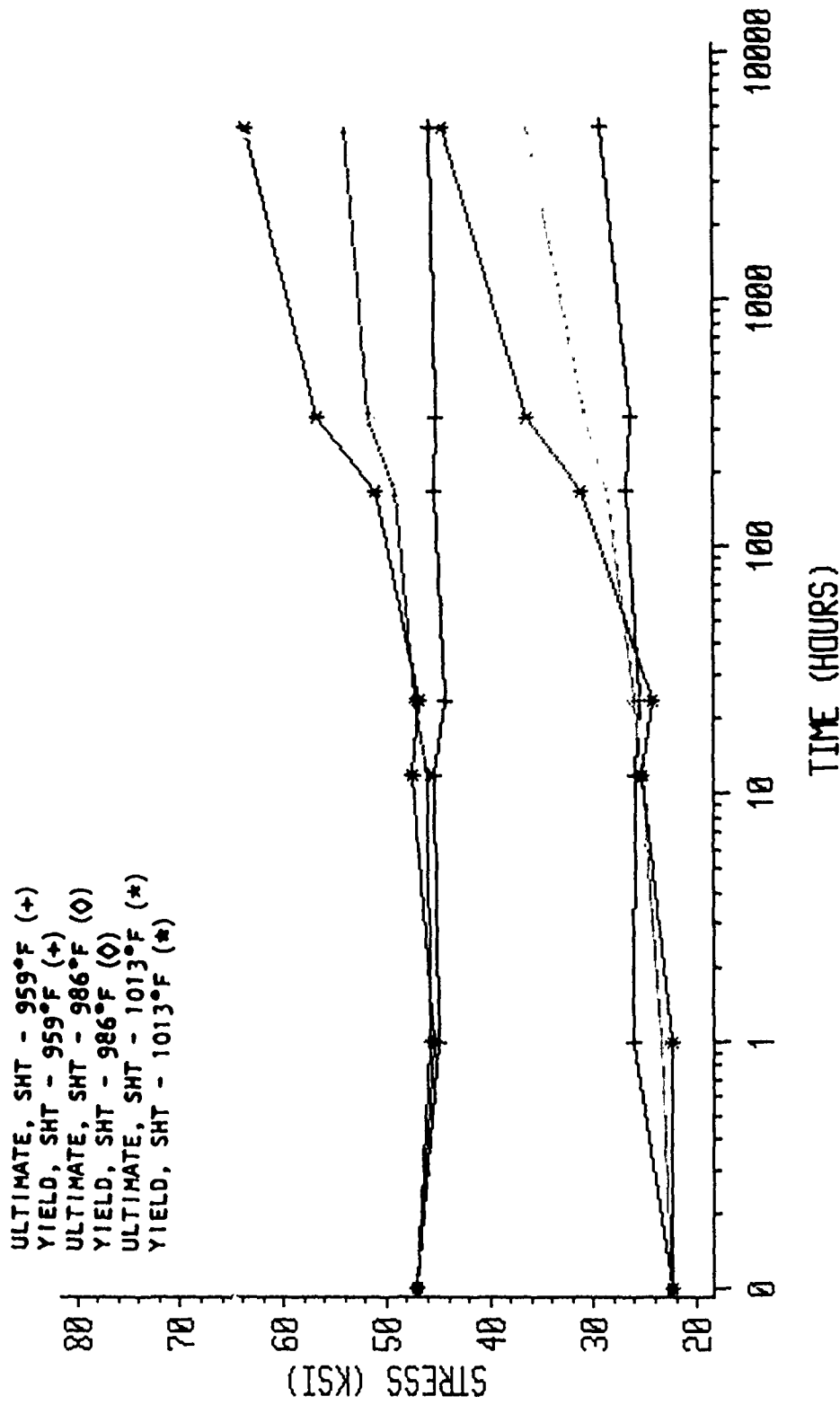YIELD, NA AT 68°F (∗)

TIME (HOURS)

STRESS (KSI)

Figure 2-65. Graphical Illustration of the Ultimate Tensile Strength and Yield Strength Values for As-rolled Material After Solution Heat Treatment at 1013°F, 1.25 Hours, and Aging at 68°F, 329°F, and 365°F.
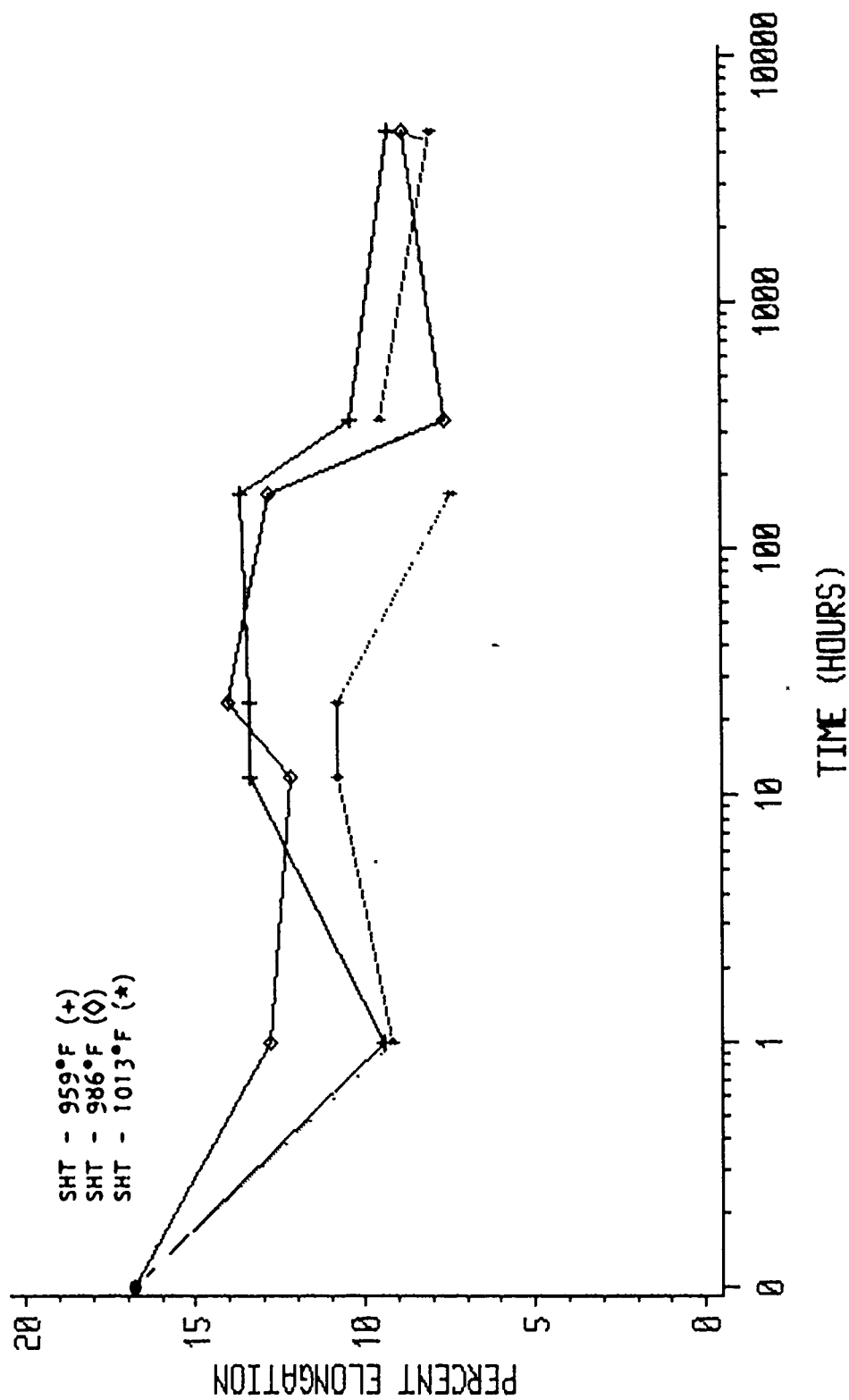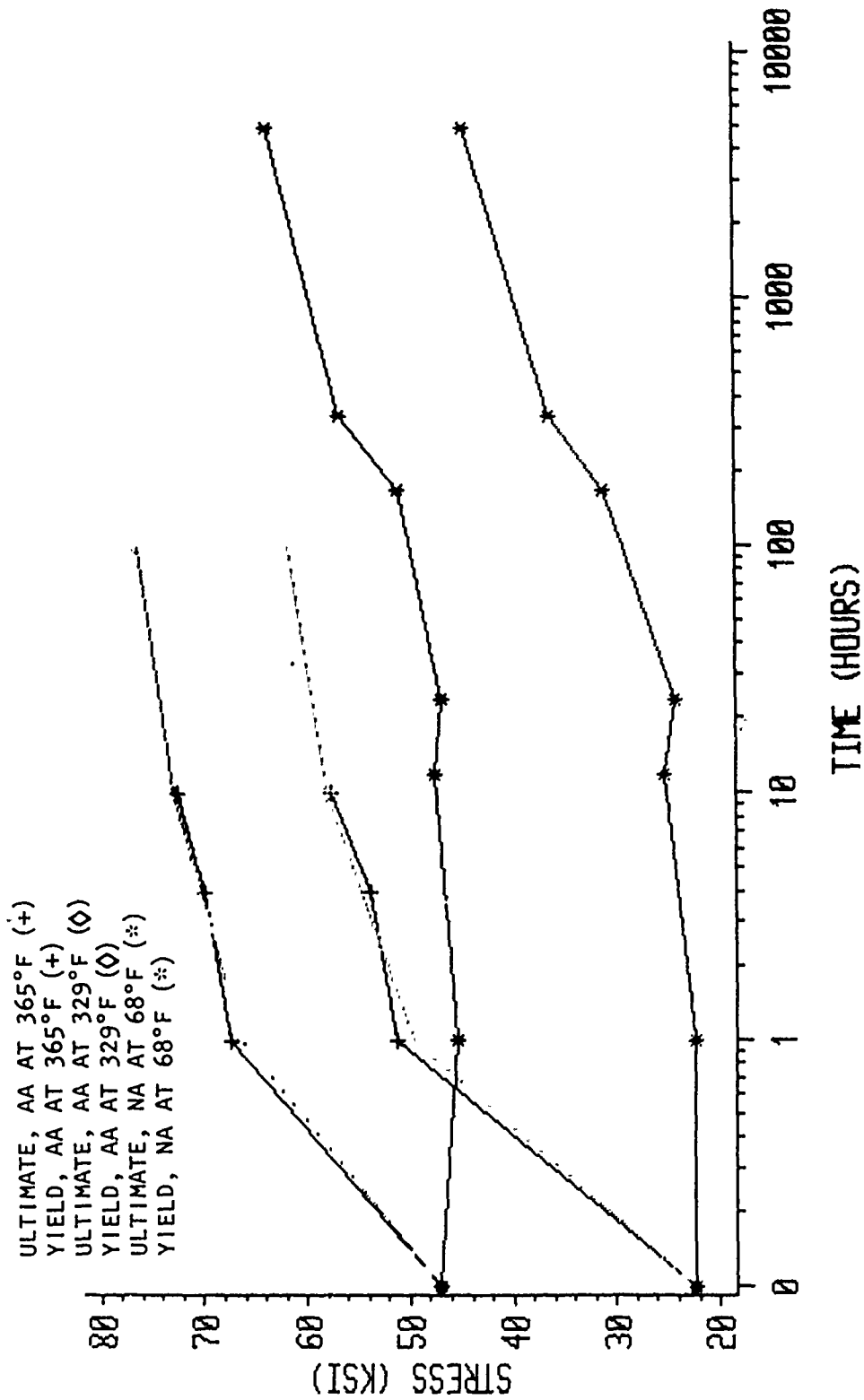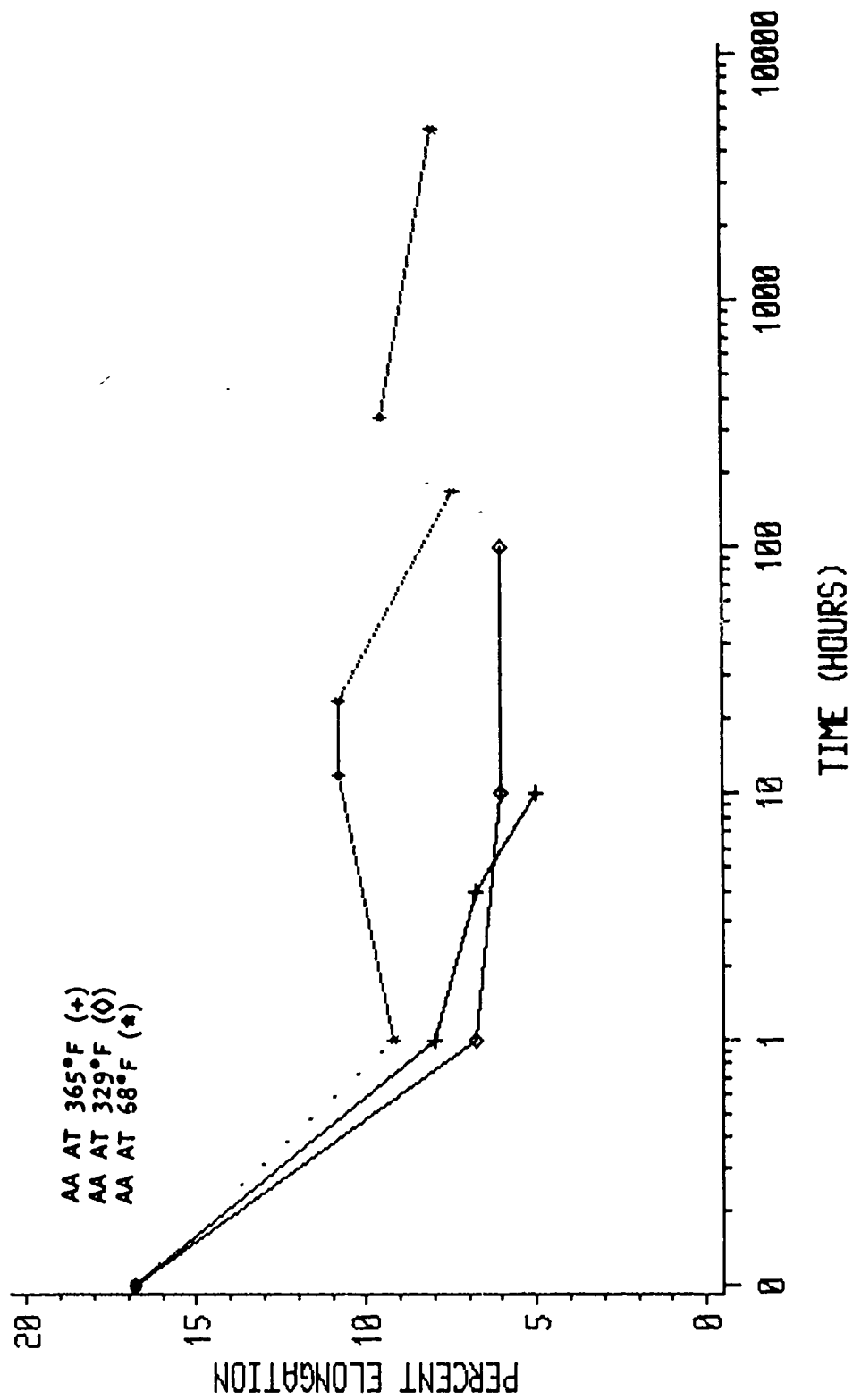
Figure 2-66. Percentage Elongation Values for Strength Data Shown in Figure 2-65.

data sets will be repeated as part of the Washington State University investigation and should be available shortly.

2.2.4.8 Isothermal Aging of SPF 8091 Al-Li

The hardness and tensile data from the 8091 Al-Li which had undergone superplastic forming are discussed in this section. Figure 2-67 graphically illustrates the hardness data for the SPF material after solution heat-treatment at 1013°F for 1.25 hours and the as-received 365°F artificially aged hardness data. The 338 and 365°F aging temperatures resulted in the highest initial hardness values, while the 329°F curve displayed peak hardness values at 336 hours of aging. Clearly, there is not a significant difference among the three aging temperatures. After approximately 20 hours of aging, the aging response of the SPF material becomes comparable to that of the as-received material. In general, the SPF material requires longer aging to reach the hardness levels displayed during the as-received study. The initial portions of the SPF curves are not included because these hardness values could be measured only on the 30T scale. These values, which are inconsequential to the overall aging response data, are for aging times less than 1 hour.

The results of the SPF/8091 Al-Li tensile tests are shown in Figure 2-68. The data from the SPF test pan (provided by Rockwell Science Center and heat treated under optimized isothermal conditions) had lower strength values than the as-received material tested under non-optimized conditions. The hardness data revealed a point where the SPF material reached the levels of the as-received material at aging times of 20 hours. The SPF tensile data at 20 hours of aging was approximately 6 ksi lower in strength than the as-received material; as the aging time approached 50 hours, however, the strength differential between SPF and as-received material was less than 4 ksi. It appears that by modifying the SPF heat treatment cycle, a gain in overall strength levels may be possible.

2.3 TASK 3 - DESIGN CONCEPT EVALUATION

2.3.1 SPF DESIGN CONCEPT EVALUATION

Optimized SPF tensile test parameters (developed at the Rockwell Science Center) were successfully used to fabricate small test pans. The test pans were laboratory scale with low amounts of overall strain in the part blank. The next step in the characterization of the material was to verify the producibility of the 8091 Al-Li on medium-to-large scale SPF parts.
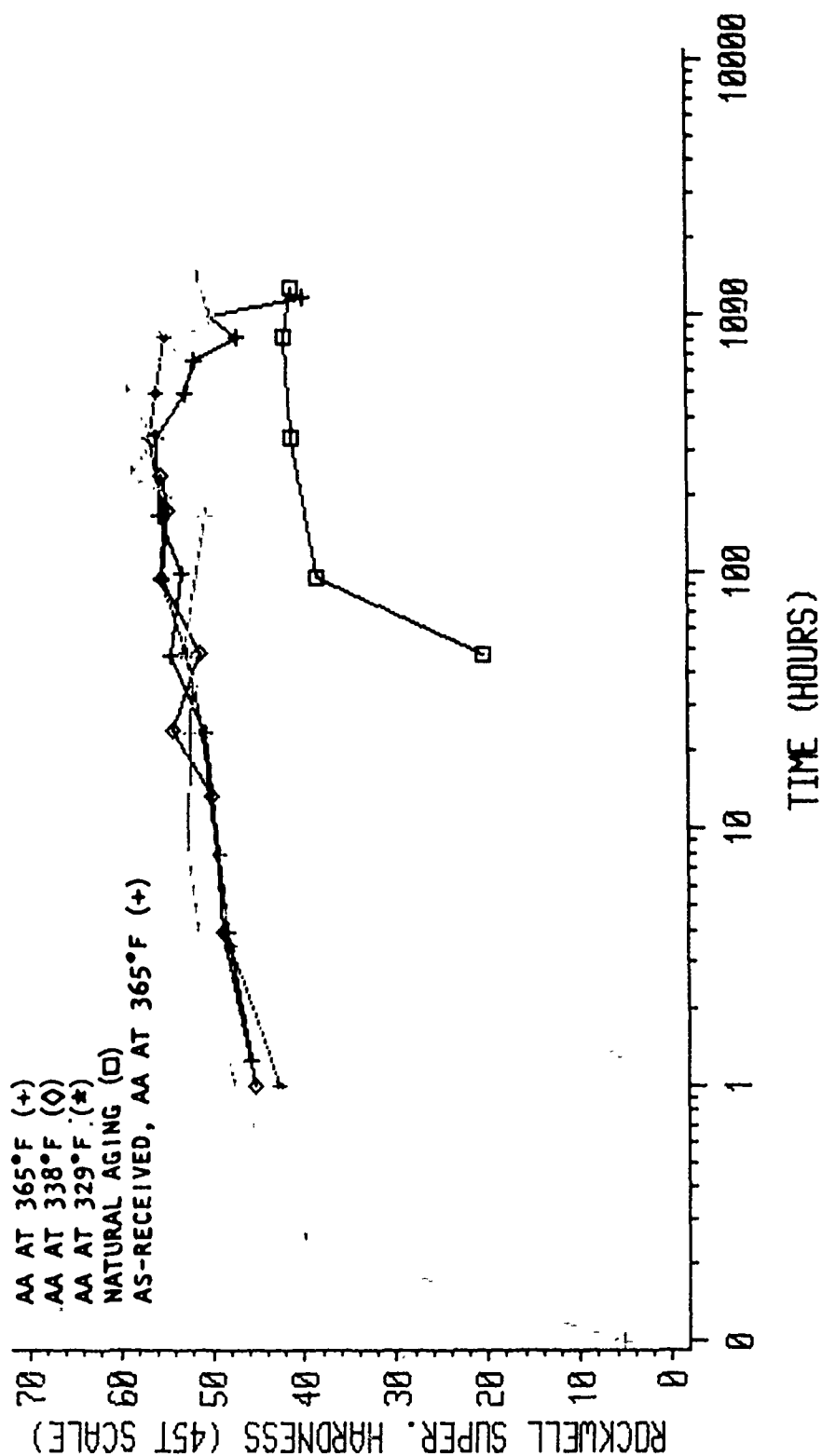
Figure 2-67. Hardness Data for Rockwell SPF Material (Test Pan 10) After Solution Heat Treatment at 1013°F, 1.25 Hours, and Aging at 68°F, 329°F, 338°F, and 365°F. Also Shown are Data for As-received Material AA at 365°F.
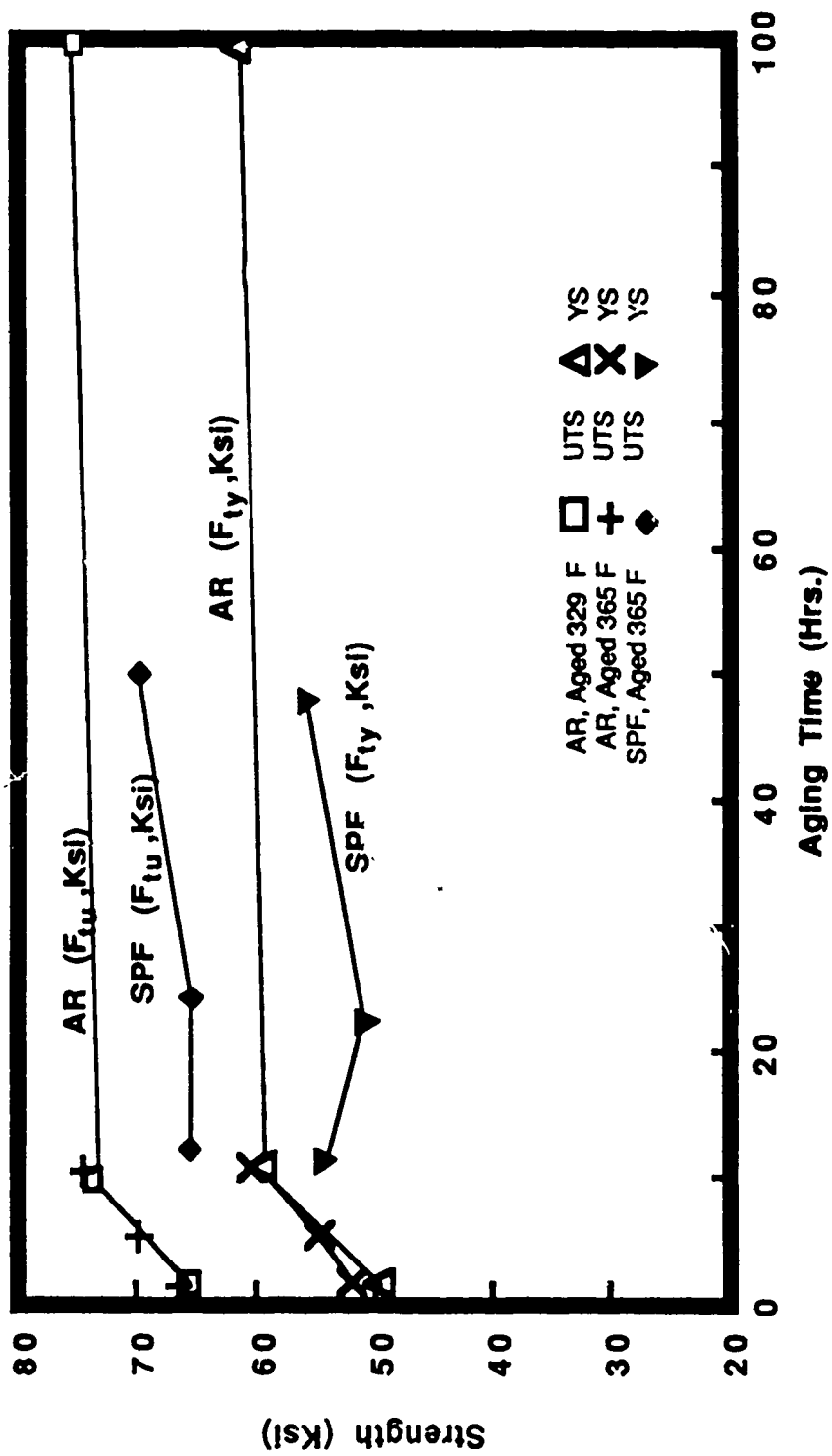
Figure 2-68. Composite Graph of 8091 Al-Li As-received Material and SPF Tensile Data

The producibility effort used existing facilities and tooling to form the parts. The four tooling configurations are delineated in Table 2-13.

TABLE 2-13

TOOLING CONFIGURATIONS FOR PRODUCIBILITY TEST PANS

Tooling Configuration (Length by Width by Height (Inch))	Aspect Ratio (Width/Height)	Length/Width	Condition
6- by 6- by 3.5	1.71	1	All pans failed.
6- by 6- by 2.5	2.4	1	Successful parts; some flaws and failures.
18- by 18- by 6	3.0	2	Good parts.
18- by 9- by 6	1.5	1	Good part.

Previous superplastic forming studies have yielded important manufacturing data for tool designs which include back pressure and lubrication techniques that will not degrade the formability or cause corrosion in the part blank.

2.3.1.1 Pressure-Time Cycles

The pressure-time cycles were generated on two systems: The first system was an in-house computer model of the tooling and optimum material parameters. The second cycle generating system used the optimum material parameters and a hemispherically shaped tooling model. Both systems required material parameters such as flow stress, strain hardening equation, optimum strain rates, temperature, and tooling constraints. Tooling constraints were the maximum amount of gas pressure that the system could contain at elevated temperatures and the tooling geometry.

2.3.1.2 Producibility Part Forming

Forming cycles used for all 13 parts are shown in Figures 2-69 through 2-71. Cycles 1 through 4 and 12 through 14 were generated using the in-house computer model; Cycles 5 through 10 were generated using the computer hemispherical tooling model. The producibility summary (Table 2-14) indicates that "hot loading" the parts and maintaining "tight" temperature control on the tooling are essential to the formability of the Al-Li material. Prolonged exposure to elevated temperatures (duration 4 to 8 hours) appears to cause excessive grain growth in the material which impedes forming. Pan 1 was loaded while the tooling was at ambient temperature and was allowed to heat along with the tooling for 4 hours. Once the tooling and part blank were at the optimum temperature, the forming cycle commenced. The part barely formed and had only a slight deflection of approximately 1.25 inches at the center of the pan.
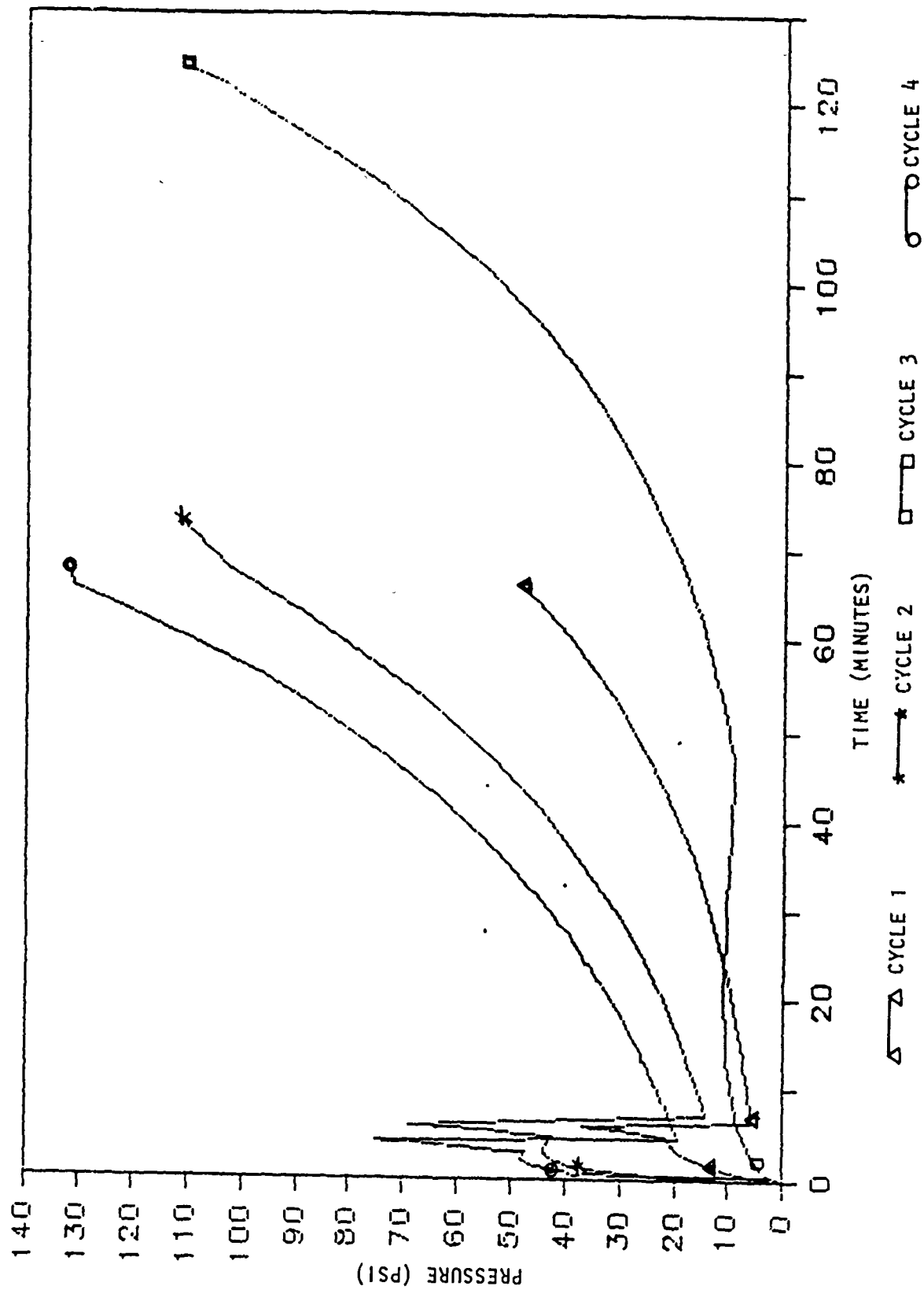
Figure 2-69. Pressure-Time Cycle for Producibility Pans 1 Through 4; 8091 Al-Li SPF
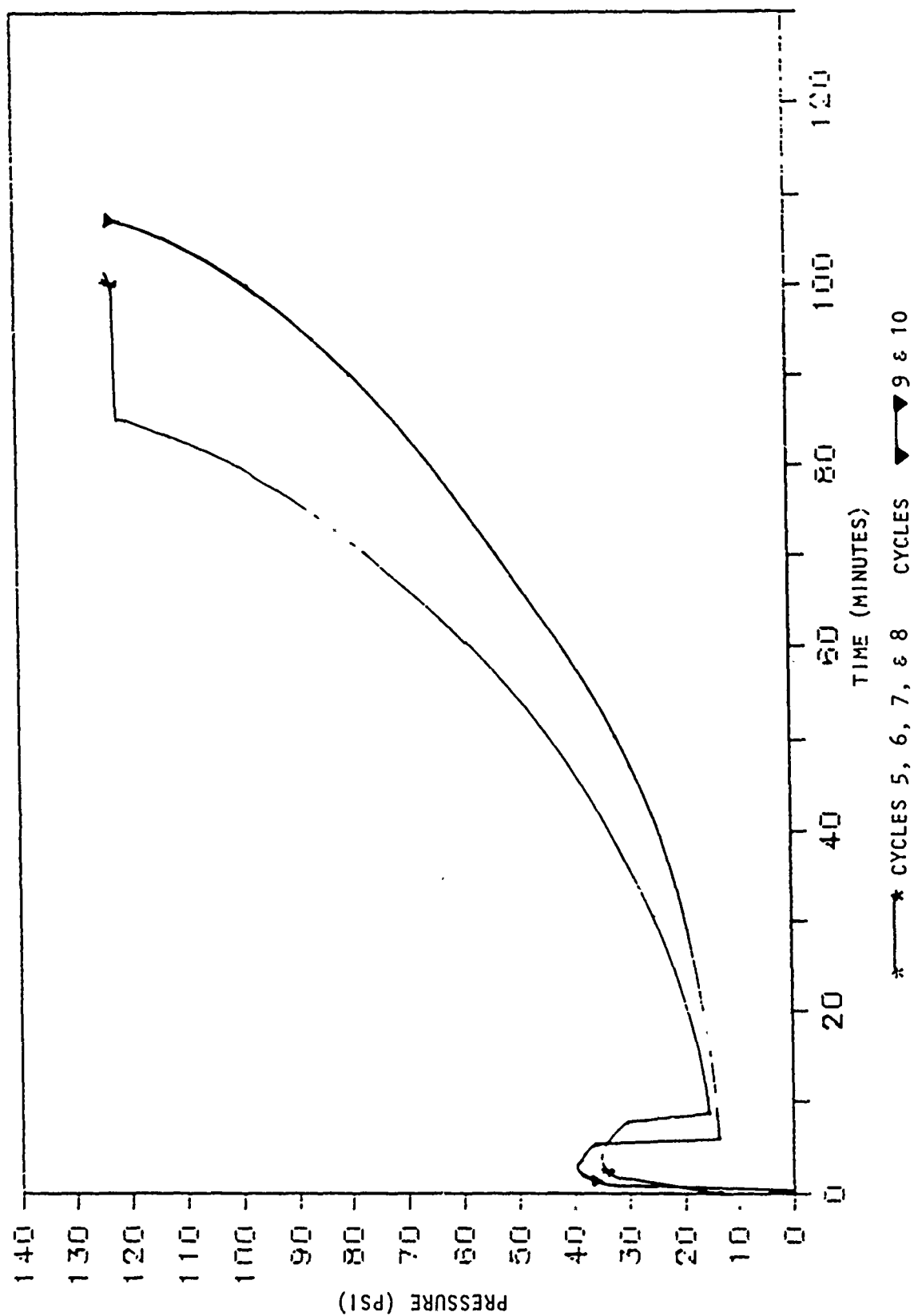
Figure 2-70. Pressure-Time Cycles for Producibility Pans 5 Through 10 (8091 Al-Li SPF)
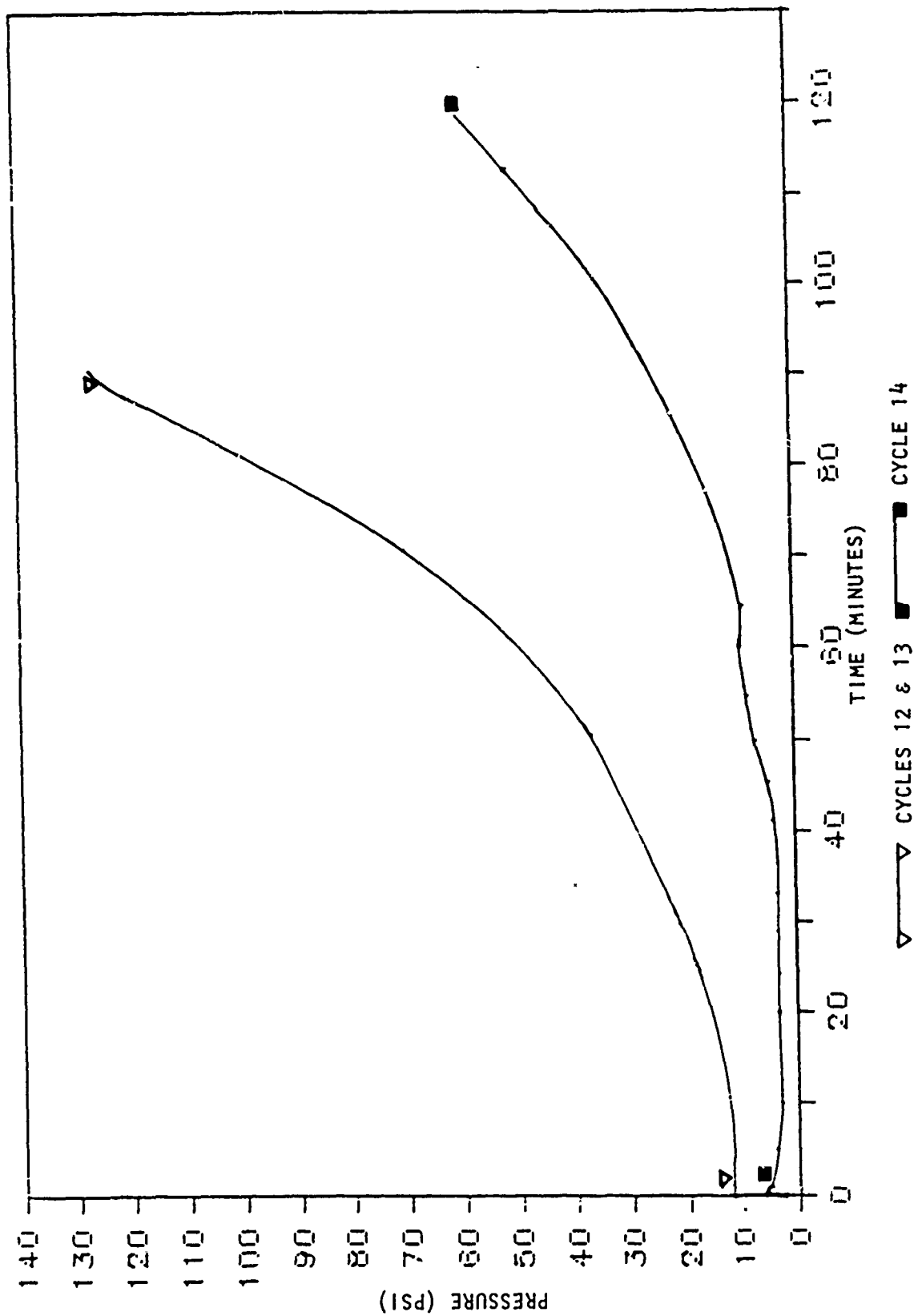
Figure 2-71. Pressure-Time Cycles for Producibility Pans 12 Through 14 (8091 Al-Li SPF)

TABLE 2-14

PRODUCIBILITY PHASE FORMING MATRIX AND PARAMETERS

Part Number	Strain Rate Used Until Indicated Strain Values	Pan Configuration W x L x D	Forming Temperature (°F)	Material Thickness (in.)	Back Pressure (psi)	Formability	Tool Condition When Part Blank was Loaded
1	2×10^{-3}/sec ϵ = .7 2×10^{-4}/sec ϵ = final value	6 x 6 x 3.5 in.	Between 950 and 1000	0.090	450	Not Formed	Cold
2	2×10^{-3}/sec ϵ = .7 2×10^{-4}/sec ϵ = final value	6 x 6 x 3.5 in.	Between 970 and 1000	0.090	400	Part failed 8 min. into cycle along draw radius and pan bottom	Hot
3	2×10^{-4}/sec ϵ = final value	6 x 6 x 3.5 in.	Between 950 and 1000	0.090	400	Part failed 90 min. into cycle	Hot
4	2×10^{-3}/sec ϵ = .5 2×10^{-4}/sec ϵ = final value	6 x 6 x 2.5 in.	Between 960 and 1000	0.090	600	Part failed 20 min. into cycle along draw radius	Hot
5	1.5×10^{-3}/sec ϵ = 1.75 2.5×10^{-4}/sec ϵ = final value	6 x 6 x 2.5 in.	Approximately 950	0.090	400	No failure: tripped gas near upper corners of draw	Hot
6	1.5×10^{-3}/sec ϵ = 1.75 2.5×10^{-4}/sec ϵ = final value	6 x 6 x 2.5 in.	Between 960 and 1000	0.090	400	Part failed at 65 psi differential pressure	Hot
7	1.5×10^{-3}/sec ϵ = 1.75 2.5×10^{-4}/sec ϵ = final value	6 x 6 x 2.5 in.	Between 950 and 955	0.090	400	Part failed at 73 psi differential pressure	Hot
8	1.5×10^{-3}/sec ϵ = 1.75 2.5×10^{-4}/sec ϵ = final value	6 x 6 x 2.5 in.	Between 970 and 980	0.090	400	No failure; gas pockets trapped	Hot
9	2.0×10^{-3}/sec ϵ = .5 2.0×10^{-4}/sec ϵ = final value	6 x 6 x 2.5 in.	Between 942 and 998	0.090	400	No failure; gas pockets trapped	Hot
10	2×10^{-3}/sec ϵ = .5 2×10^{-4}/sec ϵ = final value	6 x 6 x 2.5 in.	Between 996 and 980	0.090	400	No failure; gas pockets trapped	Hot
12 & 13	Stepped transition 2×10^{-3}/sec 2×10^{-4}/sec	18 x 18 x 6 in.	Between 986 and 990	2 sheets each 0.090	400	No flaws	Hot
14	Same as pans 12 & 13	18 x 9 x 6 in.	990	0.090	400	No flaws	Hot

ϵ = Epsilon

The pressure-time cycle developed for Pan 2 used two strain rates. The initial strain rate was used to quickly start the material moving into the tool. Once an overall strain of 0.7 was reached, a slower strain rate was used to complete the forming process. The part blank for Pan 2 was hot loaded but tore upon reaching the bottom of the tool. The part appeared to have thinned out excessively along the draw radius and pan bottom during the initial strain rate. The thinning continued until failure occurred as shown in Figure 2-72. Although Pan 3 used the same tooling configuration as Pans 1 and 2 (6- by 6- by 3.5-inch), it used only one strain rate during the entire forming cycle. Although the part formed to the bottom of the tool (as shown in Figure 2-73), it ruptured 90 minutes into the cycle.

Pans 4 through 10 were formed in the original 6- by 6-inch die box with an insert added to decrease the depth of the draw. The new configuration was 6- by 6- by 2.5-inch. Pan 4 used the two-stage strain rate cycle. The amount of strain observed in the part using the initial strain rate, however, decreased from 0.7 to 0.5 at which time the slower strain rate was used to complete the forming cycle. The amount of back pressure used during the forming process was increased to 600 psi and temperature control was improved over the preceding pans. Pan 4 failed along the draw radius 20 minutes into the cycle which is evident in Figure 2-74. The next pan to be formed used a pressure-time cycle developed by the Rockwell Science Center. The pressure-time cycle for Pan 5 used a slower initial strain rate than used for earlier cycles and increased the amount of strain into the part blank from 0.5 to 1.75 before changing to the slower strain rate. The pan formed completely but had limited cosmetic flaws at the upper corners of the sidewalls; these could be eliminated by modification of the tooling or forming cycle. Pans 6 through 8 used the same cycle and forming parameters as used for Pan 5; however, the results were somewhat different. Pan 6 ruptured in one of the bottom corners at a differential pressure of 65 psi. The forming temperature was between 940 and 968°F at the onset of the cycle and remained in the lower range throughout completion. Pan 7 also ruptured during the forming cycle at 73 differential pressure. The temperature during the cycle was in the lower range (950 to 955°F) of the optimized forming temperature. Pans 6 and 7 were almost fully formed except at corner areas at the bottom of the pan. Figures 2-75 through 2-77 illustrate different degrees of forming for Pans 5, 6 and 7. Pan 8 was the last pan to be formed using the cycle developed for Pan 5. Pan 8 completed the cycle without any problems or ruptures in the part. Temperature control was excellent and temperatures were maintained on or near 970°F throughout the duration of the cycle. The configuration of Pan 8 is shown in Figure 2-78.

Pans 9 and 10 used a second pressure-time cycle developed by the Rockwell Science Center. The new cycle used the two-step strain rate that was used for Pan 4. Pans 9 and 10 had good temperature and pressure control during the cycle and there was no failure in the parts.
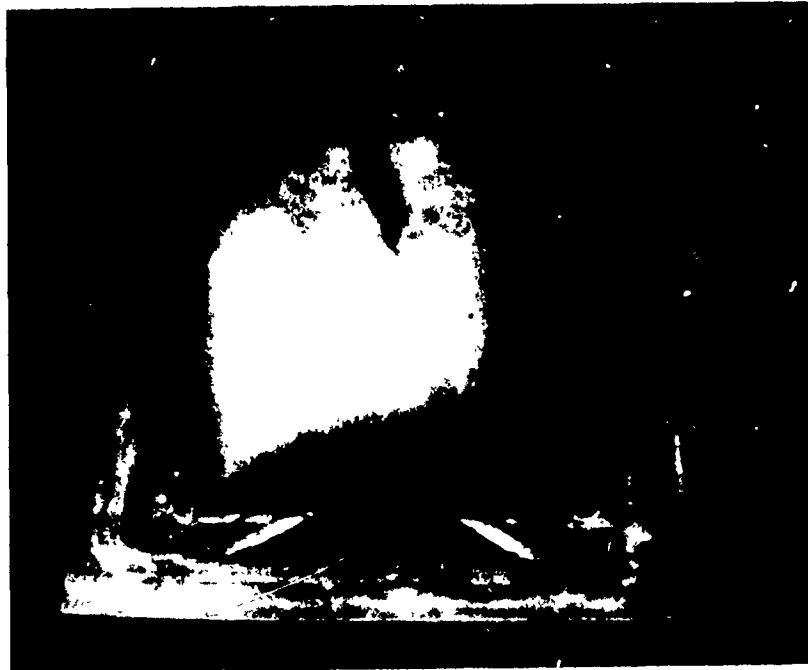
Figure 2-72. Producibility Pan 2; Failed Along Draw Radius and at Pan Bottom

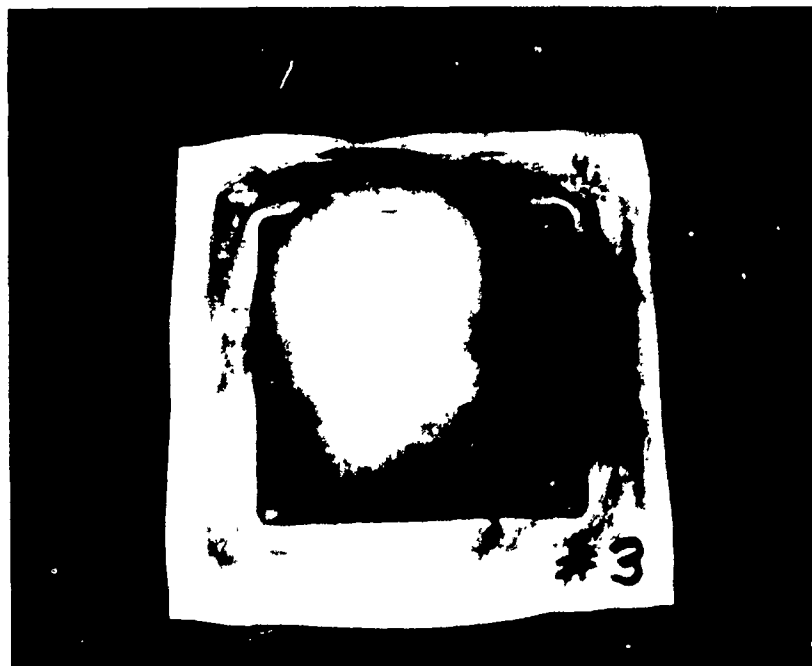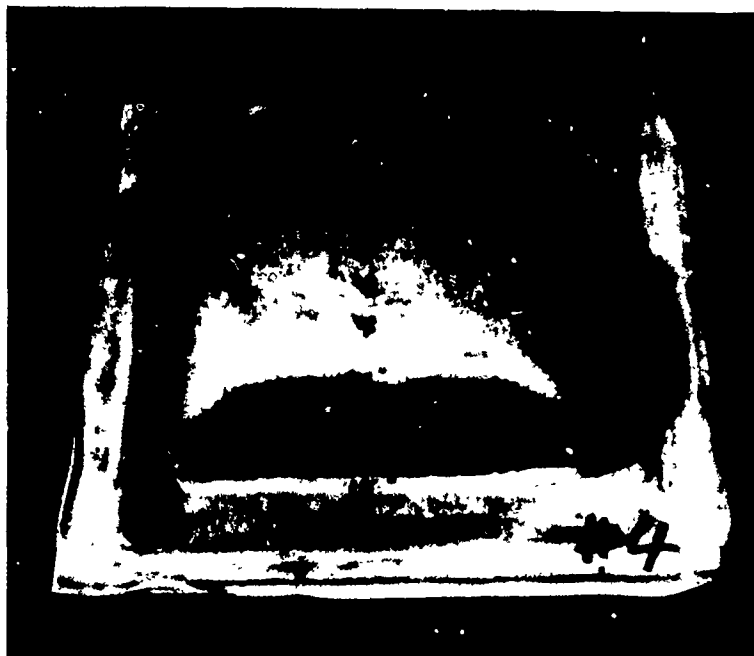Figure 2-73. Producibility Pan 3; Touched Bottom of SPF Die Before Failure

Figure 2-74. Producibility Pan 4; Failed at Draw Radius on One Side Only
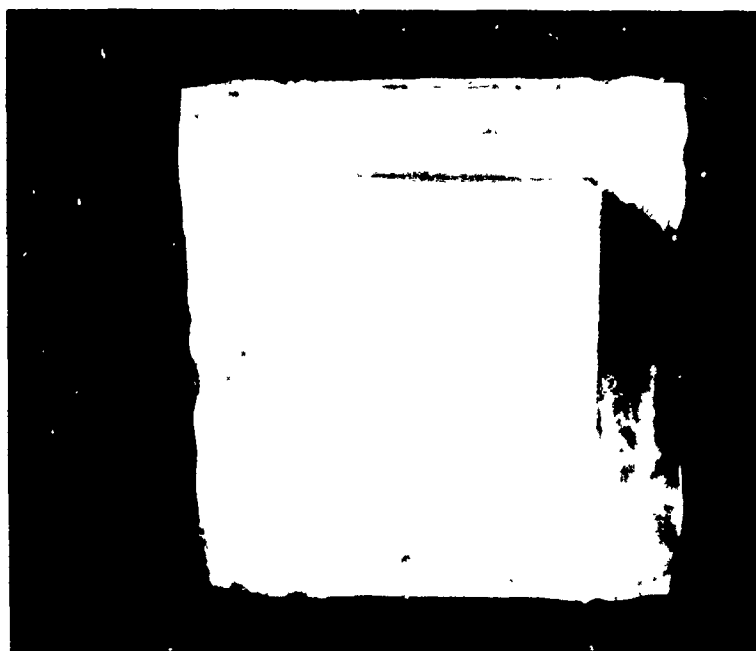

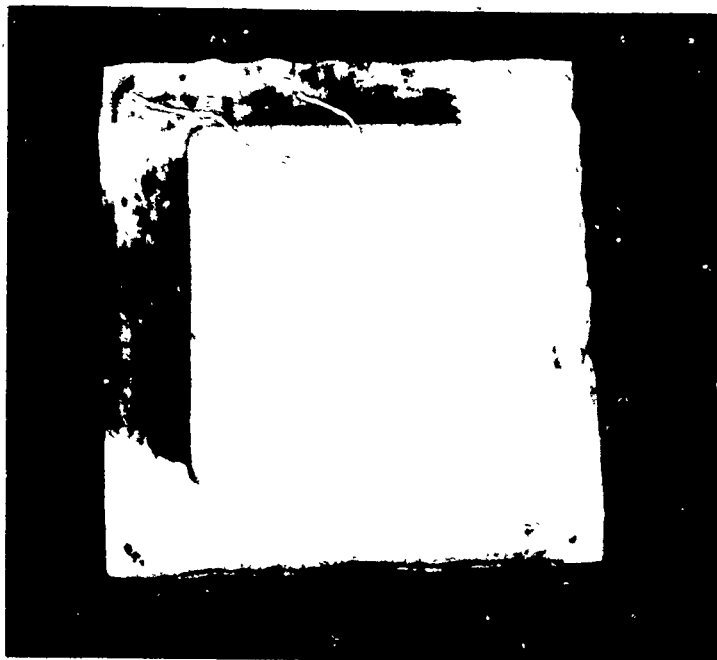Figure 2-75. Producibility Pan 5; Formed Completely Without Rupturing

Figure 2-76. Producibility Pan 6; Failed at Bottom Corner of Pan Before
Cycle was Complete
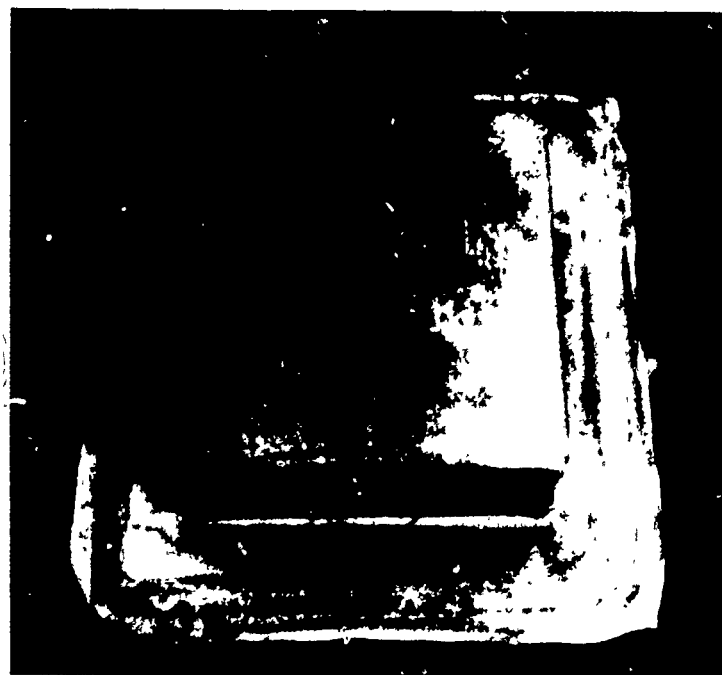
Figure 2-77. Producibility Pan 7; Failed Along Bottom Corner of pan
Before Forming Cycle was Complete
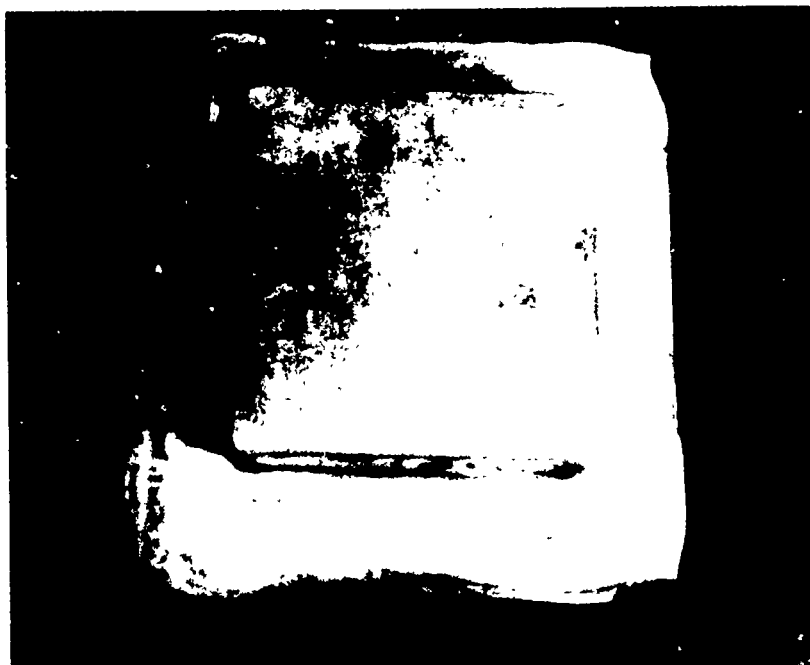
Figure 2-78. Producibility Pan 8; Followed Identical Pressure-Time
Cycle as Pans 5 Through 7 Without Experiencing any Failure

Pans 12 and 13 used an 18- by 18- by 6-inch die box. The pressure- time
cycle was developed at Rockwell-NAA using an in-house system. To conserve
forming time, the two parts were formed simultaneously. The pressure-time
cycle was developed to accommodate 0.180-inch sheet thickness (two sheets
combined) compared with the initial 0.090-inch material used for earlier
tests. The decision to "step" the strain rates reduced localized thinning
along the drawline of the part. The pressure-time cycle developed on the in-
house model was used with the optimum back pressure developed at the Rockwell
Science Center; back pressure was used on all of the producibility parts to
eliminate cavitation (refer to Table 2-14). Pans 12 and 13 were fully formed
with no cosmetic flaws (Figure 2-79). Excellent temperature control was
maintained throughout the entire cycle. Pan 14 used a stainless steel plate
covering the ceramic insert to reduce the aspect ratio in the part and to
increase the amount of overall strain in the part blank. The forming cycle
was developed with an in-house computer model and (again) produced a pan from
a stepped strain rate with no cosmetic flaws (Figure 2-80).

Figure 2-79.   Producibility Pans 12 and 13; Formed Simultaneously and Were Flawless

Figure 2-80.   Pan 14 Used a Ceramic Insert to Divide Die Cavity; Used for Pans 12 and 13 to Increase Strain in Part. Discernible Physical Flaws Observed in Part.

2.3.1.3 Thickness Distributions
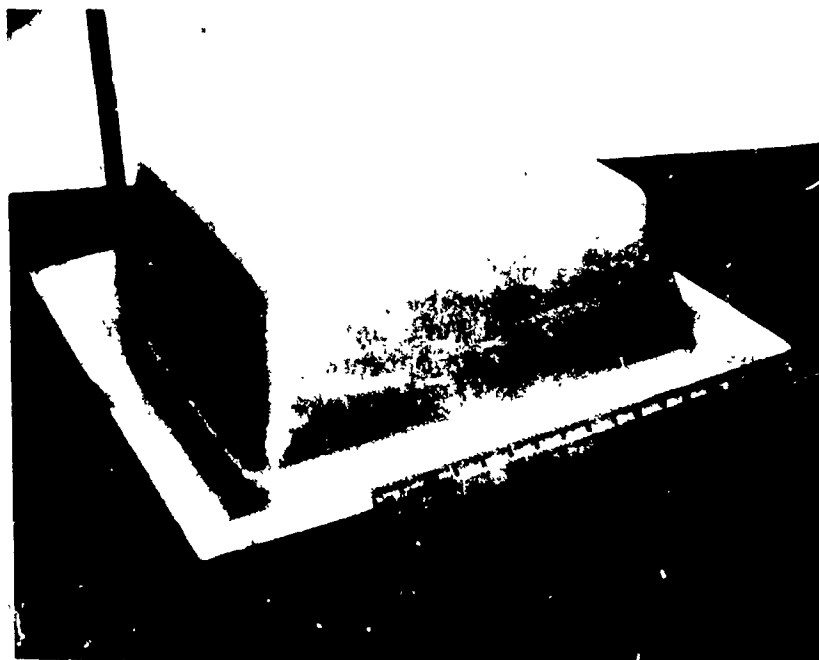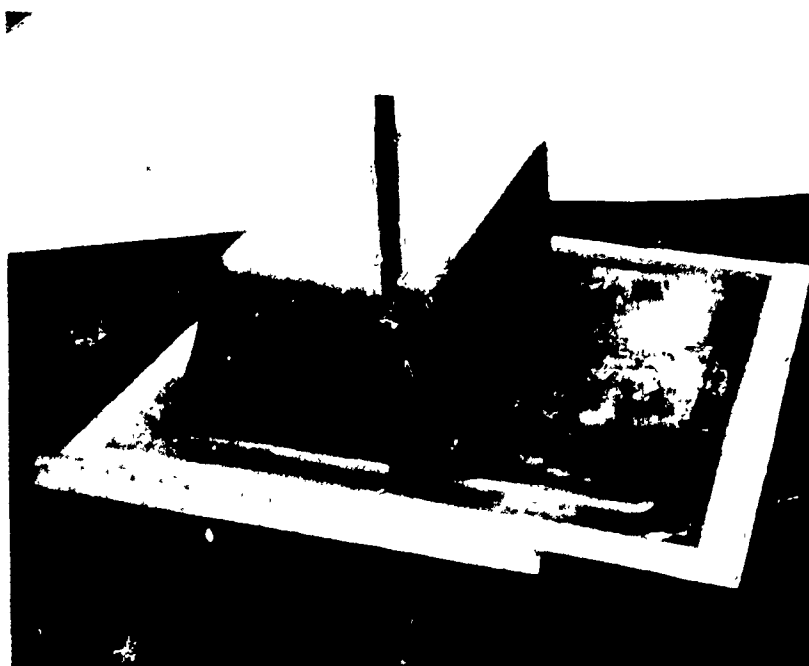
The thickness distributions for Pans 5 through 10 are graphically represented in Figures 2-81 through 2-86. The distribution of thickness appears to be more uniform for Pans 9 and 10 than for the earlier pans. Generally, Pans 9 and 10 appear to have better formability than earlier pans that used the same die box configuration. Figure 2-87 shows the thickness distribution and the degree of formability for Pan 13. The overall formability of the large producibility pans is superior to that of the smaller pans. The thinning appeared more uniform over the entire part with no areas of "orange peel" texture in the material.

2.3.1.4 Cavitation

The medium-sized parts were sectioned and evaluated for the presence of cavitation. The cavitation analysis used photomicrographs (100X and 200X) to determine the approximate level or presence of cavitation for different thickness strains. The corners of the sidewalls of the large pans were removed and examined for cavitation. The results are summarized in Table 2-15. Figures 2-88 and 2-89 illustrate the changes in the amount of cavitation in the part with thickness strain. Pans 6 and 14 were formed with 400 psi back pressure; however, Pan 6 had a considerable amount of cavitation while Pan 14 (essentially) had no cavitation. The difference between the two parts was not only the size and shape of the die box, but the way in which the strain rates transitioned during the forming cycle. Pan 6 used a strain rate of 2E-3/second for a strain of 1.75 before changing to the slower strain rate; Pan 14 used the fast strain rate for a strain up to 0.1 at which time a "stepped" strain rate transition took place which gradually decreased the strain rate to its final value at an overall strain rate of 0.5. The lack of cavitation in Pan 14 at high stress levels appears to result from the transitioned strain rates and from the excellent temperature control during the entire forming process.

Several producibility pans were sent to Washington State University for optimization of the heat treatment cycle using material which had undergone superplastic deformation. The large producibility pans were sent to Alcoa Laboratories for initiation of engineering design allowables studies. The optimum heat treatment established at Washington State University will be used for development of the material allowables and for the data generation task.

* Density coupon average thickness
(Inch)

GRAIN DIRECTION

Figure 2-81. Thickness Distribution and Thickness Measurements of
Density Coupons for Producibility Pan 5

* Density coupon average thickness
(Inch)

GRAIN DIRECTION

Figure 2-82. Thickness Distribution and Thickness Measurements of
Density Coupons for Producibility Pan 6

Figure 2-83. Thickness Distribution and Thickness Measurements of Density Coupons for Producibility Pan 7
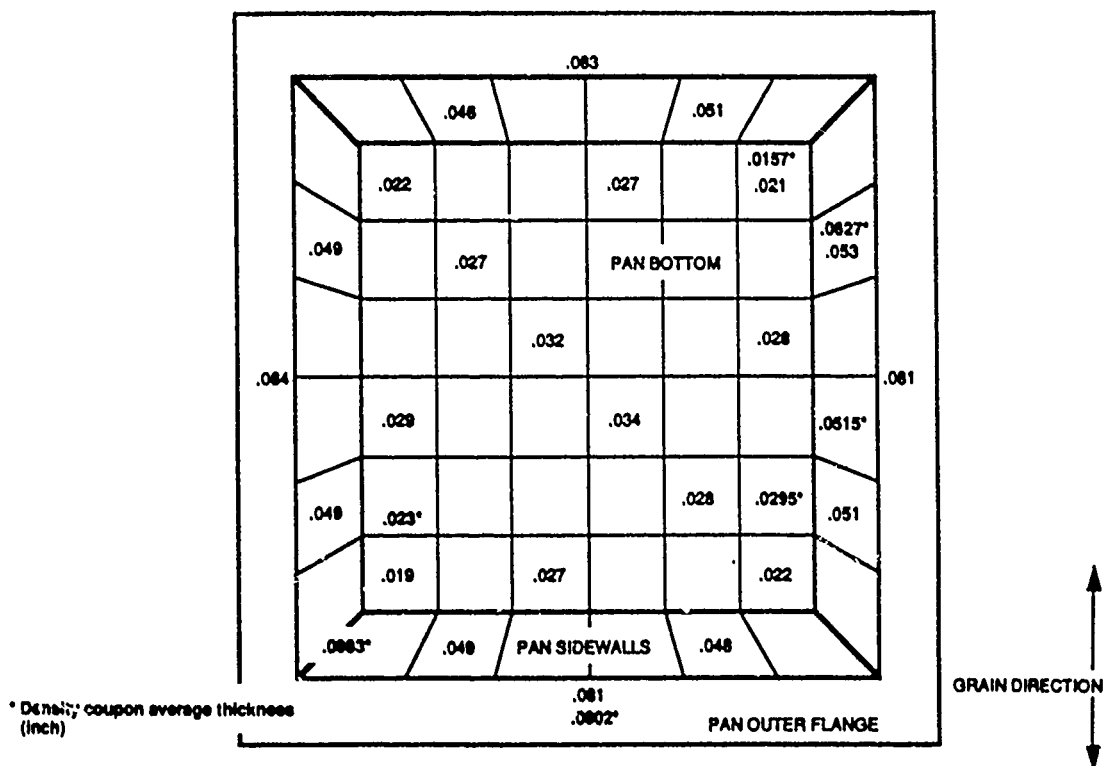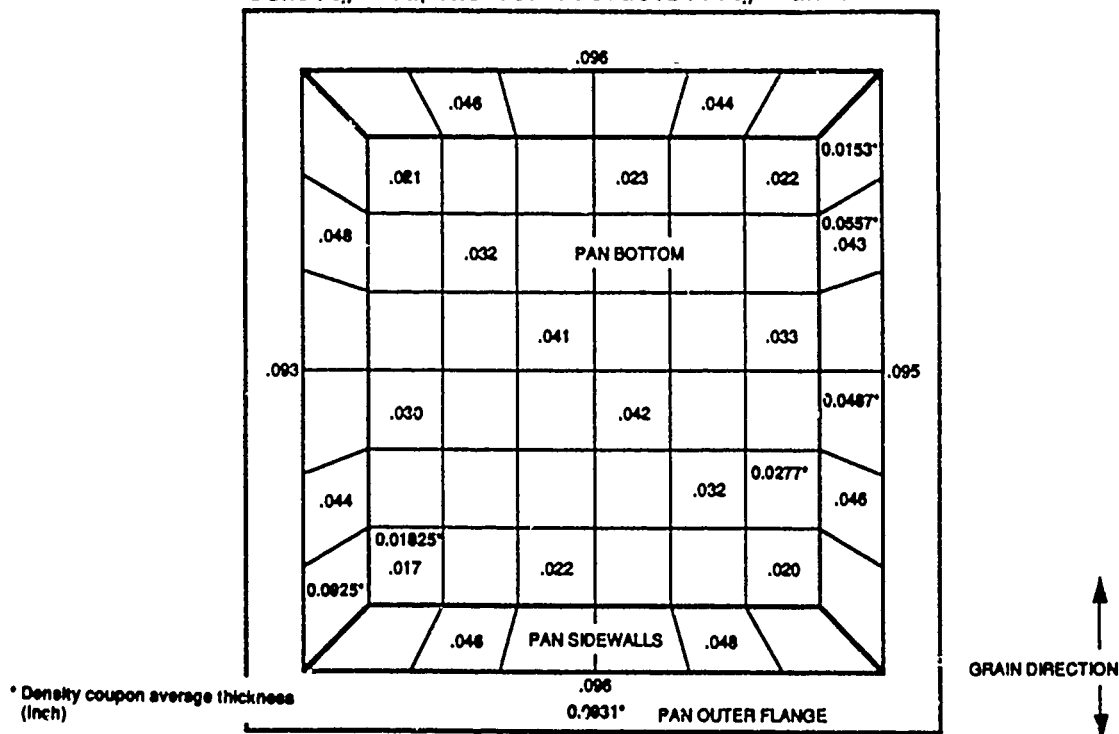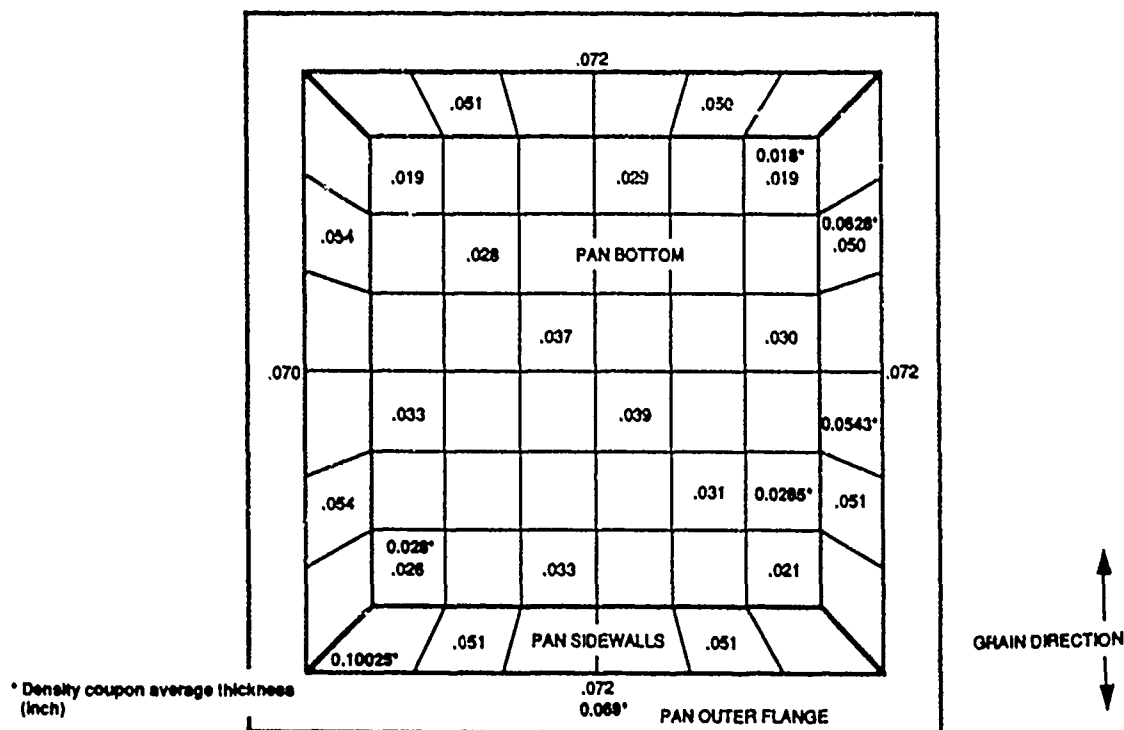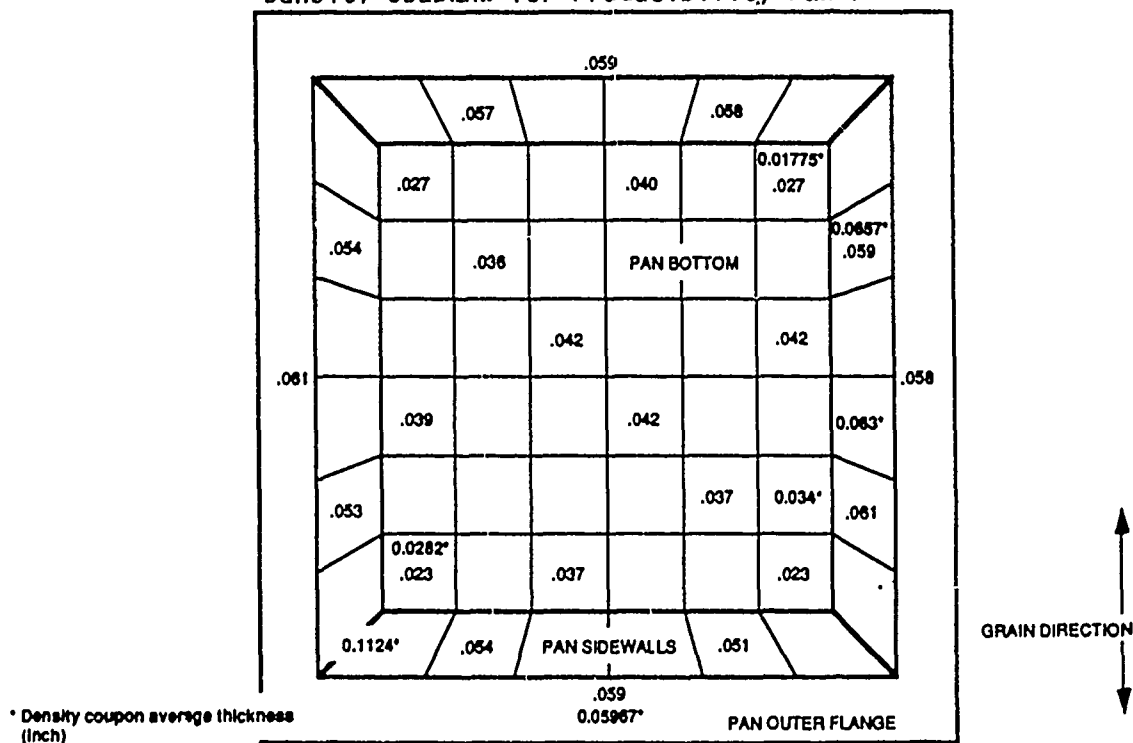

Figure 2-84. Thickness Distribution and Thickness Measurements of Density Coupons for Producibility Pan 8
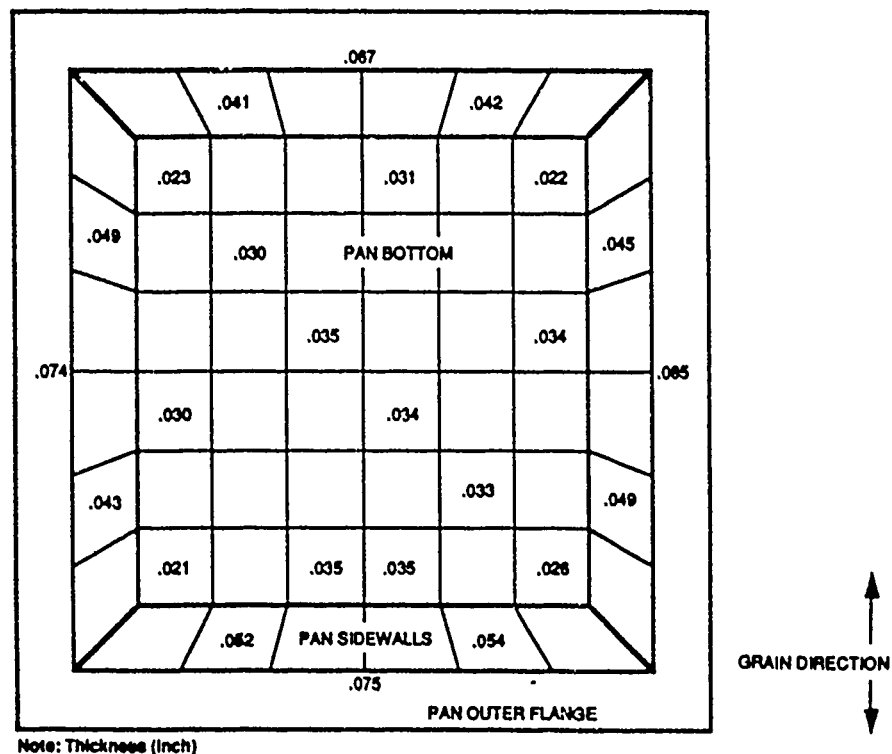
Figure 2-85. Thickness Distribution and Thickness Measurements of Density Coupons for Producibility Pan 9
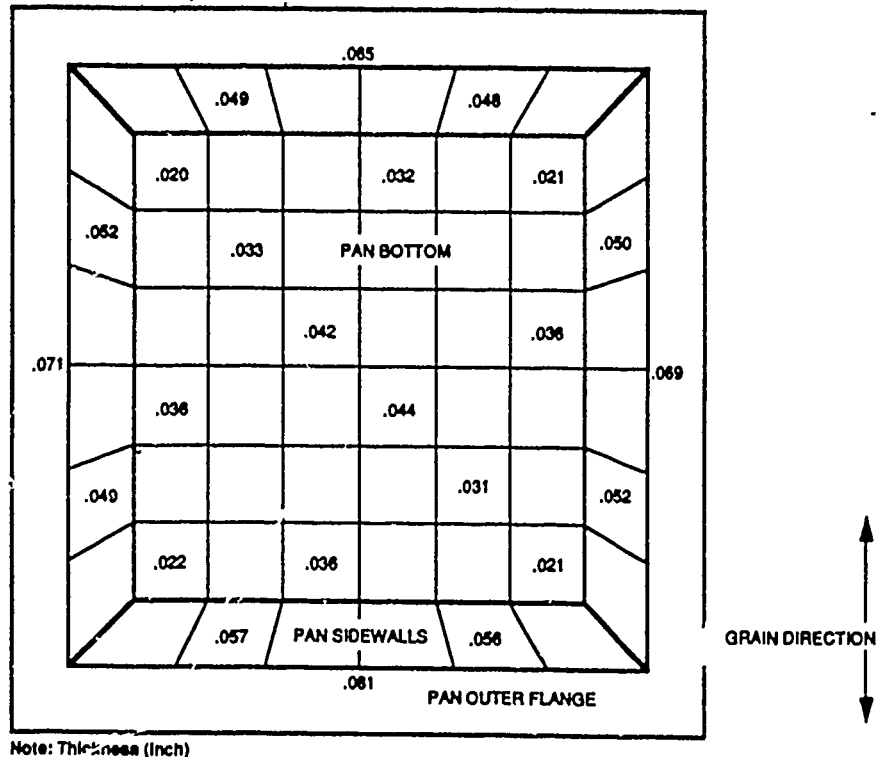
Figure 2-86. Thickness Distribution and Thickness Measurements of Density Coupons for Producibility Pan 10
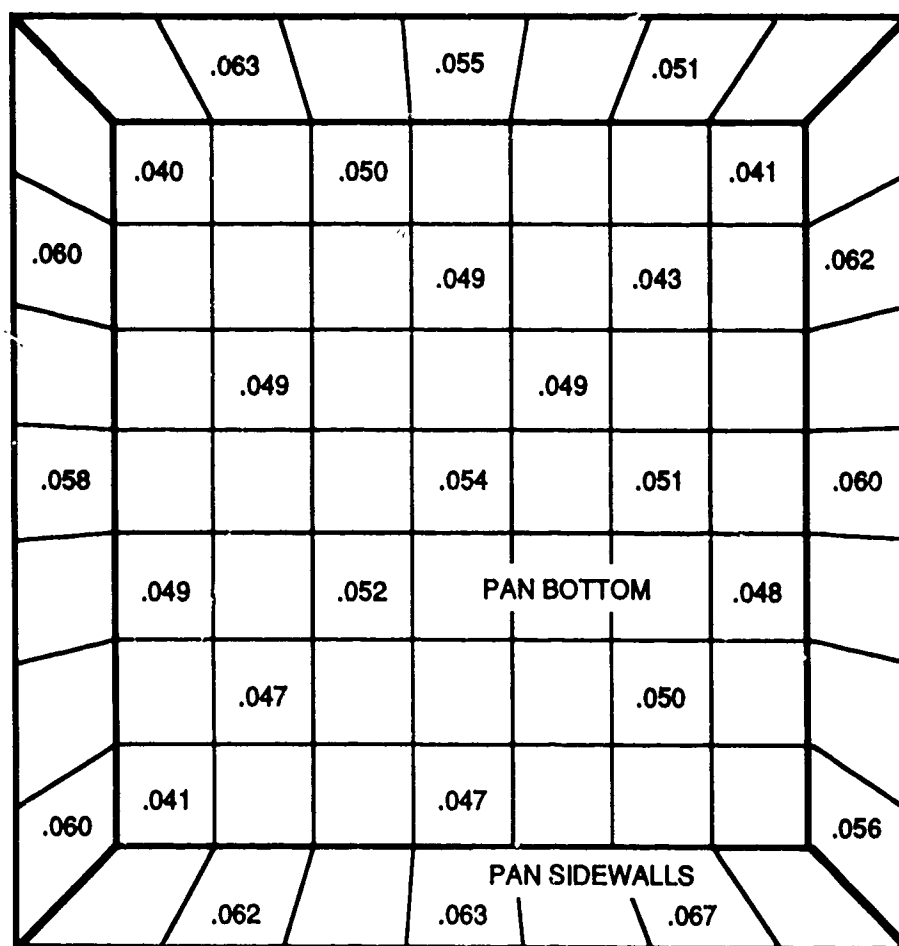
Figure 2-87. Thickness Distribution - Producibility Pan 13

TABLE 2-15
CAVITATION VALUES VERSUS STRAIN VALUES FOR PANS
WITH THREE DIFFERENT CONFIGURATIONS

Thickness Strain %	Percent Strain/Percent Cavitation					
	Pan 5	Pan 6	Pan 7	Pan 8	Pan 13	Pan 14
475 - 7500	473/7.8	488/0.68 to 1.32				
450 - 474						466/.012
425 - 449						
400 - 424			400/10.45	407/15.23		
375 - 399		393/0.098				
350 - 374						
325 - 349						
300 - 324						
275 - 299	291/1.17					
250 - 274						
225 - 249		225/1.15				
200 - 224	205/1.78		216 / 2.51 & 221 / 3.12	219/0.0244		
175 - 199						190/.0038
150 - 174				164.7/0.366		
125 - 149					143/.06 & .01	143/.004
100 - 124						
75 - 99		85 / 2.93				
50 - 74	74.7/1.17		65.7/0.97	50.8/0.0488		50 / 0
25 - 49	43.5/1.07			36.9 / 0.244 & 42.8 / 0.732	28 & 32 / .18 & .01	
0 - 24					0/3.2 & .01	0/.0005

PAN 6

STRAIN = 448%
MAXIMUM PERCENT
CAVITATION = 1.3
MAGNIFICATION = 200X

PAN 6

STRAIN = 225%
MAXIMUM PERCENT
CAVITATION = 1.4
MAGNIFICATION = 200X

PAN 6

STRAIN = 85%
MAXIMUM PERCENT
CAVITATION = 2.92
MAGNIFICATION = 200X

Figure 2-88. Photomicrographs of Cavitation at Different Thicknesses
(SPF 8091 Aluminum-Lithium)
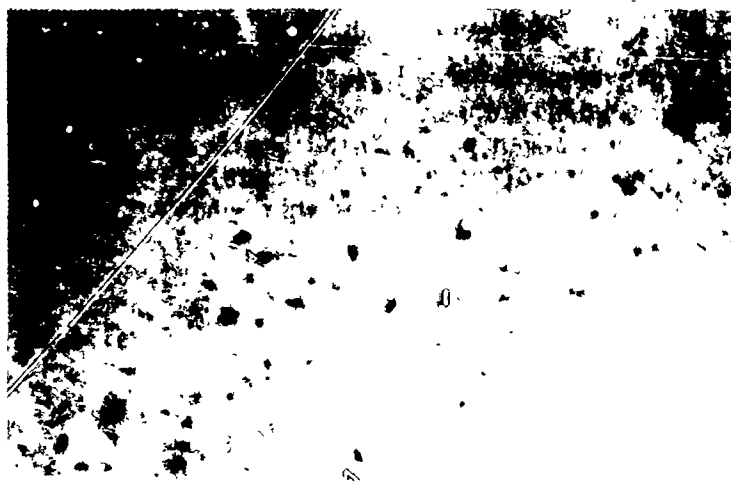
PAN 14

STRAIN	= 446%
PERCENT CAVITATION	= 0.013
MAGNIFICATION	= 200X

PAN 14

STRAIN	= 200%
PERCENT CAVITATION	= 0.004
MAGNIFICATION	= 200X

PAN 14

STRAIN	= 0
PERCENT CAVITATION	= 0
MAGNIFICATION	= 200X

Figure 2-89. Photomicrographs of Cavitation at Different Thickness Strains in SPF 8091 Al-Li

2.3.2 JOINING CONCEPT EVALUATION

Advanced joining methods provide alternatives to the conventional mechanical fastening and adhesive bonding currently used in aluminum airframe structures. Some benefits of the advanced joining methods are: 1) a capability to overcome some of the deficiencies of current joining methods which would reduce labor-intensive assembly, reduce weight and fatigue crack initiation, and reduce fuel leakage and maintenance, 2) apply during the superplastic forming process to provide unique monolithic expanded structures.

The most promising candidates for advanced joining of Al alloys for airframe structures are discussed in the following paragraphs.

2.3.2.1 Metal-to-Metal Joining

Several metallic joining methods are of interest in fabricating structures with Al-Li alloys. Broadly speaking, these methods fall into the categories of solid-state joining and fusion welding. Solid-state joining includes diffusion bonding with or without a transient liquid phase formation and deformation bonding to break up surface oxide. Fusion welding involves gas/metal arc electron beam or laser welding processes. These methods, in principle, can be used for building multisheet trusscore structures as well as for joining end pieces or other structural elements. For this program, roll-bonding and laser welding experiments on Al-Li alloy are described.

2.3.2.1.2 Roll-Bonding

Texas Instruments has developed a unique process for making expanded metal structures by roll-bonding and thermal expansion. Two or more sheet layers containing a "stopoff" material (ink) between them (in a suitable pattern) are roll-bonded. The panel is subsequently heated to a temperature at which the ink decomposes, releasing a gas which expands the part in the areas where bonding did not occur. Many complex configurations have been made in this manner with both similar and dissimilar metal sheets. The process of bonding involves extremely thorough surface cleaning, followed by silk-screening the ink material. The screened materials are deformed 60 percent in one step under very high pressures. The 60 percent deformation ruptures the oxide film (which remained after cleaning) and achieves a metallurgical bond. Subsequent annealing treatments improve the strength of the bond by allowing further diffusion and spheroidization of the impurities. In addition to the flexibility of various shapes, this process is readily adaptable to dissimilar metal joining such as Al/SiC. Another attractive feature of this process is the low-cost aspect of the process elements. The 8091 Al-Li sheets were shipped to Texas Instruments for roll-bonding and experimentation is are in progress.

2.3.2.1.3 Laser Fusion Welding

In-house work at both NAA and the Science Center has extended the general findings that the ingot-melt Al-Li alloys may be readily fusion-weldable. Special surface preparation of Al-Li alloys is essential prior to welding, but thereafter weld cracking and porosity may be effectively controlled. Related research and development on advanced joining of aluminum sheet structures using high-powered, continuous-beam lasers have demonstrated the attractive design and manufacturing benefits of laser welding. Laser welding appears to be particularly compatible with superplastic forming, provided there is either a prebonding with subsequent superplastic expansion between the welded joints or a post-bonding of caps, doublers, etc.

The major sources of porosity encountered during aluminum welding are: (1) traces of hydrogen or moisture in the shielding gas (2) traces of hydrogen in the base and filler metal, and (3) surface contamination of the base metal with moisture or hydrocarbons.

Liquid aluminum dissolves large quantities of hydrogen and its solubility decreases rapidly with decreasing temperatures. During cooling of the weld pool, hydrogen gas bubbles are formed. Bubbles which do not have time to escape to the free surface can be trapped as pores during weld solidification. The following methods were evaluated to minimize porosity: (1) use of hydrogen getters and (2) effect of salt bath heat treatments. Al-Li sheets were shipped to Laser Institute, Ohio and experimentation are in progress.

2.3.2.2 Metal-to-Composite Joining Methods

The initial phase of bonding Al-Li to composite materials examines the influence of process parameters on flame-spraying thermoplastics onto 8091 Al-Li and Cypac. Process parameters currently being examined are the surface treatment of the substrate, the kind of thermoplastic or thermoset to be sprayed, the adhesive coating thickness, and flame-spraying conditions. The adhesion of the coating to the Al-Li and composite material is the key factor to bond strength. The final phase of the study, the actual Al-Li to composite bonding, will commence once the adhesion strength requirements are met for the initial phase.

2.3.2.2.1 Test Methodology

A primary focus of the adhesion effort was on the testing procedure. ASTM C633-79, "Adhesion or Cohesive Strength of Flame-Sprayed Coatings," specified the use of adhesives to bond a metal plug to a substrate. Of the several adhesives tested, none adhered well to the thermoplastic (Ryton PPS) coating used. In some tests, where the ASTM specification was used, failures occurred at the coating-adhesive interface rather than at the coating-substrate interface. Failure at the coating-adhesive interface substantially reduced the significance of the data. A modification to the ASTM test procedure (flame-spraying a thermoplastic onto the surface of a steel plug and onto a 1- by 3-inch Al-Li or Cypac substrate) was examined. Immediately after flame-spraying, while the polymer was still molten, the steel plug was placed onto the substrate with the flame-sprayed coatings together and allowed to harden. The thermoplastic flame-sprayed coating was the "adhesive" and "coating" in this particular test. Steel plugs were used for the initial phase demonstration tests on bond strength. The steel plugs were grit blasted followed by a cleaning operation before the spraying.

The adhesion strength of the substrate-adhesive-steel plug bond was tested by a tensile pull. The coupon plug combination was mounted onto a plate with a projection for mounting into an Instron testing machine and clamped (substrate to plate) for testing (Figure 2-90). The steel plug also
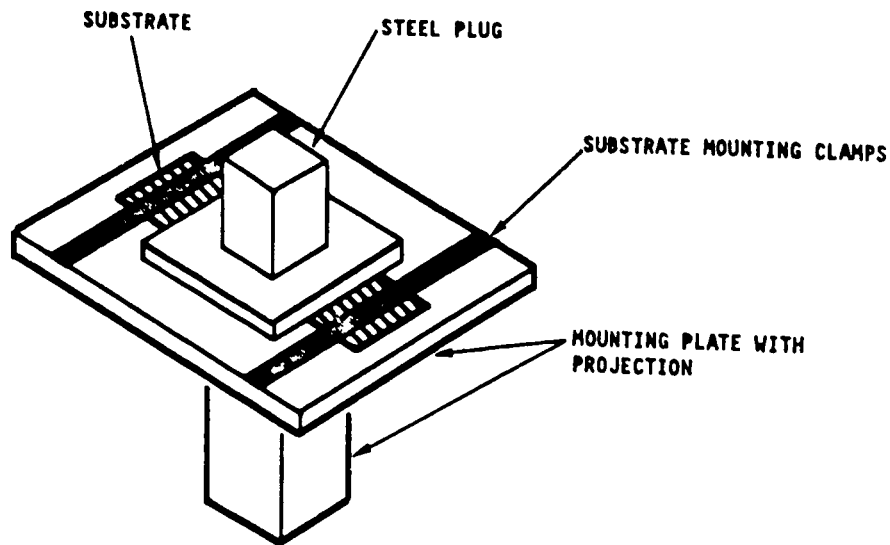
Figure 2-90. Test Setup for Measurement of Adhesion Strength
of Substrate-Adhesive-Steel Plug Bond

has a projection for mounting into the other jaw of the tensile machine. The
bonding combinations were tested by a straight tensile pull.

2.3.2.2.2 Adhesives

The thermoplastics being tested as adhesives are polyethylene (PE),
polyphenylene sulfide (Ryton-PPS), Nylon 11, polyester, and polyetherimide
(Ultem). These thermoplastics are used as a powder for flame-spraying.
Preliminary tests demonstrated that polyethylene and polyphenylene sulfide
powders can successfully be flame-sprayed. The polyethylene and polyester
powders did not satisfy the necessary thermal requirements to support the
program and were eliminated as possible adhesives. A polyetherimide powder
(Ultem or related to it) was purchased and tested. Experiments were conducted
on flame-spraying a coating of polyetherimide onto steel, but this produced
unsatisfactory results since the polyetherimide material did not appear to
fuse well and resulted in a loose, gritty coating. Several additional tests
will be conducted with the material.

Several thermoset polymers were examined as candidate adhesives; they
were polyester-urethane, polyether sulfone, polyacrylates and an epoxy
polyester material. Polyester-urethane, examined for thermal performance at
temperatures above 280°F, retroreacted (cross-linking breakdown) at
temperatures approaching the range of 350 to 550°F. It was determined that
the retroreaction did not satisfy the thermal requirements to support the
program. Preliminary tests conducted on polyether-sulfone resulted in good
adhesion to steel and Al-Li coupons. Tests conducted with an epoxy polyester
material resulted in a smooth surface appearance with good adherence to the
coupon. Polyacrylates are being sought in powder form for testing.

Three different adhesives will be examined once the preliminary examination of available thermoplastics and thermoset polymers is complete. Thus far, of the material tested, polyphenylene sulfide, polyether sulfone, and the epoxy polyester material appear to have the best adhesive-substrate interface and flame-spraying characteristics.

2.3.2.2.3 Flame-Spraying Procedure

The flame-spraying equipment available at Edison Welding Institute was modified to improve equipment performance. Powder and gas flow rates can be accurately controlled separately which allows the flame to preheat the coupon before powder flow is initiated. A spray booth which monitors the substrate heating process both before and during the flame- spraying operation was constructed. A single pass of the spray puts down a film thickness of about 0.010-inch while two passes puts down a thickness of 0.020-inch, etc.; however, powder does periodically collect in the feed line which can result in uneven spraying. Further modifications to the flame-spraying equipment should alleviate this problem.

2.3.2.2.4 Testing

Al-Li sheets used for the first group of tests were heated in an open air oven at 950°F for 15 minutes and water quenched. The heat treatment parameters have been altered for the second group of tests (scheduled to begin in May 1988) to a solution heat treatment of 1010°F for 30 minutes immediately followed by a water quench and an artificial age of 24 hours. The modification to the heat treatment will result in a condition in the 8091 Al-Li sheet similar to the post-SPF and heat-treated condition before flame-spraying.

The first group of coupons were removed from a sheet of 8091 Al-Li, heat treated at 950°F, and divided into two test sections for surface preparation. Coupons for Test Section 1 were grit-blasted and cleaned prior to coating. Test Section 2 coupons were etched by immersing the coupon in a 20-percent sodium hydroxide solution at 120°F until the surface was uniformly attacked, washed, dipped in concentrated nitric acid to remove the black smut and, finally, washed and air-dried prior to coating. The results from flame-spraying and testing the adhesion strength of the coupons are summarized in Table 2-16. The variability and relatively low values of the adhesion strengths are attributed to the test method employed. The Al-Li coupons (0.060-inch thick) bent during the test and created notches at the ends of the test bond. The bending of the thin coupons created areas of high shear which resulted in premature bond failure. The use of thicker Al-Li coupons resulted in much higher adhesive values: up to 900 psi for etching coupons; cohesive failure occurred with the Nylon 11.

One sample sprayed with Nylon 11 (a preheat temperature of 200°F) did not adhere to the substrate. A loose plastic strip was produced. Preheat temperatures of 350°F and above produced film with good adherence. As the

TABLE 2-16

PEEL TEST ADHESION STRENGTH OF 0.006-INCH THICK A1-LI COUPONS TO STEEL WITH NYLON 11

Preheat Temperature (^{O}F)	Surface Preparation	Coating Thickness (Inch)	Adhesion Strength (psi)
400	Grit Blasted	0.01	160
400	Grit Blasted	0.028	257
400	Grit Blasted	0.038	105
400	Etched	0.014	43
400	Etched	0.04	141
400	Etched	0.022	76
400	Etched	0.023	259
425	Grit Blasted	0.011	175
425	Grit Blasted	0.011	60
425	Grit Blasted	0.012	105
425	Grit Blasted	0.014	245
425	Grit Blasted	0.018	198
425	Grit Blasted	0.02	160
425	Grit Blasted	0.024	170
425	Grit Blasted	0.024	406
425	Grit Blasted	0.032	305
425	Etched	0.007	0
425	Etched	0.01	7
425	Etched	0.014	70
425	Etched	0.026	30
425	Etched	0.028	0
450	Etched	0.026	157
450	Etched	0.028	0
475	Etched	0.023	0
475	Etched	0.026	249
475	Etched	0.031	139

NOTE: Different preheat temperatures and surface preparation methods are represented.

preheat temperature of the substrate increased, the smoothness of the adhesive film improved.

The Cypac material was successfully sprayed using a preheat temperature of 200°F. The resultant coating was rough, but appeared to have good adhesion to the substrate.

Cross sections of the Nylon 11 coating on the Al-Li coupons were examined microscopically for bond integrity. The coupons were examined at the interface of the Al-Li and Nylon 11 at different process parameters. From the photomicrographs it showed that coupons processed by etching had a smoother Al-Li to Nylon 11 interface than grit blasted coupons. The grit blasted versus etched interface is shown in Figures 2-91 and 2-92. Photomicrographs of coupons flame-sprayed at different temperatures are shown in Figures 2-93 through 2-95. Tensile tests will be conducted with 0.125-inch 8091 Al-Li to verify bond integrity for both the etched and grit-blasted coupons.

Edison Welding Institute provided the flame-sprayed coupons to Rockwell for examination of coating textures at different temperatures. The coupons sprayed with the Nylon 11 had improved coating smoothness as the preheat and spraying temperatures increased. The coupons sprayed with the epoxy polyester powder did not appear improved in smoothness as the temperature increased. The epoxy polyester was sprayed at temperatures significantly less than the thermoplastic materials which could account for the difference in spraying behavior. A representation of the smoothness relative to flame-spraying temperature is shown in Figure 2-96.

Additional pieces of 8091 Al-Li were shipped to Edison Welding Institute to continue the flame-spraying tests.
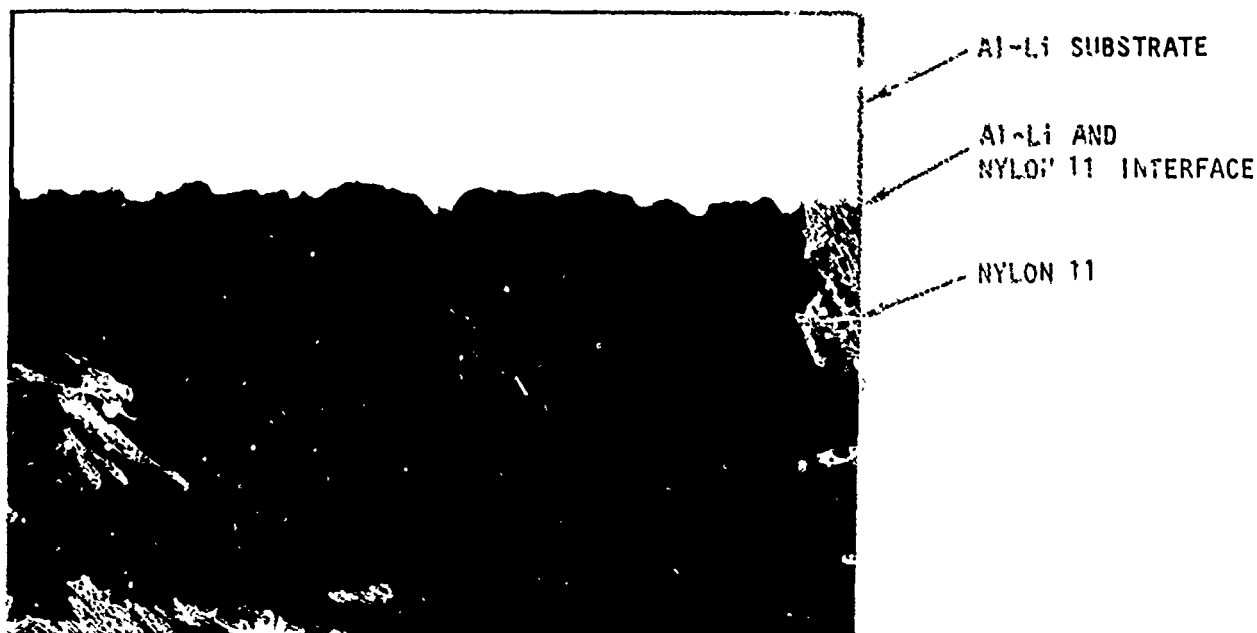
Figure 2-91. Flame-sprayed Nylon 11 on Grit Blasted Al-Li Substrate; Coating
Thickness of 0.014-Inch was Deposited at a Preheat
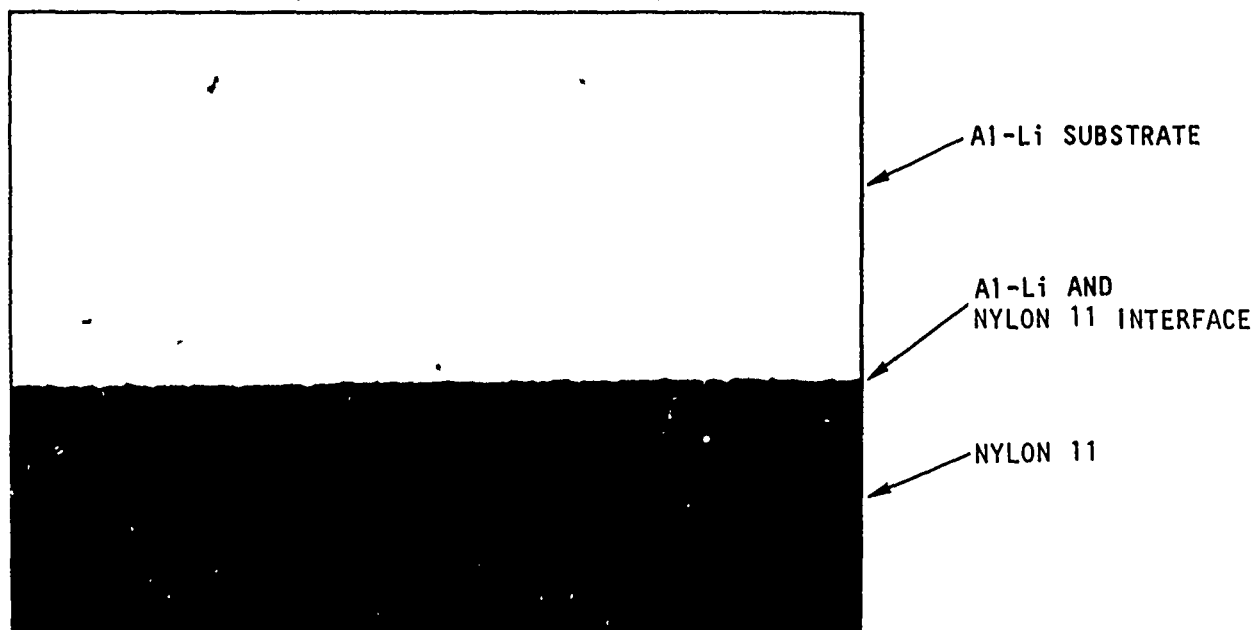Temperature of 400°F.   Magnification = 200X

Figure 2-92. Flame-sprayed Nylon 11 on Etched Al-Li Substrate;
Coating Thickness of 0.010-Inch was Deposited at a
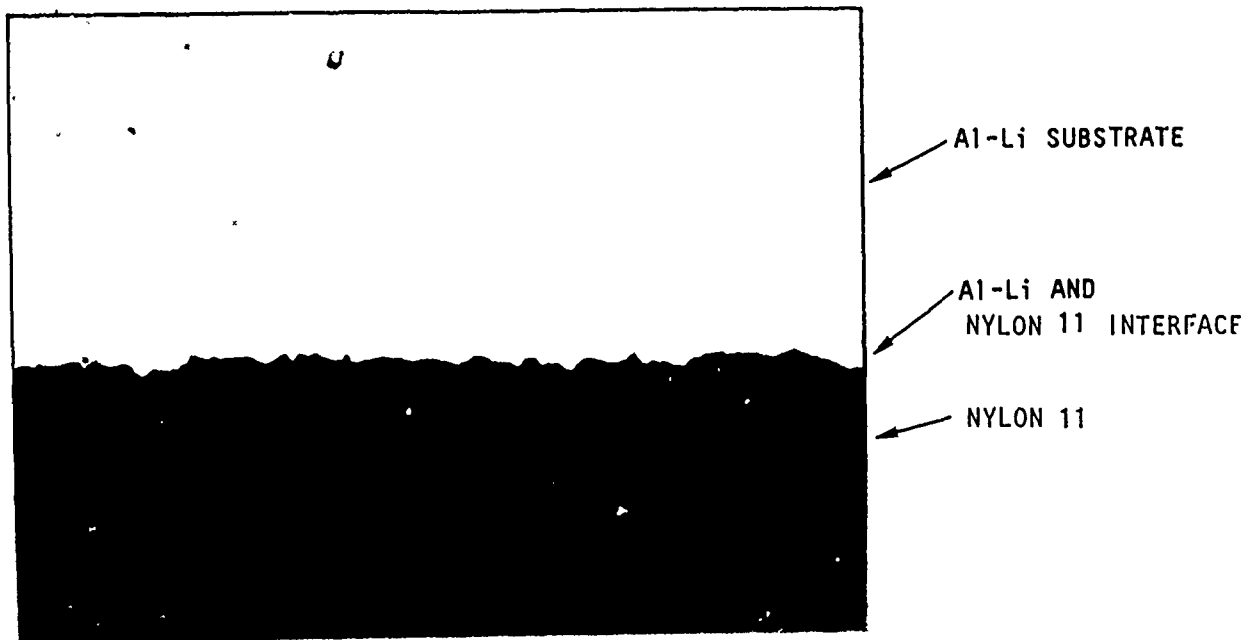Preheat Temperature of 400°F. Magnification = 200X

Figure 2-93. Flame-sprayed Nylon 11 on Grit-blasted Al-Li Substrate;
Coating Thickness of 0.014-Inch was Deposited at a Preheat
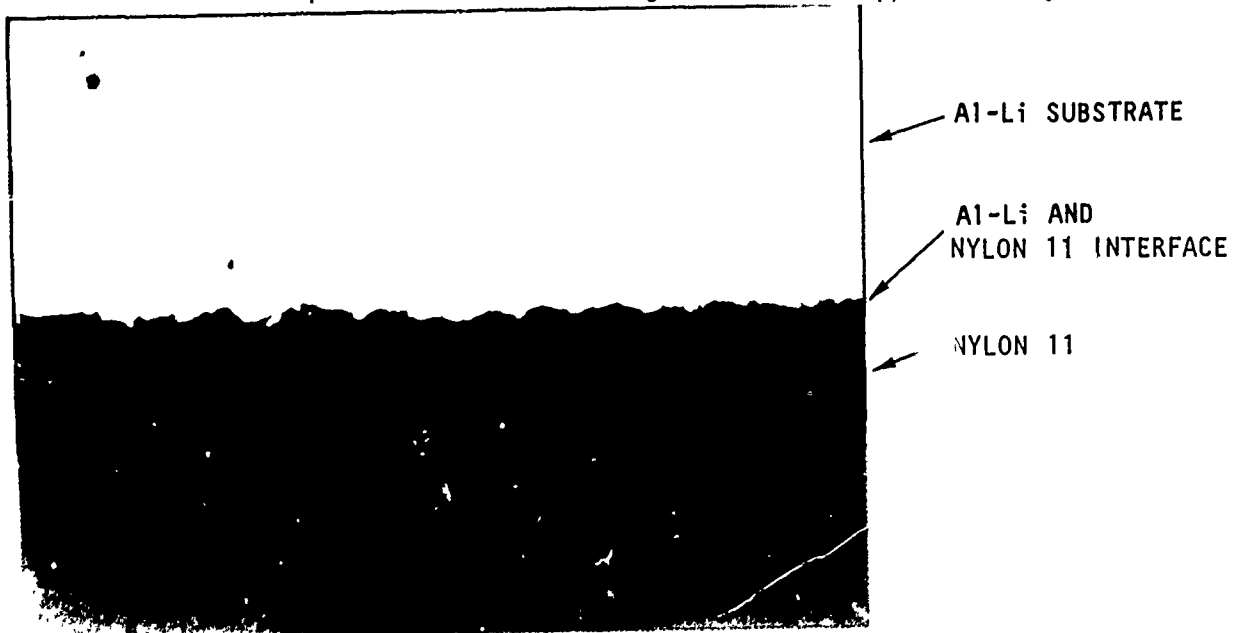Temperature of 425°F. Magnification = Approximately 150X

Figure 2-94. Flame-sprayed Nylon 11 on Grit-blasted Al-Li; Coating
Thickness of 0.028-Inch was Deposited at a Preheat
Temperature of 450°F. Magnification = 100X

←— AL-LI SUBSTRATE

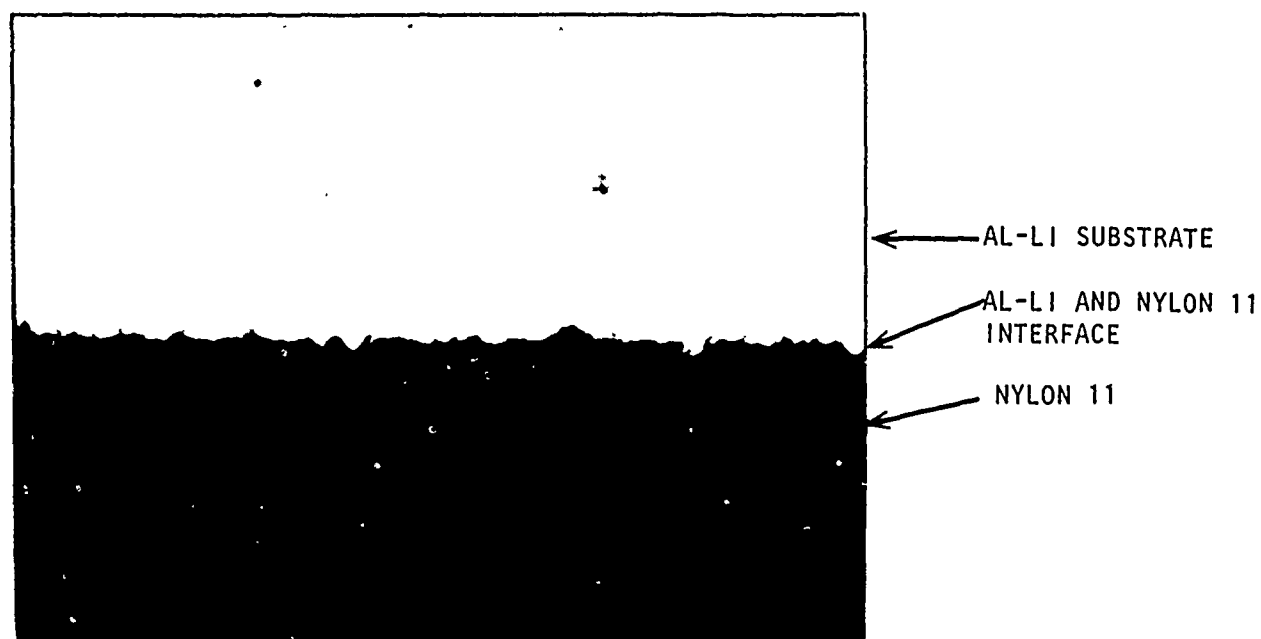←— AL-LI AND NYLON 11 INTERFACE

←— NYLON 11

Figure 2-95. Flame-sprayed Nylon 11 on Grit-blasted Al-li; Coating Thickness of 0.026-Inch was Deposited at a Preheat Temperature of 475°F. Magnification = 100X
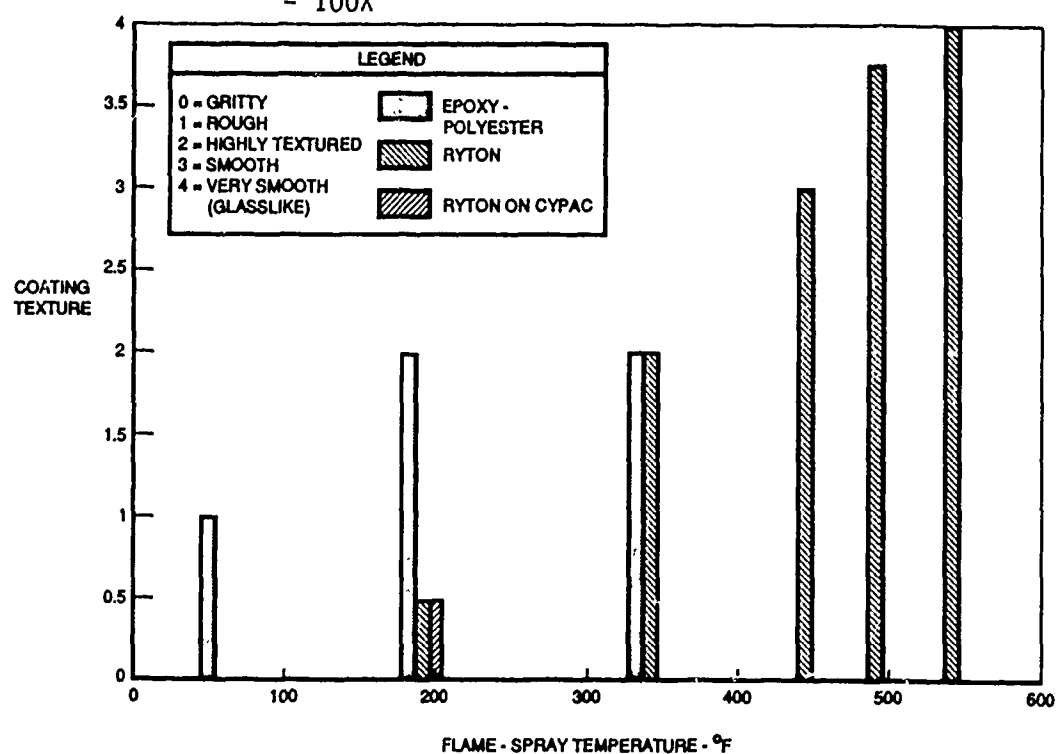

Figure 2-96. Representation of Smoothness Relative to Flame-spraying Temperature

3.0 REFERENCES

1. Ghosh, A. K., "Characterization of Superplastic Behavior of Metals," Superplastic Forming of Structural Alloys, proceedings of a symposium sponsored by the Shaping and Forming Committee and the Titanium Committee of the Metallurgical Society of AIME and the Process Modeling Activity of American Society for Metals, San Diego, California, 21-24 June 1982, pp 85-103.

2. Laycock, D. B., "Superplastic Forming of Sheet Metal," proceedings of a symposium sponsored by the Shaping and Forming Committee and the Titanium Committee of the Metallurgical Society of AIME and the Process Modeling Activity of American Society for Metals, San Diego, California, 21-24 June 1982, pp 257-271.